


October 2020

New Mechanisms That Regulate DNA Double-Strand Break-Induced Gene Silencing and Genome Integrity

Dante Francis DeAscanis
University of South Florida

Follow this and additional works at: <https://digitalcommons.usf.edu/etd>

 Part of the [Molecular Biology Commons](#)

Scholar Commons Citation

DeAscanis, Dante Francis, "New Mechanisms That Regulate DNA Double-Strand Break-Induced Gene Silencing and Genome Integrity" (2020). *USF Tampa Graduate Theses and Dissertations*.
<https://digitalcommons.usf.edu/etd/9533>

This Thesis is brought to you for free and open access by the USF Graduate Theses and Dissertations at Digital Commons @ University of South Florida. It has been accepted for inclusion in USF Tampa Graduate Theses and Dissertations by an authorized administrator of Digital Commons @ University of South Florida. For more information, please contact scholarcommons@usf.edu.

New Mechanisms That Regulate DNA Double-Strand Break-Induced Gene Silencing and
Genome Integrity

by

Dante Francis DeAscanis

A thesis submitted in partial fulfillment
of the requirements for the degree of
Master of Science
Department of Cell Biology, Microbiology, and Molecular Biology
College of Arts and Sciences
University of South Florida

Major Professor: Younghoon Kee, Ph.D.
Kristina Schmidt, Ph.D.
Huzefa Dungrawala, Ph.D.

Date of Approval:
October 13, 2020

Keywords: Transcription, DNA Damage, Polycomb, Nucleoporins

Copyright © 2020, Dante Francis DeAscanis

Dedication

I would like to dedicate this thesis to my family who inspire me to always keep challenging myself and who have always been there for me throughout the ups and downs of life. However, I would particularly like to dedicate this to my mother, Kristina. Throughout the years, she has truly shown me what it means to conquer the adversities of life. Her and I have certainly been through a lot together, and she has always offered me her love, support, and friendship no matter the situation. Her strength and compassion have surely contributed to shaping me into the person that I strive to be. Additionally, I would like to also thank my father, David, and my sister, Gianna. To my father you have made many sacrifices over the years for our family to which I am forever grateful. Your encouragement and friendship have greatly inspired me throughout the rigors of both life and graduate school. You made frequent trips to Tampa to see me during my time in graduate school and you always made time to talk about the things that we enjoy together, particularly sports. To my sister Gianna, you have a great sense of humor and whenever we get together it is always just fun to be with you and laugh together. Thanks Gianna, for being a great friend to me and congratulations on soon graduating with your bachelor's degree! To my Aunt Lisa and Uncle Ron, you guys have also shown me what it means to be family readily opened your home to me for occasional weekend trips and it was always enjoyable to spend time with you guys. With everyone's support, you all were able to inspire me throughout my graduate career. Thank you to everybody, and I love you all!

Acknowledgements

Firstly, I would like to thank Dr. Younghoon Kee for taking a chance on me and providing me with an excellent research opportunity. Under his guidance, he allowed me to grow as a scientist and gave me the opportunity to prove my capabilities. The knowledge I have gained while working under his leadership has shown me what it takes to be a successful scientist and to constantly be thinking about innovative solutions to contribute to new findings in the scientific community. I would also like to thank my committee members, Dr. Kristina Schmidt and Dr. Huzefa Dungrawala for their helpful insight and critiques for the development of this thesis. I would like to thank the previous Kee lab members and their undergraduate volunteers who helped me troubleshoot problems and while also providing insight. Particularly, thanks to Angelo de Vivo and Anthony Sanchez for their patience and for being great mentors. Anthony helped with my benchwork techniques, was always willing to help with questions that I had, and I am sure he will have a successful post-doc career on his way to becoming his own principle investigator. Angelo was also very helpful in assisting me with troubleshooting and always had a new perspective. I know he is more than capable of achieving his future goals to contributing to new scientific research and potentially owning his own lab one day. Thanks to all the previous lab members for also being good friends, maintaining a great lab atmosphere, and for providing encouragement. Additionally, thank you to Robert Hill for offering help with the confocal microscope and for keeping it operational to contribute to this work.

Table of Contents

List of Figures	iii
List of Tables	v
Abstract.....	vi
Chapter One: Ubiquitination and Its Role as a Histone Epigenetic Marker	1
Introduction to Ubiquitination	1
Introduction to Polycomb Proteins	2
Polycomb Protein Architecture Regulates Its Catalytic Activity.....	3
Polycomb Proteins Elicit Context-Dependent Gene Silencing Mechanisms	4
PRC1 Interacts with Cohesin at Polycomb-Targeted Genes to Elicit Transcriptional Repression.....	7
Introduction to The Nuclear Pore Complex, Nucleoporins, and Their Interactions with Chromatin	9
Nuclear Lamina Filaments Maintain PRC1 Architecture and Transcriptional Repression in the Nucleoplasm	12
Chapter Two: The Roles of Gene Silencing in the DNA Damage Response (DDR)	14
Introduction to the DNA Damage Response.....	14
Transcriptional Repression Mechanisms in Response to DNA Damage.....	16
Polycomb Proteins Are Involved in Cell-Cycle Regulation and DDR Activation in Response to DNA Damage.....	20
Polycomb Proteins in Modulating DNA Replication Stress	22
The Role of Nucleoporins in The DDR and DSB Mobilization.....	23
Rationale and Hypothesis for The Potential Role of PRC1 in DNA DSB-Induced Gene Silencing	24
Chapter Three: Methodology.....	28
Cell lines, Plasmids, and Chemical Reagents	28
Site-Directed Mutagenesis of SAM-Domain L307R Mutant.....	29
PEGFP-PHC2 Wild-Type Overexpression Plasmid Design	30
DNA Transfections.....	32
RNA Interference (RNAi)	33

Western Blot and Antibodies	34
Immunofluorescence and Image Quantification	35
Ptuner263 DSB Transcriptional Reporter Assay and Quantification	36
Transcriptional Elongation Assay At UV-Induced Lesions and Image Quantification.....	37
Immunoprecipitation (Exogenously Expressed)	37
Mass Spectrometry Immunoprecipitation.....	38
IPpol Nuclease Induced DSBs and Chromatin Immunoprecipitation (ChIP)	39
Generation of BMI1 Knockout.....	41
Chapter Four: PHC2 Regulates PRC1 Architecture and Transcriptional Repression at Damaged Chromatin	44
PHC2 Depletion Contributes to Transcriptional Misregulation at Sites of DNA Damage	44
PHC2 Localizes to Damaged Chromatin and Regulates BMI1 Foci Accumulation.....	48
PHC2's SAM-Domain Controls Polycomb Body Formation and Contributes to Transcriptional Repression Flanking DSBs	54
Conclusions and Future Directions	60
Chapter Five: Elucidating the Dynamics of Transcriptional Repression at DSBs Through Interactions with Nuclear Pore Complex Proteins.....	67
Nuclear Pore Y-complex Proteins contribute to transcriptional repression at DSBs	67
NUP107 Forms Nucleoplasmic Foci and Localizes to DSBs	73
NPC Y-Complex Proteins Regulate NUP107 Expression and Foci Formation	76
Chapter Six: Conclusions, Future Directions, and Clinical Significance	81
Polycomb Proteins in Cancer.....	81
Implications of Nucleoporins in Disease.....	84
Potential Impact of Polycomb Proteins in Laminopathies	86
References	88
Appendix I: Supplemental Information	94

List of Figures

Figure 1. Schematic for ubiquitination catalysis.....	2
Figure 2. PRC1 proteins forms multiple sub-complexes.....	4
Figure 3. cPRC1 and ncPRC1 contribute differently to H2AK119-ub	5
Figure 4. PHC2-SAM polymerization contributes to gene silencing	7
Figure 5. Schematic for NPC Structure	13
Figure 6. Schematic for an ATM-dependent cascade and DSB repair	16
Figure 7. Transcriptional regulation is required for genomic stability.....	18
Figure 8. Model of potential PRC1-mediated gene repression.....	27
Figure 9. Site-directed mutagenesis workflow	30
Figure 10. Cloning strategy for PHC2_b into pEGFP-C1 mammalian expression vector	32
Figure 11. Schematic for CHIP at DSBs induced by IPpol nuclease	41
Figure 12. Workflow for generation of BMI1 KO in HeLa cells	42
Figure 13. PRC1 contributes to transcriptional derepression at DSBs	46
Figure 14. PRC1 components BMI1 and PHC2 regulate transcription at UV-induced lesions.....	48
Figure 15. PHC2 localizes to damaged chromatin	50
Figure 16. PHC2 depletion decreases polycomb nuclear body formation.....	52
Figure 17. BMI1 localization to damaged chromatin is regulated by PHC2.....	53
Figure 18. Schematic of PHC2-SAM domain.....	56

Figure 19. Overexpression of wild-type PHC2 enhances polycomb nuclear body formation while the L307R mutant diminishes formation	57
Figure 20. Overexpression of the PHC2 L307R mutant does not affect BMI1 binding	58
Figure 21. Reconstitution of PHC2 wild type but not PHC2 L307R mutant can rescue the transcription repressive phenotype	60
Figure 22. Sequencing information for PHC2 knock-in cell lines	64
Figure 23. The L307R homozygous mutation depletes polycomb body formation	65
Figure 24. Workflow for immunoprecipitation mass spectrometry analysis.....	69
Figure 25. Screen of NUPs that contribute to transcriptional repression at DSBs.....	72
Figure 26. NUP107 forms visible foci at DSBs.....	75
Figure 27. NUP107 localizes with DSBs in the nucleoplasm	76
Figure 28. NUP107 expression profile after various NUPs knockdowns.....	77
Figure 29. NUP107 is retained at DSBs over prolonged DSB induction	79
Figure 30. Cancer genomic profile of PHC2-associated cancers.....	84
Figure 31. LMNA localizes to DSBs	86
Supplemental Figure 1. PHC2 L307R mutation fails to repress transcription at DSBs	94
Supplemental Figure 2. PHC2 L307R mutation contributes to spontaneous DSB formation	95
Supplemental Figure 3. PHC2 L307R mutation contributes to replication stress	96

List of Tables

Table 1. List of siRNA.....	34
Table 2. List of Antibodies.....	36

Abstract

Proliferating cells are constantly threatened by genotoxic stressors that can potentially lead to genomic instability. Breaks in the DNA, namely double-strand breaks, are detrimental sources of damage that must be repaired to maintain genomic integrity and prevent potential tumorigenesis. Here we discuss a gene silencing mechanism flanking damaged chromatin. Gene silencing and transcriptional repression at damaged DNA are necessary to prevent potential genomic aberrations from occurring through conflicts with the DNA repair machinery. BMI1, a core polycomb protein in the polycomb repressive complex 1 (PRC1) has been known to play a role in gene silencing at damaged chromatin. However, the function of BMI1 in transcriptional repression at damaged DNA in coordination with other PRC1 members remains to be fully understood. We first investigate the role PHC2, a member of PRC1 and binding partner of BMI1, in maintaining transcriptional repression at DNA damage in a concerted effort with BMI1 in the PRC1. We show that PHC2 is also essential along with BMI1 for maintenance of gene repression flanking damaged chromatin. Furthermore, our data indicates a transcriptional repression mechanism dependent on PHC2 and polycomb body formation in response to damage. Secondly, we investigate the role of nuclear pore proteins in gene silencing at double-strand breaks to elucidate double-strand break peripheral nuclear localization in human cells. We show that specific nuclear pore proteins contribute to transcriptional repression at double-strand breaks and form nuclear foci.

Chapter One: Ubiquitination and Its Role as A Histone Epigenetic Marker

Introduction to Ubiquitination

Ubiquitin is an essential reversible post-translational modification that is used as a modification onto proteins [1]. For instance, linking of ubiquitin chains onto proteins signal them for proteasomal degradation [2]. Additionally, ubiquitination conjugation to proteins provides a regulatory mechanism with implications in gene expression [3]. Ubiquitination of DNA histone substrates allows for further epigenetic modifications to regulation gene expression [3, 4]. For example, this ubiquitination conjugation is facilitated by a cascade of related ubiquitinating enzymes (Figure 1) [5]. First, the ubiquitin activating enzyme (E1) utilizes ATP to conjugate to the ubiquitin protein to form a thioester bond [6]. The E1 then transfers the ubiquitin to a ubiquitin conjugating (E2) enzyme at the cysteine residue in its active site to form a thioester bond [6]. Finally, a ubiquitin ligase (E3) catalyzes the conjugation of the ubiquitin to the lysine of the substrate by forming an iso-peptide bond [6]. E3 ligases contain a really interesting new gene (RING) domain that contains a zinc-binding motif with the catalytic activity necessary to ubiquitinate substrates [7]. As an example, the formation of polyubiquitination chains on a conserved lysine at residue 48 of histones targets them for proteasomal degradation [2]. However, not all ubiquitination signals are necessarily linked to proteasomal degradation and are responsible for eliciting multiple mechanisms. For instance, polycomb protein RING1B (RNF2) is an E3 ligase containing a RING domain possessing the catalytic activity necessary for the

monoubiquitination of histone H2A on the lysine 119 residue (H2Ak119ub) which has suggested implications in mediating gene silencing [8].

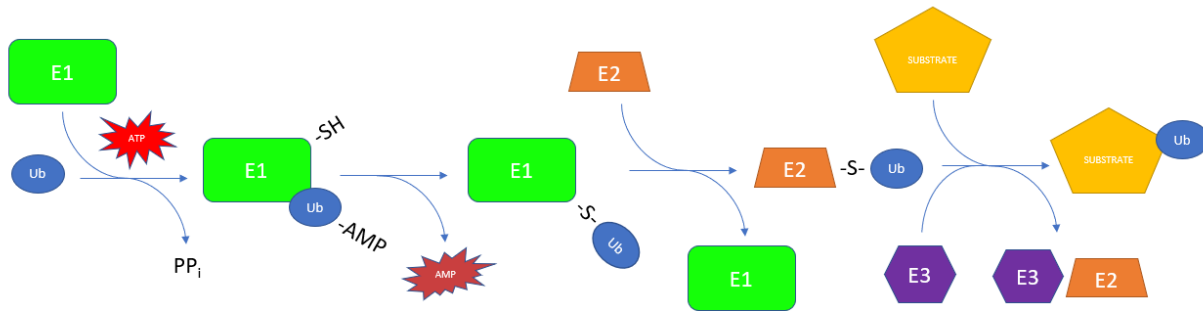


Figure 1. Schematic for ubiquitination catalysis. Through ATP hydrolysis, The E1 enzyme binds to ubiquitin. The E2 ligase is recruited and ubiquitin is transferred forming a thioester bond. Finally, the E3 ligase catalyzes the transfer of the ubiquitin molecule to the appropriate substrate which also displaces the E2 enzyme. Adapted from Nguyen, et al. (2014) [5].

Introduction to Polycomb Proteins

Transcriptional regulation is an essential function proliferating cells must utilize to promote cellular differentiation, regulate tissue development, and maintain genomic integrity [9]. For instance, transcriptional regulatory mechanisms such as epigenetic histone modification and 3-dimensional chromosomal arrangement are elicited in complex pathways to achieve transcriptional regulation [9-11]. Studying the role of polycomb group (PcG) proteins as mediators of gene silencing and transcriptional repression has come to the forefront in understanding epigenetic regulation in transcriptional repression. PcG proteins have been identified as evolutionary conserved transcriptional regulators of developmental *Hox* genes first identified in *D. melanogaster* [11, 12]. However, the scope of understanding their regulatory mechanism has extended from developmental genes to include stem cell proliferation and

tumorigenesis [13, 14]. Thus, polycomb proteins have been implicated in regulating multiple essential cell maintenance activities, but the mode of gene silencing elicited in each pathway reveals to be more complex than previously suggested.

Polycomb Protein Architecture Regulates Its Catalytic Activity

Mammalian PcG proteins have increased complexity and are divided into two different complexes, polycomb repressive complex 1 and 2 (PRC1 and PRC2), that differ in both their composition and enzymatic activity [9, 11]. PRC2 consists of the core subunits EED, SUZ12, and EZH2 to catalyze tri-methylation of lysine 27 on histone H3 (H3k27me3) [9, 11, 15, 16]. On the contrary, PRC1 facilitates the mono-ubiquitination of lysine 119 on histone H2A (H2Ak119ub) [8, 16-20]. PRC1 is also further divided into either the canonical (cPRC1) or non-canonical (ncPRC1) based on the subunits present in the complex (Figure 2). To further add to the complexity, PcG proteins that form PRC1 contain multiple paralogues which accounts for many different combinations. cPRC1 contains either RING1A/B (RNF1/2), one chromobox domain family protein (CBX 2,4,6,7, or 8), PCGF2/4 (MEL-18/BMI1), and one Polyhomeotic-like protein (PHC 1-3) [9]. However, ncPRC1 contains the RING1 and YY1 binding protein (RYBP), PCGF 1-6, and either RING1A or 1B but is deficient of CBX or PHC subunits [18, 21-23]. Original studies suggested a hierarchical mechanism where PRC2 is recruited to a genetic locus and facilitates H3k27me3 which then further recruits cPRC1 to epigenetically mark H2Ak119ub for transcriptional repression (Figure 3) [15]. In this hierarchical model, EZH2 possesses the methyl transferase activity to facilitate the catalysis of H3K27me3. Once the histone H3 is methylated, this provides a docking station for recognition by the CBX proteins of cPRC1 through its chromobox domain. RING1A/B then possesses the ability to catalyze H2Ak119ub through its E3 ubiquitin ligase

activity. However, RING1A/B also forms a heterodimer through RING-RING domain interactions with Mel-18/BMI1 [8, 9, 11, 19]. This interaction further enhances RING1A/B catalytic potential while the PCGF proteins have not been shown to have any catalytic activity themselves. Furthermore, Mel-18/BMI1 bind with the PHC proteins which have been suggested to facilitate cPRC1 activity [21, 24]. Considering this originally proposed hierarchical model, the ncPRC1 pathway has been shown to promote H2A ubiquitylation independent of PRC2 (Figure 3) [25]. As a result, there has been recent controversy over the contribution that H2Ak119ub plays in mediating transcriptional silencing by the various cPRC1 and ncPRC1 complexes.

Polycomb Proteins Elicit Context-Dependent Gene Silencing Mechanisms

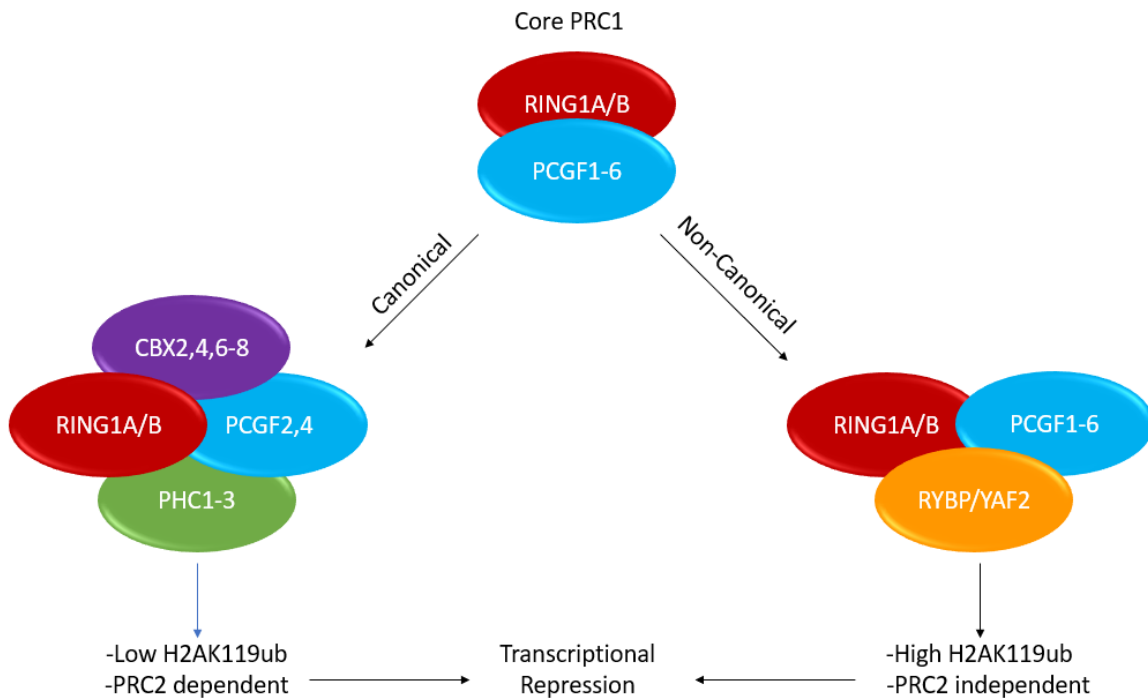


Figure 2. PRC1 proteins forms multiple sub-complexes. The polycomb proteins RING1A/B and PCGF1-6 form a heterodimer and make up the catalytic core of PRC1. From there, the core heterodimer can form either canonical or non-canonical PRC1 variants. In the canonical variant, either PCGF 2 or 4 forms a heterodimer with RING1A/B. CBX 2,4,6-8 and PHC1-3 variants also bind to make up the canonical PRC1. In the non-canonical version, PCGF1-6 bind with RING1A/B and either RYBP or YAF2. Together, these PRC1 variants contribute to gene silencing via H2AK119ub. Adapted from Cohen et al. (2020). [9].

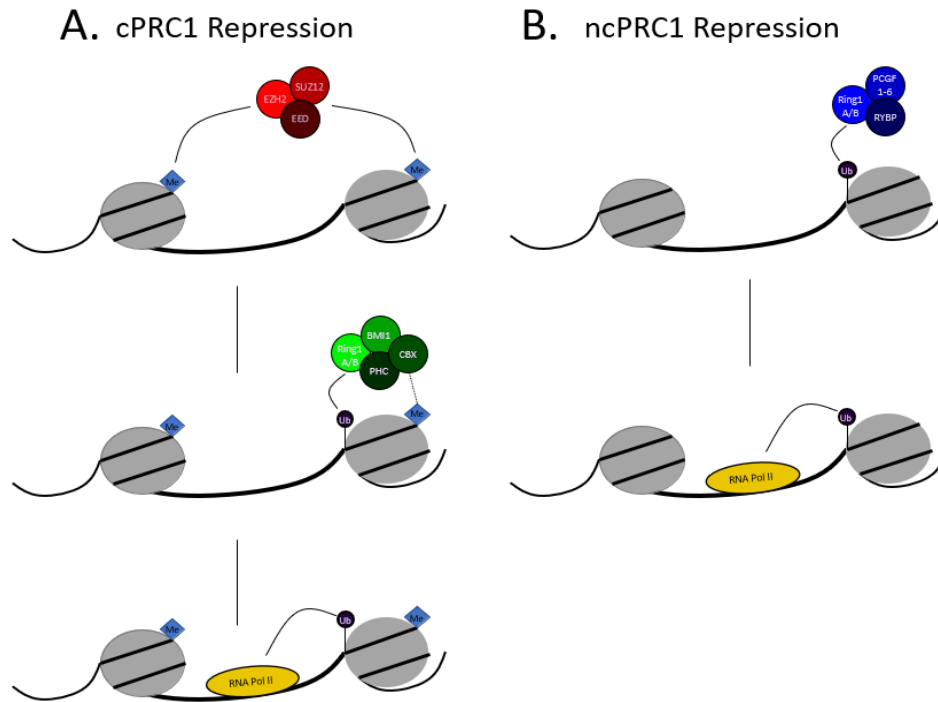


Figure 3. cPRC1 and ncPRC1 contribute differently to H2AK119-ub. A. The cPRC1 must first recognize the H3K27me3 marker deposited by PRC2. CBX proteins bind to the H2K27m3 marker where RING1A/B can catalyze H2AK119ub and prevent transcription. B. The ncPRC1 does not require the H3K27me3 marker to catalyze H2AK119ub to repress transcription.

Over the last decade there has been extensive research in understanding the mechanism by which PRC1 variants contribute to gene silencing. While original evidence suggested a canonical role for PRC1-mediated H2Ak119ub, more recent evidence points to alternative mechanisms. For example, *in vitro* studies suggest that the RING1A/B-Mel-18/BMI1 heterodimer that forms the core of cPRC1 possesses relatively low H2Ak119ub catalytic activity compared to that of the ncPRC1 (Figure 2) [20, 26-28]. Rather, other evidence points to a mechanism where cPRC1 is recruited to H3k27me3 marked by PRC2 and facilitates chromatin compaction and condensation to elicit transcriptional repression [18, 20, 28]. On the contrary, ncPRC1 variants have shown a marketable increase in H2Ak119ub deposition and may not require H3k27me3 catalysis by PRC2 to monoubiquitinate H2A [18, 28]. As a result, studying the involvement of

PRC1-mediated gene silencing is context-dependent and depends on PRC1 architecture and interactions with other genomic maintenance factors.

A prevalent context for which PRC1 architecture influences its activity is prevalent in the presence of PHC2, a binding partner of BMI1. PHC2 contains a sterile alpha motif (SAM) domain that binds with another PHC2 protein through interactions with the end helix (EH) of one PHC2 protein and the mid-loop (ML) of another [29, 30]. By doing so, this polymerizes the cPRC1 to form higher order cPRC1 structures that condense and increase their deposition onto chromatin to further enhance gene silencing (Figure 4) [31, 32]. As a result, when canonical proteins, such as BMI1, PHC2, or RNF2 are visualized via immunofluorescence, distinct nuclear body foci are seen. These nuclear bodies have been denoted as polycomb bodies and are suggested to play a role in transcriptional repression and chromosomal architecture [32]. However, there is little evidence on the precise function and mechanism by which polycomb bodies mediate transcriptional repression. Nonetheless, their presence at cPRC1 targeted genes coincides with evidence supporting a mechanism dependent on modulating chromatin for condensation and 3-dimensional chromatin organization [20, 32]. Other evidence suggests cPRC1 interacts with other nuclear components to further aid in this model of chromatin modulation to facilitate gene silencing.

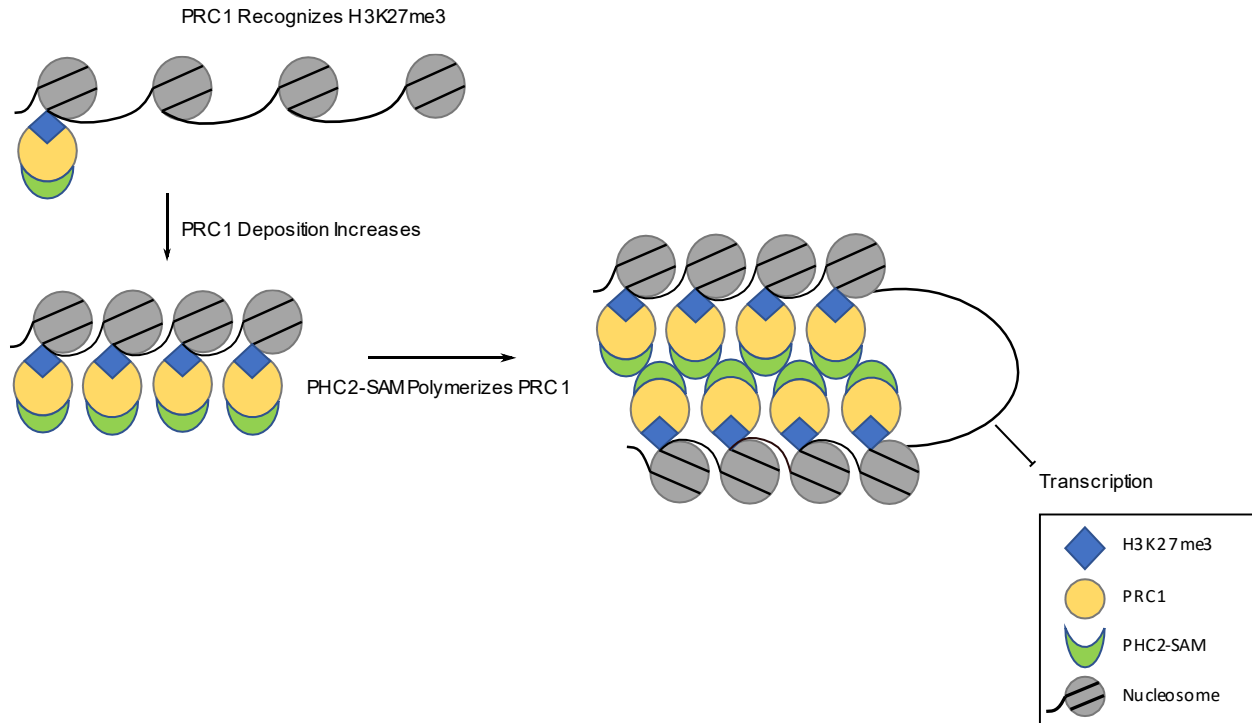


Figure 4. PHC2-SAM polymerization contributes to gene silencing. PRC1 recognizes the H3K27me3 epigenetic marker catalyzed by PRC2. An increase in PRC1 deposition onto chromatin occurs. Adjacent PHC2 proteins bind and further polymerize multiple chromatin bound PRC1. The increase in polymerization results in an increase in PRC1 contacts and facilitates chromatin compaction. This compaction hinders RNA Polymerase II accessibility and blocks transcription. Adapted from Isono, et al. (2013).

PRC1 Interacts with Cohesin at Polycomb-Targeted Genes to Elicit Transcriptional Repression

In addition to PRC1's architecture shaping its activity, coordination with other nuclear regulatory factors shapes PRC1's mode of silencing. For instance, cohesin exists as a complex containing the subunits SMC1, SMC3, and Rad21 [33]. However, the complex possesses two variants that differ depending on the presence of SA1/2 (STAG1/2) [33, 34]. Cohesin has been canonically known to function in the cohesion of replicated sister chromatids in S phase prior to mitotic division. However, cohesin has emerging roles in gene silencing pathways in interphase cells independent of its known role in sister chromatid cohesion. For instance, it has been recently shown that the cohesin-SA2 complex interacts with PRC1 to facilitate long-range

chromosomal interactions to Polycomb domain-mediated in embryonic stem cells [35]. In the context of developmental genes in *D. melanogaster*, long-range interactions occur between Hox gene clusters in which PRC1 occupancy at these genetic loci increases gene repression in a cohesin-SA2 dependent manner. Conversely, there also has been previous studies reporting an antagonistic connection between cohesin and PRC1 in regulating developmental genes in *D. melanogaster*. As a result, there is an unclear understanding of the mechanism by which the cohesin-PRC1 axis regulates gene silencing. To shed some light on this discrepancy, Cuadrado et al., (2019) showed that cohesin-SA1/2 preferentially contributes to distinct chromosome architecture and transcription in mESCs. In this finding, cohesin-SA2 was found to promote PRC1 recruitment and establish long-range interactions of distant polycomb domains to enhance transcriptional repression. On the contrary, the cohesin-SA1 was found to disrupt PRC1-dependent gene silencing of the Hox gene network while preserving topologically associated domain (TAD) contact to silence genes [35]. Thus, these results suggest an alternative pathway where the cohesin-SA2 mediates chromatin looping to maintain polycomb repression at target genes. In line with this cohesin-SA2 dependent gene repression mechanism, increasing evidence is suggesting that cohesin-SA2 contributes to gene silencing in interphase of human cells where mutations in the SA2 subunit are frequently associated with cancers [36]. Based on the canonical function of cohesin, it would be expected that defects in cohesin would negatively affect chromosomal segregation resulting to aneuploidy and subsequently resulting in cancer. However, mutations in the SA2 subunit are not necessarily associated with aneuploidy phenotypes in cancers suggesting that cohesin-SA2 operates in an alternative mechanism to maintain genomic stability. It was thusly concluded that cohesin-SA2 specifically contributes to

transcriptional repression at damaged chromatin in which mutations in SA2 contribute to chromosomal rearrangements and fail to suppress transcription in response to damage [37]. Simultaneously, PRC1-containing protein members have also shown similar involvement in gene repression at damage [38], so it is tempting to speculate a concerted effort between cohesin-SA2 and PRC1 to facilitate gene silencing at damaged DNA. This topic of PRC1-mediated gene repression at damage will be discussed in more detail in a later section. Nonetheless, it is still unclear whether the cohesin-SA2 and PRC1-mediated gene silencing mechanism occurs in interphase of human cells. Additionally, it is also unclear as to a distinct interaction between cohesin-SA2 and either the cPRC1 or ncPRC1 architecture would consequently influence the mode of polycomb repression and bring to fruition to what extent H2Ak119ub plays in this repression.

Introduction to The Nuclear Pore Complex, Nucleoporins, and Their Interactions with Chromatin

The nuclear pore complex (NPC), which is a large protein channel embedded in the nuclear envelope, is comprised of a multitude of A multitude different nucleoporins (NUPs) that facilitate the transport of macromolecules between the nucleus and the cytoplasm [39-41]. The structure of the NPC consists of an inner ring structure that is embedded in the plane of the nuclear envelope [41]. Additionally, there are nuclear and cytoplasmic ring structures that reside on the periphery and connect the inner ring structure to either the nucleoplasm or the cytoplasm [41]. There are also cytoplasmic filaments that protrude from the outer ring structure at cytoplasmic side which aid in both funneling cargo into the nucleus and channeling exported molecules to cytoplasmic proteins [41]. On the other side of the membrane in the nucleus, there is also a nuclear basket that connects to the inner ring structure to further increase interactions

scaffolding between nuclear proteins and the NPC [40]. Finally, there exists nuclear lamina proteins at the nuclear periphery in the nucleoplasm in proximity to the NPC which shape the structural integrity of the nucleus which will be discussed further in a future section [42]. Despite the NPC's original observed function as a factor for both import and export into and from the nucleus, there is emerging evidence for the NPC in genomic organization and regulating transcriptional dynamics [43, 44].

The notion that chromosomes and specific genetic loci occupy distinct microenvironments within the nucleus as opposed to being dispersed randomly is a phenomenon currently being uncovered [45]. In fact, it has been observed that chromatin organization can differ depending on the tissue or cell type in addition to the species [40]. Additionally, it has been observed that heterochromatin regions are in proximity to the nuclear periphery which is a phenomenon categorized from yeast to metazoans [46]. Furthermore, there is evidence in yeast that actively transcribed genes are relocated to the NPC to facilitate gene repression [40]. On the other hand, there is evidence suggesting that the chromatin associated with specific NUPs simultaneously contributes to activation [47]. Furthermore, these phenotypes have mainly been pursued in yeast with little insight into mechanisms pertaining to mammalian cells so it remains to be fully clear how NUPs influence transcriptional dynamics in higher order metazoan organisms [40]. Nonetheless, more research with the past decade has aimed to shed light on the mechanisms by which the NPC and the nuclear periphery interact with chromatin and influence transcriptional activity.

Recent research has implicated specific NUP proteins in facilitating modes of transcription dependent on interactions with transcription-dependent proteins. For instance, Gozalo, et al.

(2020) analyzed through ChIP-seq experiments in fruit flies that Nup93 targets polycomb-repressed genes to facilitate polycomb-mediated repression at the NPC. This proposed interaction was suggested to regulate a subset of repressed polycomb genes. Through ChIP-seq analysis, Nup93 was found present at polycomb target genes along with PRC1 components and the PRC2 H3k27me3 epigenetic marker [44]. Further ablation of Nup93 resulted in derepression of polycomb target genes suggesting that the Nup93 aids in forming long-range clustering of polycomb sites occurring at the nuclear pore. This result subsequently aided to link PRC1-dependent gene repression with the NPC. A caveat to this finding is that the mechanism was identified in *D. melanogaster* with PRC1 homologs while also being largely uncharacterized in mammalian cells. Additionally, in mammalian cells, NUP153 has been shown to recruit PRC1 to a subset of target genes to promote transcriptional repression at the target loci [48]. What is particularly interesting about this finding is that this interaction was observed in the nucleoplasm as opposed to the nuclear pore shown by ChIP-seq of nucleoplasmic developmentally regulated genes. Evidence like this implicates various NUPs propensity for nucleoplasmic migration away from the NPC [48, 49]. As a result, the possibility for completely different interactions between other nucleoporins and PRC1 cannot be completely ruled out. For example, the NPC “Y-complex” which is an isostoichiometric complex that comprises the nuclear and cytoplasmic ring structures and acts as a structural scaffold to the NPC [50]. At the same time, the NPC Y-complex has shown previous interactions with NUP153 for proper assembly at the NPC [51]. As a result, it is plausible that NUP153 may interact with PRC1 and the Y-complex simultaneously to promote transcriptional repression. However, it remains unclear to what mechanisms of gene repression can lead to potential interactions at either the nucleoplasm or the NPC.

Nuclear Lamina Filaments Maintain PRC1 Architecture and Transcriptional Repression in the Nucleoplasm

Within the interior of the nuclear envelope, a meshwork of nuclear lamin proteins are organized to provide structural and mechanical support for the nucleus [42]. Lamin proteins are divided into A and B subtypes where B-type lamins are ubiquitously expressed and confined to the nuclear periphery [52]. A-type lamins (Lamin A/C) however are transcribed from the LMNA gene and alternatively spliced to form distinct proteins [53]. They are also expressed in differentiated cells and form a pool of protein filaments that extend into the nucleoplasm. Due to the alternative splicing event, LAMIN A, but not LAMIN C is synthesized with a conserved CaaX (cysteine-aliphatic amino acid-aliphatic amino acid-any amino acid) motif on their C-terminus [53]. The cysteine of the CaaX motif is farnesylated by a farnesyltransferase and the aaX tripeptide is cleaved by ZMPSTE24 [53]. An isoprenylcysteine carboxyl methyltransferase (ICMT) methylates the farnesylated C-terminus and finally ZMPSTE24 cleaves the last 15 amino acid on the C-terminus. Interestingly, this final cleavage event by ZMPSTE24 is essential for mature Lamin A production where genetic mutations in the cleavage site results in age related disorders such as Hutchison-Gilford Progeria Syndrome [54]. Without the proper cleavage, progeria cells are abundant in farnesylated prelamin A resulting in amorphous cells and lack of migration from the nuclear envelope to the nucleoplasm. While this lack of migration to the nucleoplasm results in serious age-related, muscular, and cardiovascular disorders, a precise mechanism of action remains to be elucidated [55]. A previous interaction between lamin A/C and PRC1 proteins have been identified and such interaction has been proposed to occur in the nucleoplasm thus contributing to gene repression [56]. Additionally, an interplay between lamin A/C and PRC1 has

been implicated in muscular dystrophy disorders [57]. As a result, it is plausible to suggest that crosstalk between lamin A/C and PRC1 proteins facilitates gene silencing mechanisms implicated in age-related and muscular disorders.

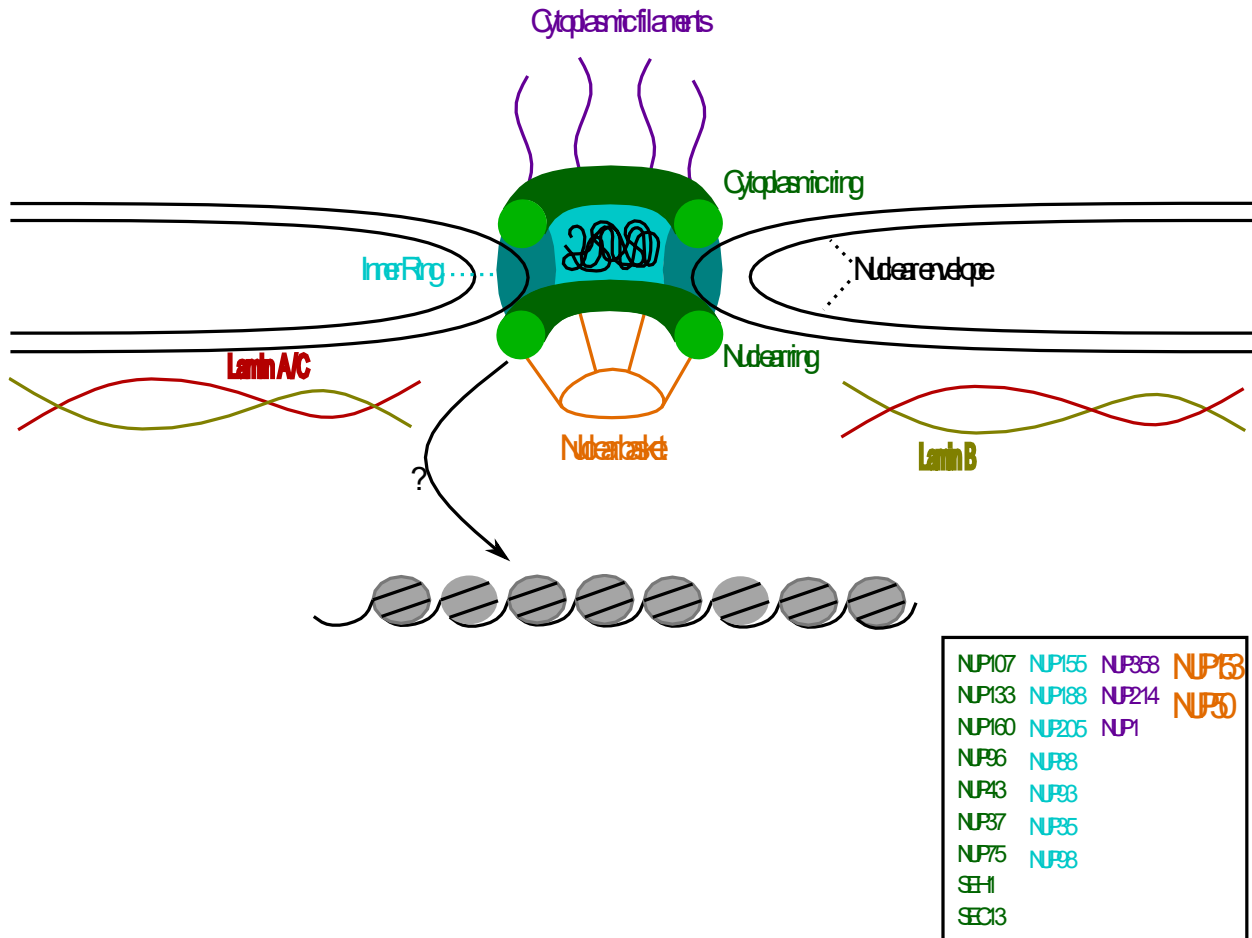


Figure 5. Schematic for NPC Structure. The NPC facilitates the import and export of macromolecules through the nucleus. The nuclear and cytoplasmic ring structures are comprised of the same nucleoporins and contact the nuclear envelope. The inner ring structure is embedded with the nuclear envelope and contains nucleoporins necessary for molecular transport. The nuclear basket allows for scaffolding between the NPC and nuclear proteins. Lamin proteins also form a meshwork along the nuclear periphery in the nucleoplasm. Genomic organization and interactions between the NPC and chromatin are currently under investigation as it remains unclear how the NPC interacts with the genome. Adapted from Raices et al., (2012) and Weberruss et al. (2016). [40,41]

Chapter Two: The Roles of Gene Silencing in the DNA Damage Response (DDR)

Introduction to the DNA Damage Response

Mammalian cells routinely encounter both endogenous and exogenous sources of damage such as reactive oxygen species and UV/ionizing radiation, respectively [58]. In either case, specific types of damage cause different DNA lesions such as bulky pyrimidine dimer adducts or breakages of the double-stranded DNA. Of interest are lesions resulting in double-strand breaks (DSBs) because these lesions are the most toxic. Both strands must be repaired efficiently before replication otherwise excess DNA damage may cause replication fork collapse to further introduce genetic mutations and threaten genomic stability that can lead to cancer [59]. As a result, the cell must elicit a robust response that elicits cell-cycle checkpoints to prevent the daughter cells from potentially inheriting deleterious damaged DNA prior to repair. In response to DSBs, ATM is an important regulator that is actively recruited to DSB where its activation and subsequent kinase activity phosphorylates downstream targets to facilitate repair, cell-cycle checkpoints, and apoptosis [60]. Upon encountering a DSB, the MRE11-RAD50-NBS1 complex (MRN) senses and binds to free double-stranded DNA ends. Upon binding, the MRN complex recruit's ATM which typically exists as a homodimer in unstressed cells.

However, once a DSB is encountered and the MRN complex recruits ATM, ATM autophosphorylates both subunits on the serine 1981 residue further dissociating the dimer [61]. Once dissociated, ATM triggers a cascade of phosphorylation events on chromatin flanking the DSBs. The histone H2A variant H2AX is phosphorylated on the serine 139 residue (γ H2AX) and spread to >10 kb from the DSB site and is further required for the accumulation of DNA repair proteins [62]. The spread of γ H2AX throughout flanking chromatin regions is mediated by the response protein MDC1. MDC1 directly binds to γ H2AX and indirectly anchors ATM through NBS1 binding which can bind both ATM and MDC1 [63]. This allows ATM to recognize nucleosomes with γ H2AX and further propagate H2AX phosphorylation events away from the DSB to allow for DNA repair factor recruitment [62,63]. Simultaneously, ATM phosphorylates the effector kinase CHK2 on a threonine 68 residue and p53 on the serine 15 residue which further signals G2/S phase and G1 phase cell-cycle checkpoints, respectively [64]. In addition, original evidence suggests that γ H2AX formation elicits specific ubiquitination post-translational modifications on histones to facilitate DNA repair [65]. For instance, ATM-dependent γ H2AX formation and MDC1 phosphorylation also recruits the E3 ubiquitin ligases RNF168 and RNF8 which facilitate the polyubiquitination of histone H2A on the lysine 13/15 residue (H2AK13/15ub) [66, 67]. This ubiquitination event further recruits the accumulation of 53BP1 and BRCA1 which are integral repair proteins for deciding repair pathway choice [68]. Recruitment of BRCA1 facilitates the homologous recombination (HR) repair event while recruitment of 53BP1 antagonizes BRCA1 and facilitates non-homologous end joining (NHEJ). NHEJ can occur in every phase of the cell cycle while HR repair is only facilitated during S/G2 phase of the cell cycle due to the requirement for a homologous template [68, 69]. Because of this, HR repair is more efficient and less-error prone

but is also limited to when it can be implemented. On contrary, NHEJ facilitates the repair by ligating the broken ends together, but this is also prone to resection of the broken ends potentially leading to loss of genetic information potentially leading to genomic instability [70].

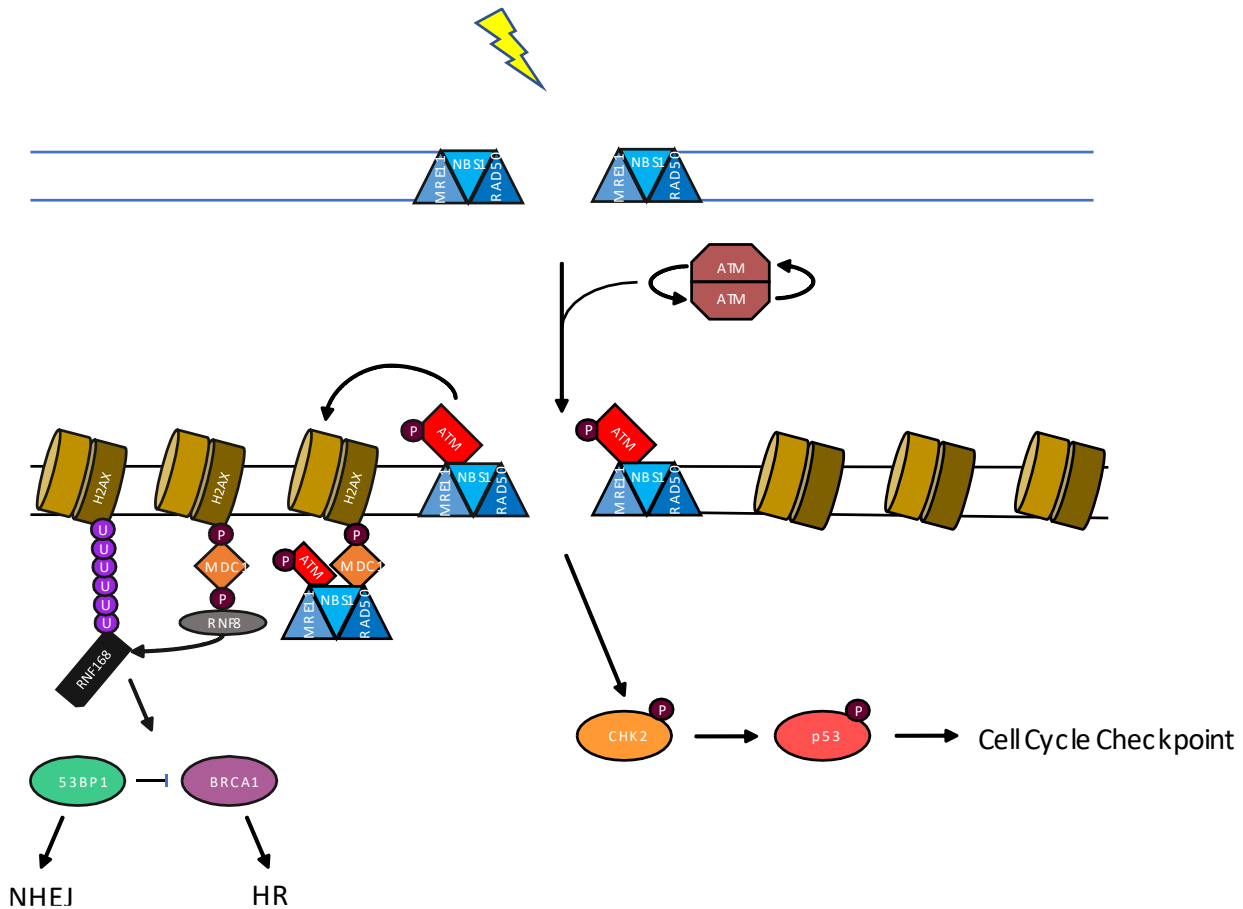


Figure 6. Schematic for an ATM-dependent cascade and DSB repair. The MRN complex recognizes DNA DSBs and recruits ATM. ATM is a homodimer that autophosphorylates itself to dissociate the homodimer. Autophosphorylated ATM binds to NBS1 of the MRN-complex and further phosphorylates the histone H2A variant H2AX. H2AX phosphorylation recruits MDC1 to which ATM indirectly binds through NBS1. MDC1 is further phosphorylated by ATM and recruits E3 ligase RNF8 and RNF168. Together, RNF8/RNF168 contribute to H2AK63ub. This polyubiquitination signal recruits 53BP1 which promotes NHEJ by blocking BRCA1-mediated HR repair. Simultaneously, ATM phosphorylates CHK2 which interacts with and phosphorylates p53 to promote cell-cycle checkpoints while the DSB is repaired. Adapted from Kinner et al. (2008) and Shaltiel et al. (2015) [69,70]

Transcriptional Repression Mechanisms in Response to DNA Damage

In response to DNA damage, a robust DDR pathway is elicited to facilitate repair to maintain genomic integrity [62-70]. Simultaneously, transcription must also be inhibited at the

damaged chromatin to prevent interference with the repair machinery and to prevent the accumulation of genetic mutations. Without this transcriptional repression, genomic stability is threatened potentially resulting in tumorigenesis [71]. Several mechanisms are elicited to mediate gene silencing. For instance, RNA polymerase II an RNA polymerase enzymes in eukaryotic cells that transcribes DNA into mRNA to be further translated into proteins. In regions of the genome that are actively transcribed, there is a consistent presence of active RNA polymerase II [72]. If a region of the genome that is actively transcribed experiences damage in the form of lesions, particularly DSBs, then the RNA Polymerase II must be stalled until the damage can be repaired [71]. This can be facilitated through directly inhibiting RNA Polymerase II elongation at the damage or through chromatin modulation [73].

In the former case, positively regulating RNA polymerase II-interacting proteins are inhibited to prevent it from progressing at the damaged lesion. For example, FACT components SPT16 and SSRP1 facilitate transcription by acting as histone chaperones for histones H2A and H2B, respectively [74]. This allows RNA Polymerase II to transcribe mRNA unhindered. However, when encountering a DSB, FACT is negatively regulated by OTUD5 which consequently inhibits RNA polymerase II elongation. OTUD5 is specifically recruited to the DSB and binds to SPT16 as a negative regulator to further inhibit RNA polymerase II [75]. Alternatively, other factors such as cohesin are suggested to increase chromatin looping in areas proximal to the damaged chromatin which decreases RNA polymerase II access to the location [37]. Nonetheless, it remains to be fully elucidated as to the extent of the upstream DDR factors that signal for this repression. For instance, ATM phosphorylated is suggested to play a role as an upstream factor in signaling for transcriptional repression [76]. However, other reports suggest that DNA-PKc, another protein

kinase, is responsible for eliciting phosphorylation propagation in the DDR at actively transcribed genes [77]. Thus, more research in the field is necessary to fully understand which signals regulate transcriptional repression at DSBs.

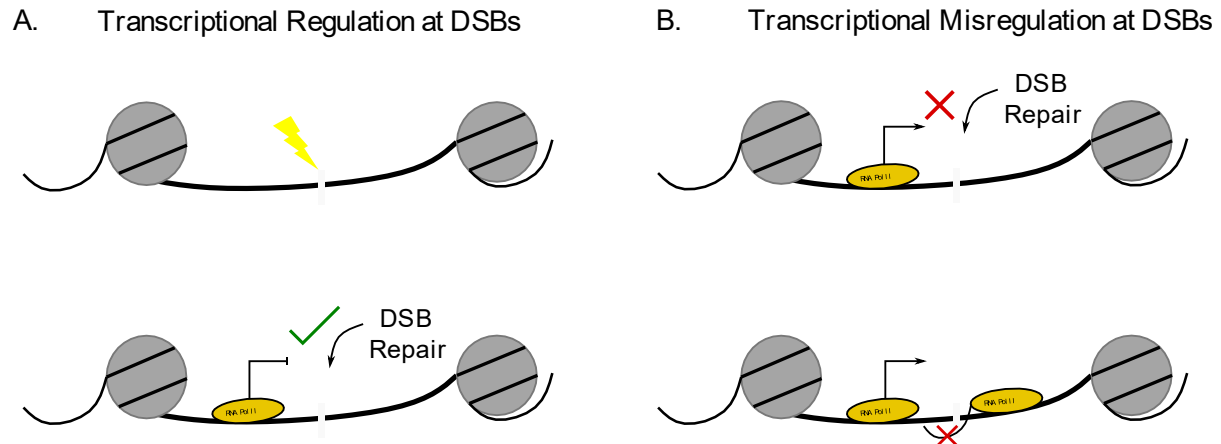


Figure 7. Transcriptional regulation is required for genomic stability. A. Upon successful repression of RNA Pol II at DNA DSBs, repair can efficiently occur at the lesion and maintain genomic integrity. B. Transcriptional misregulation can interfere with DSB repair factor activity resulting in inefficient repair resulting in potential sources of mutations and genetic instability. Additionally, failure to properly inhibit RNA Pol II can result in faulty mRNA synthesis further causing potentially mutated and non-functional protein synthesis further contributing to a decrease in cellular homeostasis.

The Greenberg laboratory proposed that ATM-dependent H2A ubiquitylation regulates transcription *in cis* to DSBs [76]. Using a unique reporter cell line their lab designed, transcriptional activity at a single induced DSB was visualized through immunofluorescence in response to various conditions. In the human osteosarcoma cell line (U2OS), a reporter was integrated at the 1p.36 genomic location. In the cassette, a lac operator array is integrated approximately 5 kb upstream of tetracycline response elements (TREs) which is doxycycline inducible. Directly downstream of the TREs are a promoter region and YFP-MS2 encoding sequence which binds to nascent RNA and the MS2 stem loop transcript after translation. In addition, DSBs are induced by a mCherry-LacI-Fok1 fusion protein. The fusion protein localizes to the lac operon where Fok1 creates a DSB with its endonuclease activity and is visualizes with the

mCherry tag [76]. Taken together, this system is used to identify nascent transcription *in cis* to a single DSB. Using this reporter cell line, Dr. Greenberg's laboratory showed that H2Ak119ub is an ATM dependent gene silencing mechanism utilized in response to DSBs. However, this mechanism was originally proposed to be mediated by the RNF8/RNF168 E3 ubiquitin ligases which together facilitate the H2Ak63ub polyubiquitination in recruiting DDR proteins [76]. However, other evidence suggested that the H2Ak119ub was mediated by BMI1-RNF2 of the PRC1 [78, 79].

Taken together with this evidence, it was shown *in vitro* that BMI1-RNF2 could promote DSB repair via H2Ak119ub [73, 78, 79]. Given that BMI1 has not shown to possess its own catalytic activity, it is suggested to be required for targeting RNF2 to DSBs and subsequent H2Ak119ub in an ATM-dependent manner [19, 78, 79]. In addition, this recruitment was independent of RNF8 which indicated that BMI1-mediated H2Ak119ub functions in a different pathway in the DDR [79]. Furthermore, the Downs laboratory showed that BMI1 and EZH2 were required for H2Ak119ub recruitment to DSBs [73]. Further depletion of BMI1 and EZH2 increased YFP-MS2 accumulation at Fok1 positive spots using the U2OS transcriptional reporter cell line. This evidence suggests that PRC1 and PRC2 may cooperate to catalyze H2Ak119ub for gene silencing at DSBs in an ATM-dependent manner. However, it was unclear as to the mechanism by which ATM signaling BMI1-mediated gene silencing. It was then proposed that ENL, a transcriptional elongation factor, interacts with BMI1 in an ATM-dependent pathway [80]. In this mechanism, ENL is recruited to sites of transcriptional elongation by RNA polymerase II (RNA pol II). After encountering a DSB, ATM is recruited to the site and phosphorylates H2AX along with ENL. This

subsequent phosphorylation increases the interaction between ENL and BMI1 to increase BMI1-RNF2 enrichment *in cis* to the DSB to catalyze H2Ak119ub and promote gene silencing [80].

Despite the evidence that BMI1 facilitates gene silencing via H2Ak119ub, given the recent evidence in the controversy over the ability of cPRC1 vs ncPRC1 to facilitate this epigenetic modification, there is reason to suggest that an alternative pathway may mediate the gene repression. Our previous work identified an H2Ak119ub-independent mechanism for BMI1 gene silencing at damaged chromatin [38]. Our laboratory showed that UBR5 interacts with BMI1 and FACT subunits SPT16 and SSRP1. In this way, the BMI1-UBR5 interaction repress RNA pol II elongation by antagonizing SPT16. In BMI1 and UBR5 depleted cells, transcriptional derepression occurs where SPT16 foci is enlarged at the damaged site [38]. Depletion of SPT16 in BMI1 and UBR5 knockout HeLa cells reverses the transcriptional derepression by RNA pol II elongation. Thus, these results suggest that BMI1 shows propensity for H2Ak119ub-independent gene silencing pathways in break repair. In addition to roles in gene silencing in the DDR, there are implications of polycomb proteins having roles in the maintenance of DNA replication.

Polycomb Proteins Are Involved in Cell-Cycle Regulation and DDR Activation in Response to DNA Damaged

As previously mentioned, PcG proteins have been extensively researched in understanding developmental gene regulation and stem cell differentiation. Interestingly however, PcG proteins have also been implicated in the DDR through an unknown mechanism where PcG protein deregulation affects cell-cycle progression and induces DNA damage checkpoints ultimately contributing to cancer development [81-83]. As a result, there is increasing evidence for a role of polycomb proteins in double-strand break repair and checkpoint

regulation [13, 14, 84, 85]. BMI1, a key protein in the PRC1, has been at the forefront over the last decade in uncovering the role polycomb proteins and PRC1 play in the DDR.

Original *in vivo* studies where a homozygous knockout of *Bmi1* $-/-$ was generated resulted in 50% lethality [84]. Surviving mice showed a severe reduction in hematopoietic stem cells with a reduction in survivability to only about 20 weeks at maximum [84]. Interestingly, in this same study, depletion of the *Ink4a/arf* locus in *BMI1* $-/-$ did not show rescue the phenotype. However, an additional homozygous knockout of *CHK2* $-/-$ in the *BMI1* $-/-$ lineage resulted in an improved overall survivability of the mice suggesting a role for BMI1 in the DDR independent of the *Ink4a/arf* locus. Simultaneously, BMI1 loss in *BMI1* $-/-$ *Ink4a* $-/-$ *arf* $-/-$ mouse embryonic fibroblasts (MEFs) leads to an accumulation of cells in G2/M with an increase in CHK2 phosphorylation. This evidence shows that BMI1 is associated with checkpoint activation independent of the *Ink4a/arf* locus [84-86]. Further studies have implicated BMI1 in the DDR through its interaction with other DSB repair factors [76, 78, 79, 84, 87, 88]. Upon initiation of a DSB, ataxia telangiectasia mutated (ATM) becomes auto phosphorylated and further initiates the phosphorylation of the histone variant H2AX to form γ H2AX and signal the recruitment of downstream DDR repair factors [61, 62, 76, 87]. BMI1 is shown to colocalize with γ H2AX at irradiated sites and depletion of BMI1 results in persistent γ H2AX formation compared to control cells [78, 79, 86, 88]. In addition, BMI1 depletion alone results in increased γ H2AX indicating BMI1 is involved in the DDR signaling cascade pathway. BMI1 deficiency has also been linked to defects in HR repair suggesting that BMI1 contributes to accurate DNA repair [78, 86]. Together, this evidence shed light into the role PcG proteins plays in the DDR. However, given that BMI1

functions as a part of the PRC1, investigation into its H2Ak119ub capacity in the DDR will be an important aspect in elucidating a mechanism in the DDR dependent upon gene silencing activity.

Polycomb Proteins in Modulating DNA Replication Stress

The identification of PcG proteins in mediating replication was observed in BMI1 depleted cell lines where they were subjected to anticlastogenic agents camptothecin (CPT) and Aphidicolin (APH), and Hydroxyurea (HU) [86, 89]. CPT is a topoisomerase inhibitor, APH inhibits DNA polymerase, and HU depletes the dNTP pool so that all these drugs can halt cells in S-phase. Upon treatment, cells were hypersensitive to the anticlastogenic agents causing spontaneous chromosomal breaks as well as limiting progression into G2/M phase of the cell cycle after S-phase arrest. Other replication defects were observed at common fragile sites (CFSs) which are evolutionarily conserved AT-rich regions, late-replicating regions particularly susceptible to replication stress, associated with genomic stability and cancer [90]. However, it is unclear as to the precise mechanism that contributes to cancer at CFSs. Using ChIP at CFSs in APH treated HeLa cells, BMI1 is actively recruited and accumulates at CFSs [78]. This suggests a role for PcG proteins in regulating replication fork stability. Recently published results show BMI1 and RNF2 knockdown limits cell cycle progression into G2/M phase after cells are stalled in S phase [91]. Furthermore, RNF2 knockout in ovarian epithelial cells (T80) shows a significant increase in RNA pol II elongation at stressed replication forks. This irregular transcription at replication defected CFSs leads to transcription-replication conflicts (TRC) [71, 92]. The temporal activity of both cellular machineries at replicating genomic regions can cause conflicts that threaten genomic stability. How exactly might these conflicts specifically contribute to the perceived genomic instability? TRCs increase R-loop formation causing the nascent transcript to reanneal to its

template strand and displacing a ssDNA strand [93]. While R-loops are previously mentioned to be involved in mediating normal transcriptional repression/activation, their overproduction can also be detrimental to cellular survival and contribute to increased genomic instability by TRCs [93, 94]. Our laboratory also showed that the TRC in RNF2 deficient cells resulted in an increase in R-loop accumulation at CFS replication forks while also requiring Fanconi Anemia proteins for fork protection and survival [91]. Other evidence suggests that RNF2 interacts with MDM2 to prevent R-loop accumulation as well [95]. Despite the evidence for PcG proteins' involvement in replication stress, it is unclear whether PRC1 is involved in modulating R-loops and TRC.

The Role of Nucleoporins in The DDR and DSB Mobilization

Regarding the DDR, the yNup84 has been previously shown recruitment of damaged DNA to nuclear pores in yeast [96]. Several mutations in multiple proteins of the yeast nup84 sub-complex (Nup84, Nup120, Nup133, Nup60) rendered cells sensitive to DNA damaging agents suggesting a role in DNA repair [96]. Additionally, it was observed that specifically persistent DSBs and collapsed replication forks mobilized and were associated with the NPC [97, 98]. These reports further suggest that that the NPC may provide a docking station for the coordination of DNA repair observed in yeast. For instance, it was observed that replication forks encountering expanded CAG repeats transiently relocated to the nuclear periphery. A suggested mechanism for DSB and collapsed fork localization is achieved through a SUMOylation-dependent manner [97, 98]. In this way, SUMO ligases, particularly the Slx5/8 complex, operate in "on-site" SUMOylation at DNA lesions to relocate to the NPC where it interacts with the Nup84 sub-complex [96]. However, the scope of DNA relocalization to the nuclear periphery in a Nup84-dependent manner has been primarily observed in yeast. The effects of DSB mobilization has

been pursued in human cells, but there is debate over the extent of mobilization in human cells. Previous reports suggest that DSBs are rather immobile and do not relocate to repair stations [99]. On the contrary, there is also evidence suggesting that DSBs show an increase in mobility in either an ATM-dependent pathway or a 53BP1-dependent pathway mediated by microtubules and the LINC complex [100, 101]. Also considering recent evidence that nucleoporins contribute to transcriptional dynamics in coordination with polycomb proteins, there is a concerted effort to understanding the mechanism by which nuclear organization contributes to transcriptional repression at DNA lesions [48]. Doing so would bring to fruition new DSB repair dynamics and potentially introduce new therapeutic targets for cells with persistent DNA lesions.

Rationale and Hypothesis for The Potential Role of PRC1 in DNA DSB-Induced Gene Silencing

To investigate the role that PRC1 plays in promoting gene silencing in the DDR and modulating replication stress, it is necessary to identify if it is dependent on polycomb body formation. The multitude of evidence has focused on the BMI1-RNF2 heterodimer in mediating these interactions, but are these PcG components acting alone or in coordination with the PRC1? Previously discussed evidence has suggested that EZH2 plays a role in mediating the DDR, but it is unclear to what extent PRC2 and PRC1 interact to contribute to gene silencing at damaged chromatin [73]. Studies examining the molecular structure of PHC2 is particularly intriguing. PHC2 is a well-known binding partner of BMI1 in the cPRC1 and contributes to PRC1 condensation resulting in polycomb body formation [28, 31, 32]. Interestingly, understanding the function of PHC2's SAM domain may provide some evidence to link PRC1 to having a role in gene silencing at DSBs. SAM domains are conserved domains functioning in protein-protein interactions and other lines of evidence show that mutations in SAM domains are linked to defects in cancer

signaling pathways and result in disorders [102, 103]. Despite these roles' SAM domains play in regulating other pathways, it is still unclear as to the role PHC2's SAM domain plays in maintaining genomic integrity by promoting gene silencing at DSBs. One critical point-mutation in PHC2's SAM domain has been previously identified which replaces an arginine with a leucine at the 307 residue (L307R) and eliminates its capacity for polymerization resulting in decreased gene silencing [29-31]. In mammalian cells, this mutation abolishes polycomb body formation and reduces PRC2 engagement leading to a reduction in overall cPRC1 clustering. Therefore, the PHC2-SAM domain has been suggested to facilitate PRC1 clustering consequently increasing chromatin compaction in an H2Ak119ub-independent manner. Given there is controversy over the role cPRC1 plays in catalyzing H2Ak119ub and the fact that PHC2 is a well-known binding partner of BMI1, it is plausible that PHC2 may cooperate with the BMI1-RNF2 heterodimer in the cPRC1 to elicit gene silencing at DSBs.

As previously mentioned, there are recent studies in mESCs that that suggests interaction between PRC1 and NPC-associated NUPs in promoting transcription [48] However, there is controversy over the extent of the relationship compared between mammalian cells and drosophila. For instance, recent studies in drosophila described an interactions towards the nuclear periphery at the NPC while studies in mammalian cells described a relationship towards the nucleoplasm using CHIP-seq [44, 48]. Additionally, there is parallel evidence that specific NUPs can modulate chromatin interactions and DDR repair in yeast, but has not been extensively characterized in human cells [96-98, 104]. Given that PRC1 and NUPs have shown interaction in mESCs and simultaneously have shown to exhibit defects contributing to genomic instability,

there may be a concerted mechanism where the interaction between PRC1 and the NPC inhibits transcriptional access to regions flanking DSBs to maintain genomic stability.

Taken together, there is evidence that PcG proteins are involved in promoting gene silencing flanking DSBs. However, there is still unresolved controversy over the precise mechanism by which PcG proteins, mainly PRC1, contribute to gene silencing in response to DSBs. Simultaneously, while the NPC has shown to be associated with both transcription and the DDR, the precise mechanism for these interactions are lacking in the context of human cells. While most of the previous research has focused specifically on BMI1 and RNF2 and their ability to facilitate H2Aubk119 in response to DSBs, more recent evidence argues that this catalytic activity is dependent upon PRC1 architecture. Furthermore, the role of polycomb body formation remains to be fully explored in the context of gene silencing at DSBs. As a result, further research into the role of PRC1 subunits and their coordination with the NPC would aid in understanding how gene silencing mechanisms occur in response to DSBs. For instance, it is also currently unclear to the extent by which BMI1-RNF2 is recruited to the site of DSB. It is reasonable to suggest that the entire PRC1 is recruited to the site of the DNA break. However, it is also plausible that the BMI1-RNF2 dimer is first recruited to the site where other PRC1 members, such as PHC2 and CBX4, are further recruited to facilitate polycomb body formation to enhance gene silencing activity. However, the exact architectural dynamics of PRC1 at the DSB remain to be fully explored.

Chapter Three: Methodology

Cell lines, Plasmids, and Chemical Reagents

HeLa, HEK293T and U2OS cells were grown in Dulbecco's Modified Eagles Medium (DMEM) supplemented with 10% fetal bovine serum (FBS) and L-glutamine. U2OS ptuner263 cells (a gift from Dr. Roger Greenberg) were also grown in DMEM supplemented with 10% FBS and L-glutamine. HCT116 wild type, HCT116 PHC2 L307R knock-in, and HCT116 PHC2 KO cells (Washington University in St. Louis GeiC) were cultured in McCoy's medium supplemented with 10% FBS and L-glutamine. Cells were maintained in respective media containing penicillin and streptomycin and incubated at 37°C in 5% CO₂. Plasmids used were the pBABE-FLAG-PHC2 previously developed in the Kee laboratory and the pBABE-HA-ER-IPpol vector purchased from addgene. The BMI1 double-nickase plasmid was purchased from Santa Cruz Biotechnology. PHC2 isoform b (PHC2_b) was cloned into pEGFP-C1 expression vector for expression studies. Bleomycin was purchased from Selleck Chemical. Puromycin was purchased from Fisher Scientific and was used at 2 µg/ml

Site-Directed Mutagenesis of SAM-Domain L307R Mutant

Site-directed mutagenesis following the Stratagene QuikChange Site-Directed Mutagenesis protocol was utilized to create a point-mutation in the SAM domain of the pBABE-FLAG-PHC2-WT plasmid backbone. The exact point-mutation was designed to mutate a critical hydrophobic leucine residue to an acidic arginine at the 307 residue (L307R). Forward and reverse primers were designed of 28 nucleotides in length with each primer containing the mis-paired nucleotide for point-mutation in the middle of each primer sequence. Primers were incubated with 1 µg pBABE-FLAG-PHC2-WT plasmid and amplified with PCR. The PCR reaction was followed with a Dpn1 restriction enzyme for 1 hour to digest methylated parental plasmid while leaving newly synthesized plasmid unaffected. After Dpn1 digestion, the reaction was transformed into competent Top10 cells as previously described. Transformed cells were then plated on LB agar plates containing ampicillin antibiotic overnight at 37°C. A control transformation was performed in parallel with competent Top10 cells minus plasmid transformation. By doing so, this negative control would ensure that any growth on the plate would be a result of a successful transformation of the antibiotic resistant plasmid while the competent Top10 cells do not contain any antibiotic resistance themselves. Subsequent colonies were picked and compared to the control to ensure specific growth. Picked colonies were then grown overnight at 37°C in liquid LB media containing ampicillin. Liquid LB media containing potential plasmid was miniprepmed and test digested. Potential clones containing the correct size of insert and vector were selected and sent for sequence analysis (Eurofins genomics). Each sequence was carefully analyzed for the correct nucleotide change resulting in a point-mutation. Positive clones containing the plasmid

with the point-mutation were transiently transfected in 293T cells to confirm expression via western blot. Point-mutants were then used for further experiments.

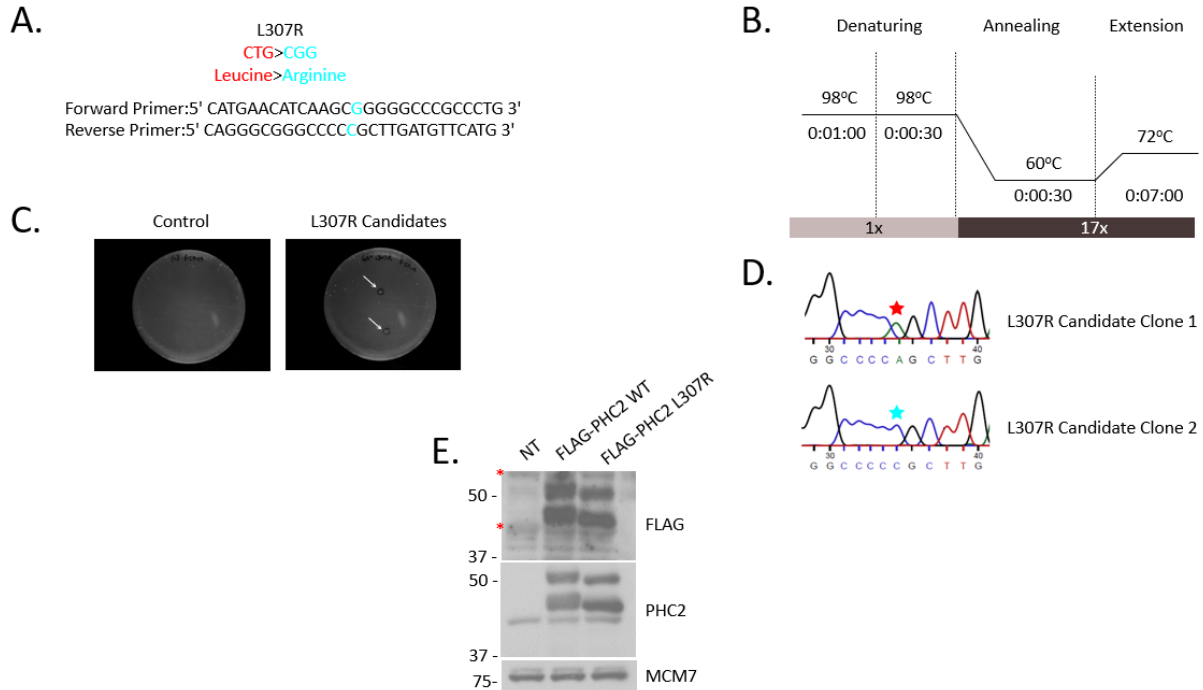


Figure 9. Site-directed mutagenesis workflow. A. Primer design to incorporate a point mutation (L307R) into the PHC2_b. B. PCR cycle used anneal primers to PHC2 sequence (60°C) and amplify DNA over a series of 17 cycles. C. Resulting PCR sample was digested with Dpn1 nuclease and transformed into competent Top10 cells. Arrows indicate potential candidates after transformation. D. Sequence chromatograph of DNA selected from positive colonies. Red star indicates wild-type amino acid while blue star indicates successful point-mutant incorporation. E. Expression test in HEK293T cells with wild-type PHC2 or L307R mutant (Red asterisk indicates non-specific bands). MCM7 was used as a loading control.

PEGFP-PHC2 Wild-Type Overexpression Plasmid Design:

PHC2 isoform b cDNA was amplified from both a T80 cDNA library and previously cloned PHC2 isoform b in a pBABE-puro vector backbone. Forward primers were designed to anneal to the first 20 nucleotides of the cDNA while the reverse primers were designed to anneal to the last 20 nucleotides of the cDNA sequence. The XhoI restriction enzyme sequence was designed into the forward primer to flank (5') the annealing sequence. Additionally, the BamH1 restriction enzyme sequence was designed into the reverse primer to flank the annealing sequence in the

same manner. The restriction enzymes were chosen that were absent within the PHC2 cDNA sequence but present in the MCS (multiple cloning site) of the pEGFP-C1 vector. Nucleotides were inserted as necessary between the restriction enzyme site and the annealing sequence to ensure that the start codon was in-frame with the N-terminal GFP. Once the primer design was finalized, PHC2 cDNA was amplified with the primers and subject to PCR using Phusion high fidelity DNA polymerase (Thermo Scientific) Forward and reverse primers were each used at a final concentration of 0.4 μM and dNTPs were used at a final concentration of 200 μM . 10x HF buffer was also added and brought up to a total volume of 50 μl with nanopure H_2O . Following the PCR reaction, the sample and 1 μg of empty pEGFP-C1 vector were digested with the 1 μl of each restriction enzymes for 2 hours at 37°C, incubated with a compatible buffer for both restriction enzymes. After incubation, the entire digestion was run on a 0.7% agarose gel and visualized. The correct bands were excised using a scalpel and subject to gel extraction using an accuprep gel extraction kit (Bioneer). After the gel extraction, the digested PHC2 insert and pEGFP-C1 empty vector were incubated with T4 DNA ligase and buffer at a 7:1 insert to vector ratio overnight at 16°C. The ligation reaction was then transformed into competent Top10 E. coli bacterial cells. Transformed Top10 cells were subject to outgrowth for 1 hour at 37°C in liquid LB media. The media containing the potentially ligated plasmid was plated on LB agar plates containing kanamycin antibiotic overnight at 37°C. Positive colonies were picked and grown overnight in liquid LB media containing kanamycin at 37°C. The LB media containing the potential plasmid was minipreped and subject to a test digestion to confirm the presence of both the vector and insert. Positive candidates through test digestion were sent for sequence analysis (Eurofins genomics). Upon confirmed sequence results for wild-type PHC2, the plasmids were transiently transfected

in 293T cells to confirm the expression of the plasmid which would be used for further experiments.

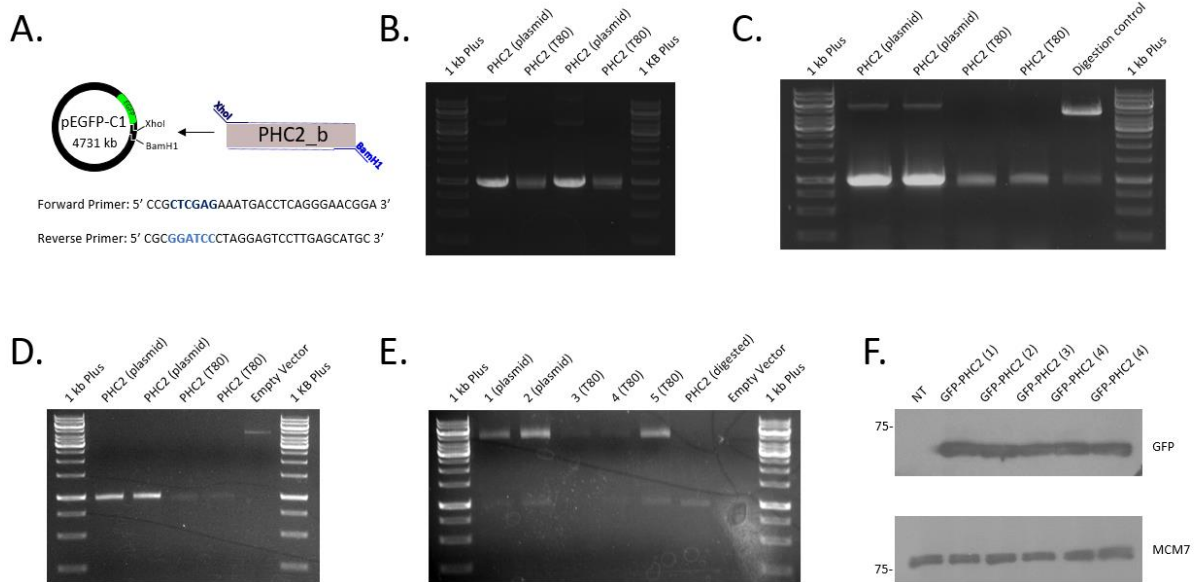


Figure 10. Cloning strategy for PHC2_b into pEGFP-C1 mammalian expression vector. A. Schematic for PCR of PHC2_b into the pEGFP-C1 vector using the indicated primers. Restriction enzyme sites were incorporated into the primer sequence to cleave and ligate into the vector. B. Agarose gel image of amplification of PHC2_b from various indicated DNA sources. C. Image taken after digestion of the amplified DNA with XhoI and BamHI. A digestion control was added to ensure successful digestion. D. Image taken after gel extraction to ensure gel extraction efficiency. E. After ligation and transformation, a test digestion was performed to verify the insert (PHC2_b) was successfully ligated into the pEGFP-C1 vector. Previously digestion PHC2 and pEGFP-C1 samples were also ran on a gel to ensure the correct sizes of the DNA base pairs. F. After sequencing, the clones were proceeded with an expression test in HEK293T cells through transient transfection. GFP is an approximate 27 kDa protein in addition to the 36 kDa PHC2_b (approximately 63 kDa). MCM7 was used as a loading control.

DNA Transfections:

Cells were cultured in penicillin-streptomycin free media. Once cells reached 70-80% confluency, they were transfected with a desired plasmid at a concentration of $1\mu\text{g}/4.32 \times 10^5$ cells (following manufacturer's protocol (Thermo Scientific)) Transfection reagents used were 1x Opti-MEM serum free media (Invitrogen) and Turbofect lipofectamine (Thermo Scientific) at a 1:100

and 1:3 DNA to mass volume ratio, respectively. Transfected cells were incubated for 24-48 hours before analyzing gene expression.

RNA Interference (RNAi)

Table 1. List of siRNA. List of siRNA used with their target sequence and company of purchase. The protein targets used with multiple siRNAs used are numbered in order. siRNA control was purchased from Bioneer.		
Protein target	Target Sequence	Company
PHC2#1	5' CUGAUGAGCGCCAUGAACA 3'	Bioneer
PHC2#2	5' CCAGGUGUUUUGUAGCAAA 3'	
PHC2#3	5' CGGUGGUCUGAGCAACAUA 3'	
PHC2#4	5' CUGAGUUGGGUUACUCAA 3'	
NUP107#1	5' GUCCUCUCUAAUGCUCCUA 3'	
NUP107#2	5' AGACAUGGUCUUGCUCUGU 3'	
NUP107#3	5' UGAUGGAUGAGUUUAGCAA 3'	
NUP43	5' GUGUGUGAGUGGGAUCCAA	
NUP85	5' CAUUGAUCUGCACUACUAU 3'	
NUP133	5' CUCUCCUGUUAAAGUCAU 3'	
NUP93	5' CUGUAUCAUUGGCAGAUGU 3'	
NUP35	5' GCUCGGAAAGCCUUAAGCA	
NUP153	5' GUCAACCAGUGUUUUCU 3'	
NUP98	5' GUGAAGGGCUAAAUAGGAA 3'	
NUP50	5' UUCACUUUCAGAAUCCUG 3'	
LMNA	5' ACAUCUGCCUAAAACCAA 3'	
NUP88	5' CUGACAUACAUCAGUCUGU 3'	
BMI1	5' CAAGACCAGACCACUACUGAA 3'	
RNF2	5' UUGGGUUGCCACAUCAGUUUA 3'	

Cells were cultured in penicillin-streptomycin free media and seeded at 30% confluency. At time of seeding, cells were also transfected with indicated siRNA at 20 nM final concentration. To increase siRNA transfection efficiency, 1x Opti-MEM and lipofectamine RNAimax (Invitrogen) were used at a 1:100 and 1:1 mass to volume ratio, respectively. Cells were treated with siRNA for total of 72 hours and subjected to subsequent experiments and analyses.

Western Blot and Antibodies

Cells were first harvested by washing with 1x PBS and scraped with polyethylene scraper (Corning). Cells were suspended and spun down at 3500 rpm for 5 minutes. The remaining supernatant was removed, and pellets were lysed and resuspended in 2x lysis buffer (0.5% SDS, 0.5 M Tris Cl). The samples were boiled at 95°C for 10 minutes and then spun down for 10 minutes at 12000 rpm to pellet cell debris. Protein concentration of each sample were determined using Protein Assay Dye (Bio-Rad) and recording optical density measurements at 595 nm. Resulting optical density measurements were compared to a standard curve of bovine serum albumin (BSA). 2x Laemmli buffer (Bio-Rad) was added to the samples and boiled at 95°C for 5 minutes and centrifuged at 12000 rpm for 1 minute. Resulting samples were loaded into SDS-PAGE gels and ran at 100 volts for 120 minutes. Proteins were then transferred onto a PVDF membrane using a semi-dry trans blot turbo. After the transfer, membranes were washed with 1x tris-buffered saline with tween (TBST) for 1 hour. Membranes were then incubated with primary antibodies overnight at 4°C and the following day, were washed in 1x TBST for 1 hour at room temperature. Membranes were then incubated with either mouse or rabbit secondary antibodies conjugated to horseradish peroxidase (Cell signaling technologies (CST)) at a 1:10000 dilution ratio in TBST for 1 hour at room temperature. Membranes were washed once more for 4 hours at room temperature and observed using the Pierce ECL Western Blotting Substrate (Thermo Scientific).

Table 2. List of antibodies. List of antibodies used with their target protein, species, and company of purchase.

Protein Target	Species	Company
BMI1	Rabbit polyclonal	Cell Signaling Technologies
MCM7	Rabbit polyclonal	
α -TUBULIN	Rabbit polyclonal	
LMNA	Mouse monoclonal	
53BP1	Rabbit polyclonal	
SSRP1	Rabbit polyclonal	
FLAG	Mouse monoclonal	Sigma Aldrich
NUP107	Rabbit polyclonal	
RNF2	Mouse monoclonal	Santa Cruz Biotechnology
NUP133	Mouse monoclonal	
γ H2AX	Mouse monoclonal	Millipore
Rpb1 (p-Ser 2 RNA Pol II)	Rabbit polyclonal	Abcam
PHC2	Rabbit polyclonal	Proteintech
NUP85	Rabbit polyclonal	
NUP43	Rabbit polyclonal	Invitrogen

Immunofluorescence and Image Quantification

Cells were seeded onto coverslips in 12-well plates and cultured in penicillin and streptomycin free media. For fixation, media was removed from the wells and washed twice with ice cold 1X PBS and then fixed to coverslips for 10 minutes in the dark using 4% paraformaldehyde (diluted in 1x PBS). Cells were washed twice with ice cold 1X PBS, permeabilized with 0.25% Triton for 5 minutes in the dark, and then washed twice with ice cold 1x PBS. Primary antibodies were diluted in 1X PBS (1:100-1:500) and 30 μ l of primary antibody were incubated on the coverslips for 1 hour in the dark at room temperature. After incubation with primary antibodies, cells were washed with 1X PBS and incubated with 30 μ l Alexa Fluor-488 rabbit and Alexa Fluor-568 mouse fluorescently labeled secondary antibodies diluted 1:1000 in 1x PBS for 1 hour in the dark. After incubation, cells were washed again with 1x PBS. Coverslips were then mounted on microscope slides using the Vectashield mounting medium for fluorescence with DAPI (Vector Laboratories

Inc). Coverslips were curated to the slide and sealed with clear nail polish. Images were taken using the Zeiss Axiovert 200 microscope equipped with a Perkin Elmer ERS spinning disk confocal imager and a 63x/1.45NA oil objective using Volocity software (Perkin Elmer). All fluorescent images were quantified using ImageJ software (refer to each section for more detail according to each assay).

Ptuner263 DSB Transcriptional Reporter Assay and Quantification

Ptuner263 cells [76] were seeded at 30% confluency in a 12-well dish onto 12 mm diameter coverslips (Fisher Scientific) with 0.13-0.17 mm thickness and cultured in penicillin and streptomycin free media. 24 hours after initial seeding, cells were treated with indicated siRNA at 20 nM for 72 hours. Ptuner263 cells were treated with Shield-1 (1 μ M) and 4-OHT (1 μ M) 3 hours prior to fixing. Additionally, transcription was induced via tetracycline (2 μ g/ml) to the growth medium 3 hours prior to fixing to induce both DSBs and transcription, respectively. For rescue analysis, the indicated plasmids were transfected, following a previously described protocol, 24 hours prior to fixing. After 72 hours, cells were subjected to immunofluorescence as previously described. Images were quantified by calculating the relative fluorescent intensity (RFI) using ImageJ. mCherry-Fok1 positive cells were selected for each siRNA condition and subsequently quantified. Each fluorescence channel was imported into ImageJ individually. The relative fluorescence intensity (RFI) was calculated by selecting individual cells followed by calculating the raw integrated density at the fok1 spot. The integrated density was corrected by normalization to the background of the individual cell. The subsequent normalized integrated density measurements were divided by the normalized average of the control. A total of 30 cells for each condition were quantified and normalized to the control.

Transcriptional Elongation Assay At UV-induced Lesions and Image Quantification

HeLa cells were seeded at 30% confluency in a 12-well dish onto coverslips and cultured in penicillin and streptomycin free media. At the same time of seeding, cells were transfected with indicated siRNA following previously described protocol (refer to *RNAi* in methods). Cells were incubated for a total of 72 hours before proceeding to fixing. 1 hour prior to fixing, the media was removed from each well and washed one time with 1x PBS. The PBS was removed from each well and the cells were irradiated with 100 J/m² UV-C (UV Stratalinker 2400) through a 3.0 µm-pore UV filter. After irradiation, cells were supplemented with pre-warmed, fresh media and allowed to recover for 1 hour with incubation at 37°C in 5% CO₂. After recovery, cells were fixed and stained following a previously described protocol (refer to Immunofluorescence and Image Quantification in methodology). ImageJ was used to analyze the RFI. Using the line tool, a vector of 100 pixels was drawn across the γH2AX at its widest diameter with the two ends at undamaged regions. The fluorescent intensity of phospho-serine 2 RNA Polymerase II staining along the vector was measured and the average RFI was calculated for 15 independent nuclei in each indicated sample.

Immunoprecipitation (Exogenously Expressed)

HEK293T cells were cultured in penicillin and streptomycin free media in 6 cm dishes. Once cells reached 70% confluency, they were transfected with either pBABE-FLAG-PHC2 WT, pBABE-FLAG-PHC2 L307R, or pBABE vehicle control vector using DNA transient transfection (refer to *DNA transfection* in methodology). Transfected cells were washed with 1 mL 1x PBS and harvested by scraping 24 hours later. Cells were centrifuged at 3500 rpm for 5 minutes in 1x PBS and lysed in a mild NP40 buffer (0.5% NP40, 100 mM NaCl, and 500 mM Tris) at 5 times the

volume of the pellet size while being kept on ice. Samples were then placed on a rotator for 10 minutes at 4°C and centrifuged at 12000 rpm also at 4°C for 10 mins to pellet cellular debris. 10% of the volume of the remaining supernatant was taken as an input and stored at -20°C. The remaining samples proceeded to immunoprecipitation and were incubated with 15 µl anti-Flag M2 affinity beads (Sigma-Aldrich) overnight while rotating at 4°C. After overnight incubation, samples were spun down at 3,000 rpm for 30 seconds. The remaining supernatant was removed making sure not to disturb the beads, and the beads of each sample were subsequently washed with ice cold 0.5% NP40 buffer 3 times in 5 times the volume of original pellet size. After washing, all samples including the inputs were resuspended with equal amounts of 2x Laemmli buffer followed by boiling at 95°C for 5 minutes and 1-minute spin at 12,000 rpm before proceeding to SDS-PAGE.

Mass Spectrometry Immunoprecipitation

Hek293T cells were cultured in penicillin and streptomycin free media and seeded at a confluency of 10×10^6 cells 24 hours prior to transfection. Once cells reached 70% confluency, cells were transiently transfected with a pBABE-FLAG-PHC2 WT plasmid. A total of 120 µg of DNA were transfected. 24 hours after transfection, cells were washed with 5 mL 1x PBS and harvested by scraping. Cells from each plate were transfer to one 50 mL conical tube and was centrifuged for 5 minutes at 4,000 rpm. The supernatant was then removed and lysed in 5 times the volume of the pellet size in ice cold mild NP40 buffer (0.5% NP40, 100 mM NaCl, and 500 mM Tris) while being kept on ice. Lysis proceeded for 10 minutes on rotator at 4°C and was then centrifuged for 30 minutes at 4°C. The supernatant was collected and 10% of the sample was stored for an input at -20°C. The remaining supernatant was used for immunoprecipitation and incubated with 15 µl

anti-Flag M2 affinity agarose beads (Sigma-Aldrich)/500 μ l supernatant overnight at 4°C while rotating. Following incubation, samples were centrifuged for 1 minute at 3,000 rpm at 4°C. The supernatant was removed making sure not to disturb the beads. The beads were then washed 3 times with ice cold mild NP40 buffer in the same volume of the original lysis. After washing, proteins were eluted from beads in 120 μ l 3% SDS in PBS and boiled for 5 minutes at 95°C. After boiling, the sample was spun down for 1 minute at 12,000 rpm and the eluate was collected. 10% of the remaining sample was removed for SDS-PAGE and stored at -20°C. The remaining eluate was submitted to Moffitt Cancer Center's Proteomics and Metabolomics Facility for mass spectrometry analysis.

IPpol Nuclease Induced DSBs and Chromatin Immunoprecipitation (ChIP)

HeLa cells were cultured in penicillin and streptomycin free media in a 10 cm dish. Once 80% confluency was reached, cells were transfected transiently with pBABE-HA-ER-IPpol plasmid [61] following previously described DNA transfection protocol for 24 hours. 3 hours prior to formaldehyde fixation, 4-OHT was added to the culture media (2 μ M). Cells were treated with formaldehyde at a final concentration of 1.42% to the culture media for 10 minutes to fix the interaction between proteins and DNA. After crosslinking, cells were quenched with 125mM glycine for 5 minutes. The media was removed, and cells were washed gently with ice cold 1x PBS combined with 0.5 mM phenylmethylsulfonyl (PMSF) protease inhibitor. Cells were then harvested by scraping and centrifuged 3,500 rpm at 4°C for 5 minutes. The supernatant was discarded and 1 mL cold FA lysis buffer (50 mM HEPES-KOH pH 7.6, 140 mM NaCl, 1 mM EDTA pH 8.0, 1% Triton X-100, 0.1% sodium deoxycholate, and 1x protease inhibitor cocktail (Thermofisher Scientific) was added to the pellet while left on ice for 1 minute. Cells were

centrifuged 12,000 RCF for 1 minute at 4°C. The supernatant was discarded, and pellet was aggressively resuspended in 500 µl FA lysis buffer with protease inhibitor cocktail following a 10-minute incubation on ice. After lysis, samples were sonicated with 45% amplitude for 10 seconds for a total of 8 times to achieve DNA fragments of 200-500 base pairs. After sonication, samples were centrifuged 12,000 RCF for 10 minutes at 4°C to pellet cellular debris. The subsequent supernatant was collected and normalized with Bradford assay to verify equal amounts of protein between all samples. 10% of the sample was saved for input and stored at -20°C. The remaining sample was divided equally for immunoprecipitation and beads only control. FA lysis buffer was added to each sample to bring to a total volume of 600 µl (25 µg of DNA). 53BP1 primary antibodies (1:200) was added to the IP samples and both IP and beads only samples were incubated while rotating overnight at 4°C. The following morning, 25 µl A/G agarose beads (Santa Cruz Biotechnology) were added to for each reaction and incubated for 2 hours at 4°C. Samples were then centrifuged 3000 rpm for 1 minute and supernatant was discarded without disturbing the beads. The beads were subsequently washed 3 times gently in 500 µl FA lysis buffer. Following the last wash, every sample including the inputs were incubated with 400 µl of ChIP elution buffer (1% SDS and 100 mM sodium bicarbonate) for 1 hour at room temperature with rotation. After crosslinking was reversed, all samples were centrifuged 14000 rpm for 1 minute and the supernatant was collected. The resulting supernatant was subjected to RNA and protein degradation. Samples were treated with 2 µl RNaseA (50 µl/mL) and incubated for 1 hour at 65°C. Proteinase K (250 µg/mL) was added to each sample and incubated overnight at 65°C. The next day, samples cooled to room temperature for 1 hour and DNA was extracted using a commercially available purification kit (Bioneer). Endpoint PCR was carried out using for each

sample using primers against specified distances from the DSB site and visualized on 2% agarose gel and proceeded with gel electrophoresis.

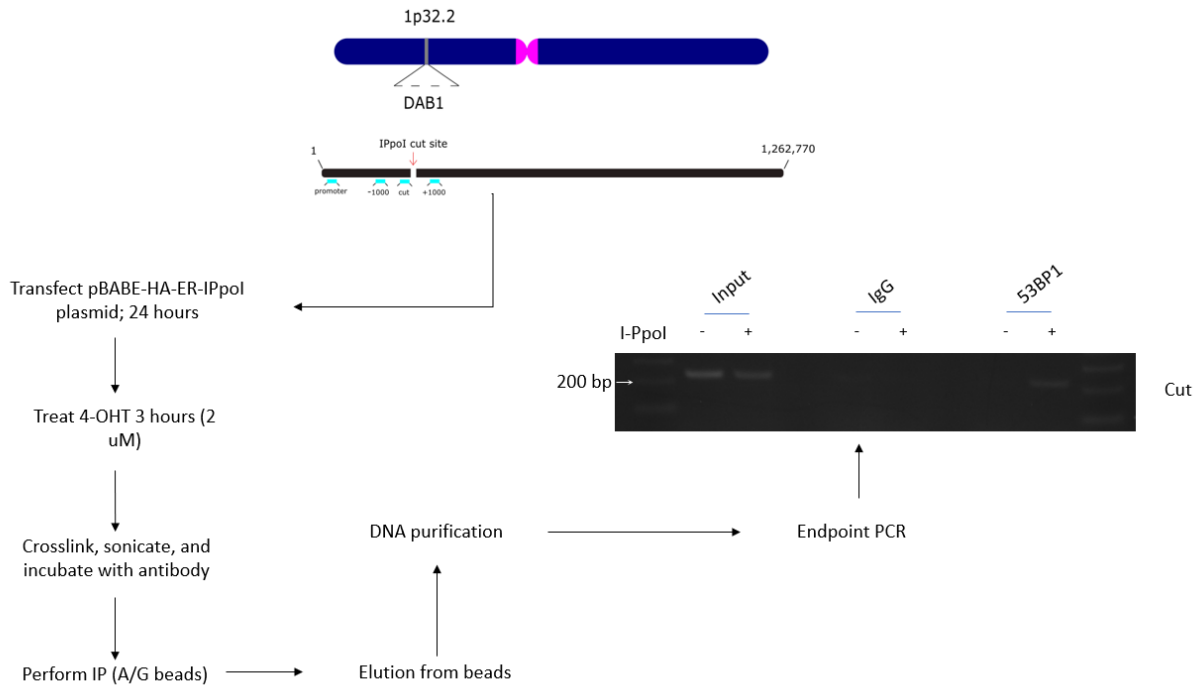


Figure 11. Schematic for ChIP at DSBs induced by IPol nuclease. The DAB1 gene is in a euchromatin region located at the 1p32.2 locus. The IPol nuclease recognizes sequence in an intronic region of the DAB1 gene to create a single DSB. HeLa cells were transiently transfected with a pBABE-HA-ER-IPol plasmid. To induce localization of the nuclease to the nucleus, 4-OHT was added to the media 3 hours prior to fixing. HeLa cells were then crosslinked with formaldehyde and sonicated to create DNA fragments. After sonication, HeLa cells were incubated with primary antibody (53BP1; 1:200). The crosslinked protein/DNA fragments were immunoprecipitated with agarose conjugated IgA/IgG beads. Following immunoprecipitation, the beads were isolated and protein/DNA interactions were eluted from the beads. Remaining RNA and proteins were eliminated with RNase and proteinase K treatment. Finally, the remaining eluate was subjected to DNA purification and PCR. PCR was confirmed on agarose gel electrophoresis with indicated primer.

Generation of BMI1 Knockout

BMI1 knockout HeLa cells were generated using the CRISPR-Cas9 system via a double nickase plasmids (Santa Cruz Biotechnology). The double nickase plasmids contain a pair of partially catalytically inactive Cas9 mutants (D10A) each capable of cleaving one strand of DNA. Each plasmid also contains a unique 20 nucleotide guide RNA (gRNA) sequence designed to target the Cas9 to the BMI1 genetic locus (Figure 12A). To verify plasmid transfection, one plasmid in

the pair contains a puromycin resistant gene while the other contains a GFP marker for visual confirmation.

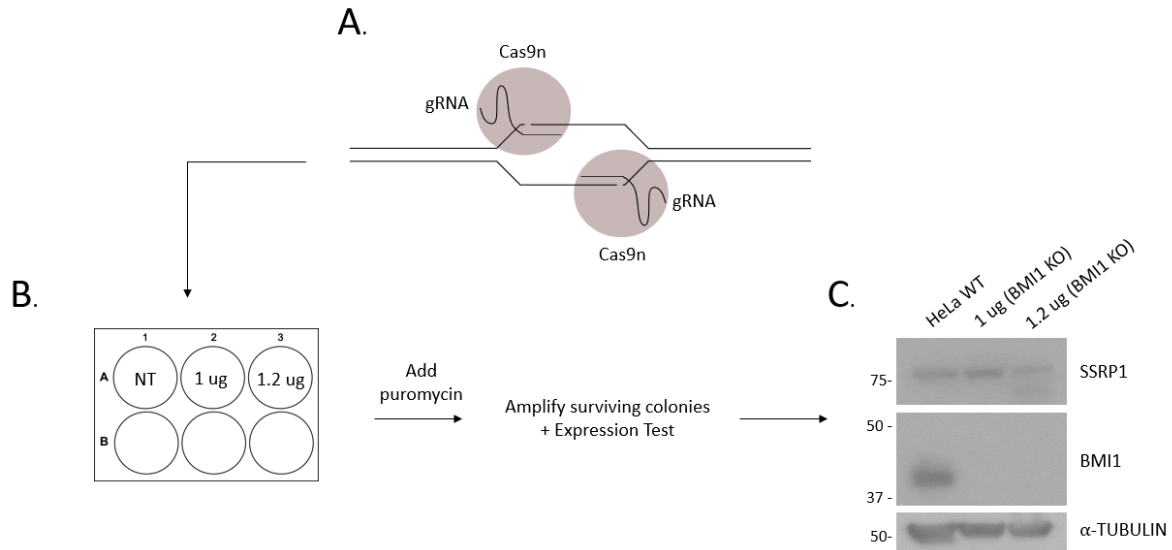


Figure 12. Workflow for generation of BMI1 KO in HeLa cells. A. The double-nickase plasmid from Santa Cruz Biotechnology contains a Cas9n (D10A) mutant that creates single strand cleavage. The gRNA scaffold anneals to target sequence where Cas9n creates single strand cleaves adjacent to a PAM sequence. The double-nickase contains two constructs to selectively target two sequences of the BMI1 gene to effectively create a double-strand break and decrease off-target effects. B. Double-nickase plasmid was transfected into a 6 well in either 1 μ g or 1.2 μ g of plasmid. 24 hours after transfection, puromycin was added to selectively kill off untransfected cells. After all non-treated cells died (72 hours), surviving colonies were amplified and proceeded to SDS-PAGE. C. Expression test of BMI1 knock-out cells compared to wild type HeLa cells.

To generate a BMI1 knockout cell-line, HeLa cells were first seeded at 30% confluency in 3 wells of a 6-well plate. Once HeLa cells reached 70% confluency, 1 and 1.2 μ g of double-nickase plasmid were transfected into two of the three wells, respectively (Figure 12B). Double-nickase plasmids were transfected using DNA turbofect (Thermo Scientific) supplemented in 1X Opti-MEM reduced serum media (Thermo Scientific). 24 hours after transfection of double nickase plasmids, potential candidate clones were selected via puromycin treatment (2 μ g/mL) for 72 hours or until all non-treated HeLa cells failed to survive. Once amplified, 2.2×10^5 cells were lysed

and proceeded to SDS-PAGE for western analysis to confirm successful knockout of BMI1 protein expression. Amplified colonies with successful knockout was stored for future experiments.

Chapter Four: PHC2 Regulates PRC1 Architecture and Transcriptional Repression at Damaged Chromatin

PHC2 Depletion Contributes to Transcriptional Misregulation at Sites of DNA Damage

The BMI1-RNF2 dimer has been previously implicated in mediating transcriptional repression at double-strand breaks [105]. However, it is unclear whether BMI1 or RNF2 act individually to perform such task (e.g. act as a diffusible factor to localize to DSB lesions) or if the PRC1-induced Polycomb body formation is necessary. Recent evidence has suggested that PHC2-BMI1 interactions may be integral to cellular survival [24]. However, it has not been fully addressed to the extent by which PHC2 may contribute to gene repression at broken DNA. To address this discrepancy, we employed the use of the Ptuner263 transcriptional reporter cell-line (refer to methods). This cell-line contains a tetracycline inducible promoter with a YFP-MS2 reporter in which MS2 tag to YFP allows for the detection of RNA at the site of transcription. Approximately 5kb upstream of the YFP promoter are a stretch of repeats of the LacO sequence (256 repeats). Simultaneously, a Fok1 endonuclease restriction enzyme is tethered to a LacI which guides the Fok1 endonuclease to the LacO where it can induce DSBs. As a result, transcription dynamics *in cis* to a DSB can be observed. Under control conditions, if transcription is repressed *in cis* to a DSB, then no YFP-MS2 accumulation would be observed at the Fok1 spot. Conversely, if YFP-MS2 expression is accumulated at the Fok1 spot, then this is an indicator of active transcription at the DSB suggesting a lack of gene silencing *in cis* to the DSB.

As a result, we wanted to address the degree to which other PRC1 factors to gene silencing flanking a DSB. Our previous work had shown that knockdown of BMI1 in the ptuner263 cell-line resulted in an accumulation of YFP-MS2 at the Fok1 spot (Figure 13A) [76]. Because RNF2 dimerizes with BMI1 forming the core of PRC1, we hypothesized that RNF2 depletion would also result in an increase in YFP-MS2 accumulation at the Fok1 spot. On the other hand, the effects of PHC2 on gene repression in response to DSBs had not been previously evaluated. Additionally, we wanted to test PHC2 because we wanted to address whether PRC1 polycomb bodies were involved in this response or if BMI1 and RNF2 acted independently. First, we used 4 different siRNAs targeting PHC2, and siRNAs targeting both BMI1 and RNF2 in ptuner263 cells to decrease the protein expression. After knockdown, we treated the cells with tetracycline to induce transcription and 4-OHT/Shield-1 to induce Fok1. After the drug treatment, we used immunofluorescence to observe the YFP-MS2 signal at the Fok1 spot in each condition. Surprisingly, we found that depleting PHC2, BMI1, and RNF2 resulted in transcriptional derepression at the Fok1 spot., thus suggesting that PHC2 is also involved in gene silencing at DSBs. In the case of all four PHC2-targeting siRNAs, we noticed a significant increase in YFP-MS2 accumulation at the Fok1 spot further enhancing the legitimacy of the finding as opposed to the phenotype resulting from some artifact (Figure 13). Consistently, we saw a similar significant increase in both the BMI1 and RNF2 knockdown samples as well (Figure 13).

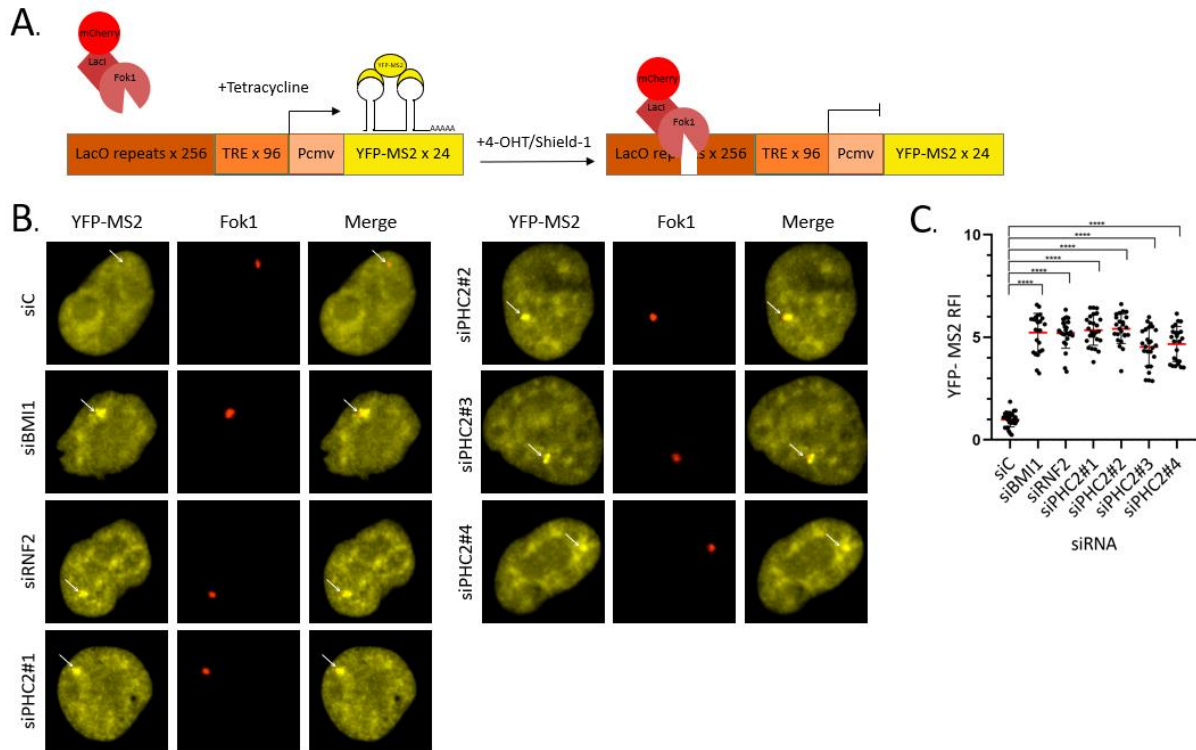


Figure 13. PRC1 contributes to transcriptional derepression at DSBs. **A.** Schematic for the ptuner263 cell-line to examine transcription in response to DSBs. In control cells, transcription is repressed after cleavage via fok1. **B.** Ptuner263 cells were transfected with the indicated siRNAs (20 nM) for 72 hours and treated with tetracycline and 4-OHT/Shield-1 (3 hours) to induce both YFP-MS2 transcription and Fok1, respectively. **C.** Quantification of the YFP-MS2 RFI compared to the control condition at the Fok1 spot. The assay was performed in triplicates (N=30) and the YFP-MS2 RFI was quantified using ImageJ (**** indicates P-value <0.0005).

One caveat to this finding is that the Ptuner263 cell line creates a single DSB at a defined genomic locus. As a result, we wanted to rule out the observed effect of PHC2 is confined to the specific DSB loci induced by the reporter system. To test whether the observed transcriptional derepression was due to some underlying artifact, we used an alternative assay to evaluate this phenotype at randomly induced damaged chromatin. We then aimed to examine the occurrence of active transcription at a UV-induced damage globally throughout the chromatin. We specifically used UV-C radiation (365 nm) which causes DSBs [106]. However, UV-C radiation can also cause other sources of damage such as single-strand breaks and pyrimidine dimers [106]. Therefore, we used γ H2AX as a DSB marker in UVC irradiated cells. To regulate transcription, RNA

polymerase II (RNA Pol II) is phosphorylated on a series of serine residues located on its carboxyl-terminal domain (CTD) [107]. CDK9 phosphorylates the serine 2 residue of RNA Pol II's CTD to engage in RNA Pol II elongation resulting the synthesis of mRNA [107]. In our lab's work, we found that depletion of BMI1 increased the presence of RNA Pol II elongation (phosphorylated serine RNA Pol II) at UV-damaged sites when compared to untreated control cells [38]. Additionally, our lab's previous work implicated UBR5 as a downstream factor of BMI1, but it remains unclear as to the precise downstream mechanism of UBR5 in this pathway [38]. It also remains unclear to what extent PHC2 plays in regulating transcription at damaged chromatin. To test whether PHC2 also contributes to transcriptional derepression at throughout chromatin, we first used an siRNA targeting BMI1 and two siRNAs targeting PHC2 to knockdown protein expression. After knockdown, we induced UV-damage through a micropore filter to irradiate a single spot within the cells. We then used immunofluorescence to detect the presence of phospho-serine 2 RNA Pol II at damaged induced γ H2AX foci formation. We chose γ H2AX because it is an established biomarker that is phosphorylated after DSB formation [87]. Interestingly, we found that depletion of PHC2 along with BMI1 resulted in transcriptional derepression marked by an increase in phospho-serine 2 Pol II overlap at γ H2AX sites (Figure 14). This evidence further suggests PHC2 facilitates transcriptional repression at damaged DNA at undefined genomic loci suggesting it may have a role in global transcriptional repression dynamics. While our PHC2 knockdown results in transcriptional derepression at damaged chromatin is consistent with previously published BMI1 knockdown phenotypes [38, 86], it is plausible that it operates in a similar but different pathway.

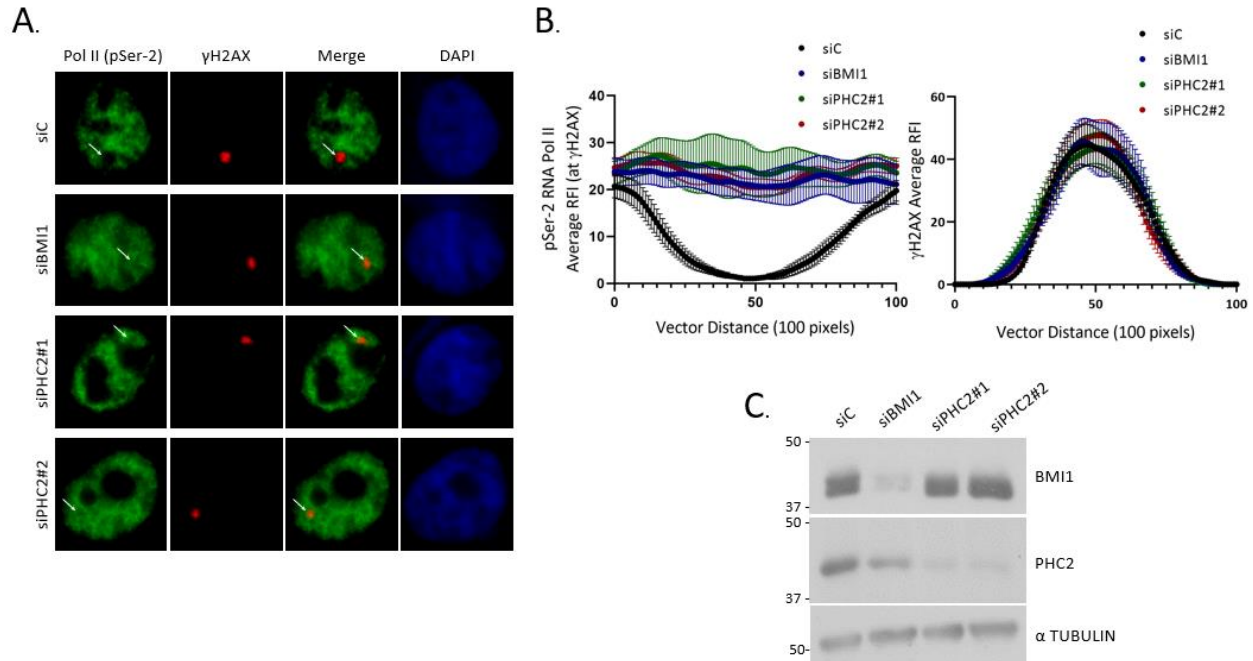


Figure 14. PRC1 components BMI1 and PHC2 regulate transcription at UV-induced lesions. **A.** Representative images of HeLa cells that were locally irradiated with UVC (100 J/m^2 ; 1-hour recovery) through $3.0 \mu\text{m}$ pore filter then costained with anti-pSer-2 RNA Pol II and anti- γ H2AX after treatment with indicated siRNA (20 nM) for 72 hours. **B.** (Left) Quantification of the average pSer-2 RNA Pol II RFI along a vector of 100 pixels across the γ H2AX spot. Values were normalized to undamaged regions. Error bars are indicated ($n=15$ each). (Right) Quantification of the average RFI of an each γ H2AX spot. Error bars are indicated ($n=15$ each). **C.** Western blot confirmation of knockdowns of BMI1 with both siRNAs targeting PHC2.

PHC2 Localizes to Damaged Chromatin and Regulates BMI1 Foci Accumulation

Thus far, we have observed phenotypes linking PHC2 to transcriptional repression at both DSBs induced via fok1 endonuclease activity and UV-C irradiation. However, it remains to be fully elucidated if PHC2 localizes to damage to directly promote transcriptional repression flanking DSBs and promote DNA repair. As previously mentioned, γ H2AX is a marker for DNA damage as its recruitment aids in facilitating repair. Therefore, if a protein is suggested to be involved in regulating a DNA repair, it can be suspected that the protein may form foci or accumulate at the γ H2AX marker. For example, original studies showed that PRC1 members BMI1 and RNF2 accumulated to damaged induced γ H2AX foci and by doing so, this suggested that BMI1-RNF2

promoted DNA repair [105]. However, early studies largely excluded the examination of BMI1's other binding partner, PHC2. Because RNF2 possesses E3 ligase catalytic activity, it was originally proposed that BMI1-RNF2 facilitated the H2Ak119-ub to promote gene silencing at the damage [78, 105]. Despite this evidence, it is still unclear as to whether the PRC1 localizes to the damaged chromatin or if the BMI1-RNF2 is solely recruited given that other PRC1 members, such as PHC2, have not been fully explored. To further address this question, we wanted to examine PHC2's propensity for recruitment to damaged-induced γ H2AX foci. Because PHC2 binds with BMI1 to form PRC1, localization of PHC2 at the damage would indicate that PRC1 is aiding in promoting DNA repair. To do so, we first irradiated HeLa cells with UV-C damage through a 3.0 μ M micropore filter. After irradiation, we allowed the cells to recover for 1-hour to allow DNA repair and γ H2AX foci formation. Following 1-hour recovery, we proceeded with immunofluorescence and costained the HeLa cells with anti- γ H2AX and anti-PHC2 antibodies. Interestingly, we found that PHC2 indeed colocalizes with γ H2AX marked irradiated cells indicating that it localized to damage to promote efficient DNA repair (Figure 15 A). As a control, we also treated cells with siRNA against PHC2 to verify that immunofluorescence signal was truly PHC2 (Figure 15 A). Additionally, we also costained HeLa cells with anti-BMI1 and anti- γ H2AX as a positive control because BMI1 has been previously shown to be recruited to damage induced γ H2AX foci (Figure 15 B) [38, 78, 79, 86]. Thus, we concluded that PHC2 is operating in a linear pathway with BMI1 to be recruited damage. This evidence further suggests that the PRC1 is localized to damage rather than solely the BMI1-RNF2 dimer. Taking into an account that we have established both PHC2 and BMI1 localizing to damaged sites, next we wanted to address whether the observed localization of

BMI1 is possibly regulated by PHC2. If so, this would suggest that PHC2 is also necessary for BMI1 accumulation at damage and would implicate PRC1 in mediating the response.

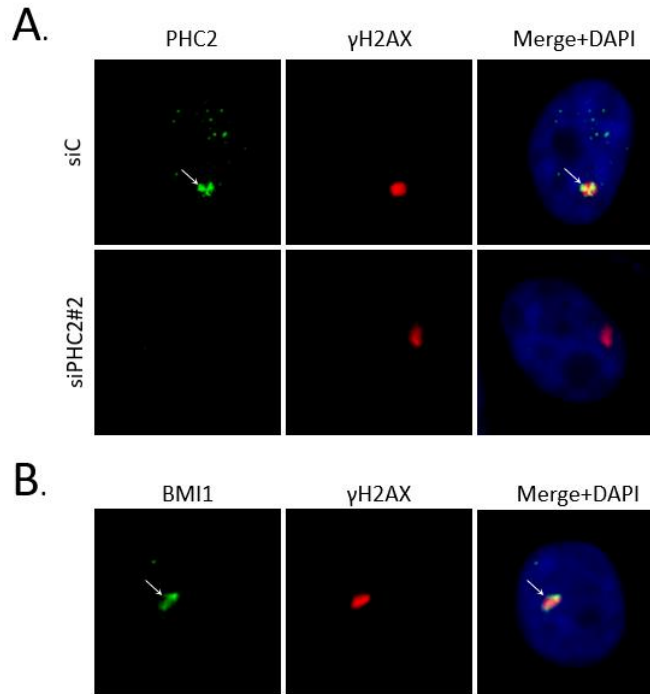


Figure 15. PHC2 localizes to damaged chromatin. **A.** PHC2 forms distinct foci in HeLa cells after damaged was induced by UV-C through a 3 μ m micropore filter (100 J/m²; 1 hour recovery) and co-stained with anti-PHC2 and anti- γ H2AX antibodies. Indicated siRNAs (20 nM) were treated for 72 hours. **B** As a positive control, HeLa cells were costained with anti-BMI1 and anti- γ H2AX antibodies after irradiation with UVC through a micropore filter as in A.

Because PHC2 is a well-established binding partner of BMI1 in the PRC1, we aimed to address whether PHC2 has the propensity to regulate BMI1 foci formation at damaged chromatin. Additionally, we wanted to address whether PHC2 depletion affects PcG body formation given that it is a key component of the cPRC1. These PcG bodies are hypothesized to form a localized transcriptional repressive environment visible by immunofluorescence of integral PRC1 proteins but little is actual known on their precise function in cells [32, 108]. In addition, it is unclear whether polycomb bodies are responsible for promoting transcriptional

repression at damaged DNA. So far, the evidence for BMI1's role in regulating transcription dynamics at DNA damage has largely excluded investigation into whether PHC2 or polycomb bodies regulate BMI1 localization to damaged chromatin. One recent study implicated that PHC2 contributes to polycomb body formation and maintaining the repressive environment of developmental loci [31]. Even though this previous data suggests that PHC2 may be involved in polycomb body formation and gene repression, it is unclear as to what extent PHC2 regulates PRC1-architecture in response to damage. Because PHC2 is a well-known binding partner of BMI1 and given our previously observed phenotypes in PHC2 depleted cells, we first wanted to test if PHC2 knockdown causes BMI1 protein levels to decrease. Secondly, we wanted to address whether PHC2 depleted cells show a decrease in polycomb body formation. In cells, we used two separate siRNA's targeting PHC2 and knocked down PHC2 protein expression. After knockdown, we used immunofluorescence and stained cells with anti-BMI1 antibody to act as a protein marker for polycomb bodies. Given that both BMI1 and PHC2 are PRC1 constituents, we expected to see a reduction in visible polycomb bodies within the nucleus. We found that PHC2 depletion fully eliminated the visible polycomb body foci while leaving nuclear BMI1 protein levels unaffected (Figure 16). This evidence further suggests that PHC2 regulates the formation of PRC1 polycomb bodies and without PHC2, the PRC1 functioning is hindered (Figure 16).

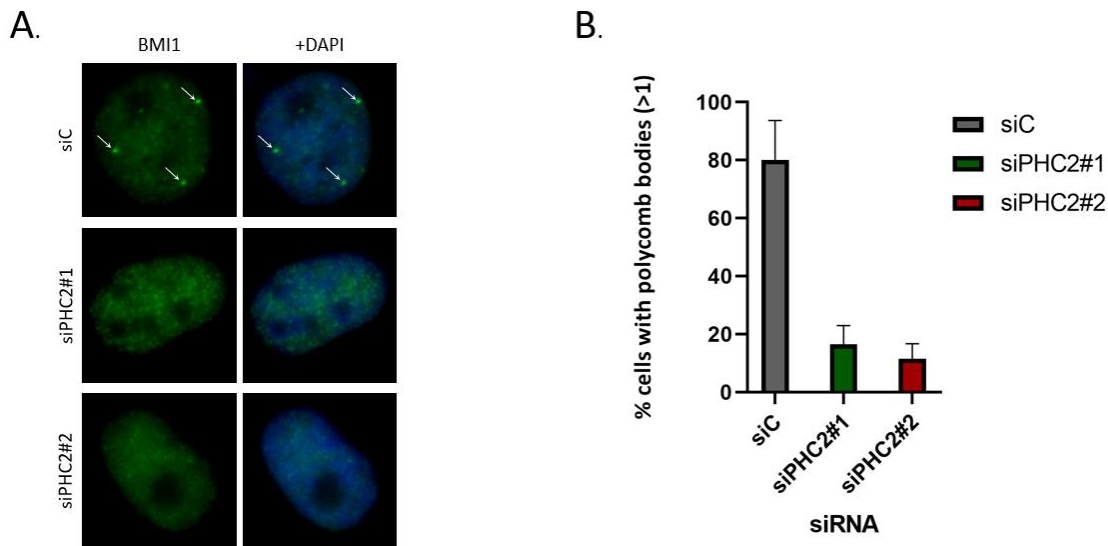


Figure 16. PHC2 depletion decreases polycomb nuclear body formation. **A.** HeLa cells were treated with indicated siRNAs (20 nM) for 72 hours, fixed and stained with anti-BMI1 antibody. **B.** Quantification of the % number of HeLa cells containing >1 polycomb nuclear body in control and knockdown HeLa cells (n=80 cells each sample).

After observing a decrease in polycomb body formation upon PHC2 depletion, we wanted to test whether this depletion would result in a decrease in BMI1 localization to damage. Our previous results have implicated that BMI1 localizes to irradiation-induced foci in cells marked by γ H2AX (Figure 15B) so therefore, we were interested in observing whether the depletion of PHC2 directly influences BMI1's propensity for colocalization with γ H2AX. To test PHC2's ability to regulate BMI1 localization to damage, we first knocked down PHC2 expression in HeLa cells using two siRNA and consequently irradiated the cells with UV damage through a micropore filter. Using immunofluorescence, we examined BMI1 foci at UV-induced lesions marked by γ H2AX. We subsequently found that depletion of PHC2 decreases BMI1 localization to the γ H2AX foci when compared to cells treated with a non-specific scramble siRNA (Figure 17). This result helped to show that BMI1 and PHC2 operate in a linear pathway where depleting BMI1's binding partner,

PHC2, decreases BMI1's localization potential to damaged chromatin. Thus, this provides an implication that perhaps the PRC1 and not solely the BMI1-RNF2 dimer is recruited to damage. As a result, we observed that PHC2 depletion both decreased polycomb body formation (Figure 16A) and decreased BMI1 localization at damaged DNA (Figure 17A) suggesting that polycomb body formation may be responsible for BMI1's observed recruitment to damage foci. However, although this evidence provides a link between the PHC2-BMI1 axis in regulating PRC1 factor recruitment, at this point it is still unclear as to the extent by which polycomb bodies or PRC1 architecture regulates Transcriptional repression flanking DSBs.

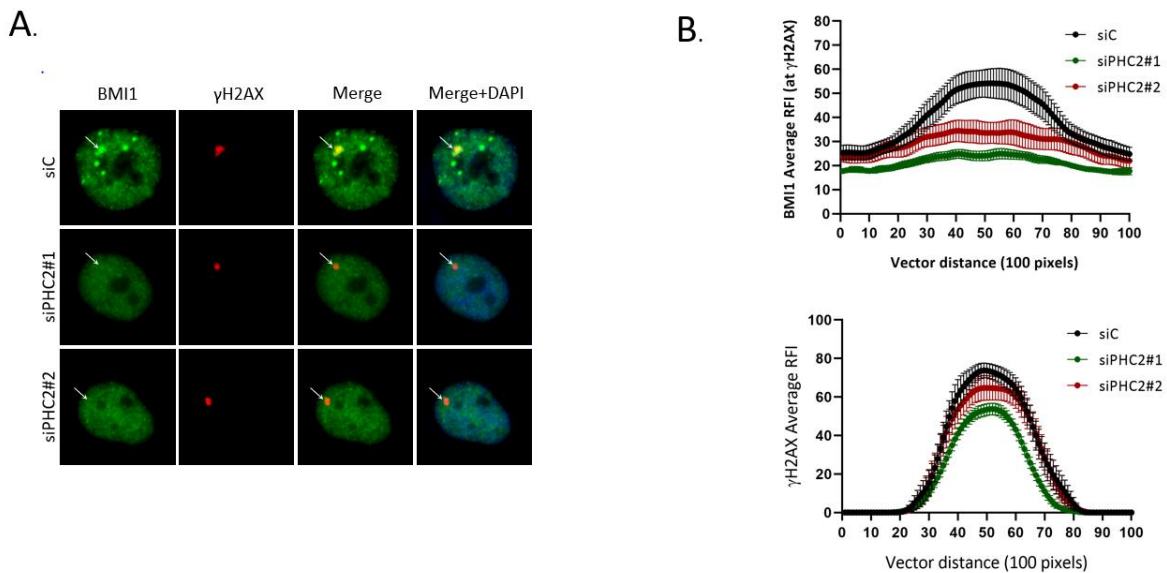


Figure 17. BMI1 localization to damaged chromatin is regulated by PHC2. A. BMI1 foci formation was induced in HeLa cells by UV-C through a 3 μ m pore filter (100 J/m²; 1 hour recovery) following the siRNA treatment (20 nM) for 72 hours. Cells were then fixed and co-stained with anti-BMI1 and anti- γ H2AX antibodies. B. (*Top*) Quantification of the average RFI of BMI1 along a vector of 100 pixels across the γ H2AX spot (n=20 each). Values were normalized to undamaged spots and error bars are indicated. (*Bottom*) Quantification of the average RFI of each γ H2AX spot. Error bars are indicated (n=20 each spot).

PHC2's SAM-Domain Controls Polycomb Body Formation and Contributes to Transcriptional Repression Flanking DSBs

Thus, we specifically wanted to address the notion that PHC2 may regulate PRC1 stability through polycomb body formation and investigate its transcriptional repressive activities specifically in response to damage. As previously discussed, PHC2 contains an essential C-terminal SAM domain. This SAM domain is a conserved domain among eukaryotic organisms with a specific structure containing a five alpha-helices bundle [29, 30, 109]. This is unique because the structure allows for binding between individual SAM domain-containing proteins [29, 30, 102, 109-111]. Furthermore, the increased potential in binding between SAM domain proteins allows for extended polymer formation. In the case of PHC2, its SAM domain facilitates binding between separate PHC2 proteins allowing for increased polymerization of PHC2 [30, 31, 109, 110]. However, PHC2 also largely exists in the PRC1 and is also bound to BMI1 through an interaction with its N-terminal homology domain 1 (HD1) and BMI1's RAWUL (Ring Associated WDR48 Ubiquitin Like) domain [24]. On PHC2's C-terminus, the SAM domain polymerizes multiple PRC1 subunits together and by doing so, this creates a positive feedback where an increase in PRC1 oligomerization further enhances its deposition and binding onto chromatin [31]. The increase in polymerization is suggested to be the culprit behind the nuclear body formation of polycomb bodies [31]. Additionally, the polymerization is suggested to further increase PRC1's transcriptional repressive capacity at target genomic loci. With our most recent phenotypes and results, we aimed to test whether this PRC1 polymerization mechanism with polycomb body formation could be a means by which PRC1 proteins BMI1 and RNF2 have been shown to be involved in transcriptional repression at damage [78, 105]. To address this potential mechanism, we

wanted to first develop a specific point-mutation that could disrupt PHC2's SAM domain interactions. Based on the literature, we found a critical point mutation that was previously identified to disrupt the SAM domain binding in PHC2's second isoform (PHC2_b) at the 307 amino acid residue [29-31]. At this location in the SAM domain resides a small non-polar leucine residue on the 5th -helices of the 5-helices SAM domain. This residue was previously shown to form a hydrophobic interface with another nonpolar residues on the 3rd -helices of a separate PHC2-SAM domain. By introducing a bulky acidic arginine residue at this location, the hydrophobic interactions are disrupted and effectively inhibits PHC2-SAM domain binding (Figure 18) [29-31]. The disrupted binding further prevents polymerization and is suggested to be critical for PRC1-mediated transcriptional repression [31]. Thus, we chose to introduce the L307R point-mutation into a wild-type PHC2 protein. We first cloned wild-type PHC2_b from a cDNA library into a mammalian pBABE-puro overexpression vector with a FLAG tag (refer to Chapter 3: Methodology, Figure 9). This method was chosen because the FLAG tag is a relatively small affinity tag used to mitigate the likelihood of altering protein secondary structure. Secondly, the pBABE-puro vector is suitable for both transient transfections and potential stable cell-line creations. After creating the pBABE-PHC2 wild-type vector, we used site-directed mutagenesis to introduce the L307R point-mutation in the pBABE-PHC2 wild-type backbone (refer to Chapter 3: Methodology, Figure 9). After doing so, we confirmed that when transiently transfected in mammalian cells, protein expression is equal among each construct (Figure 9).

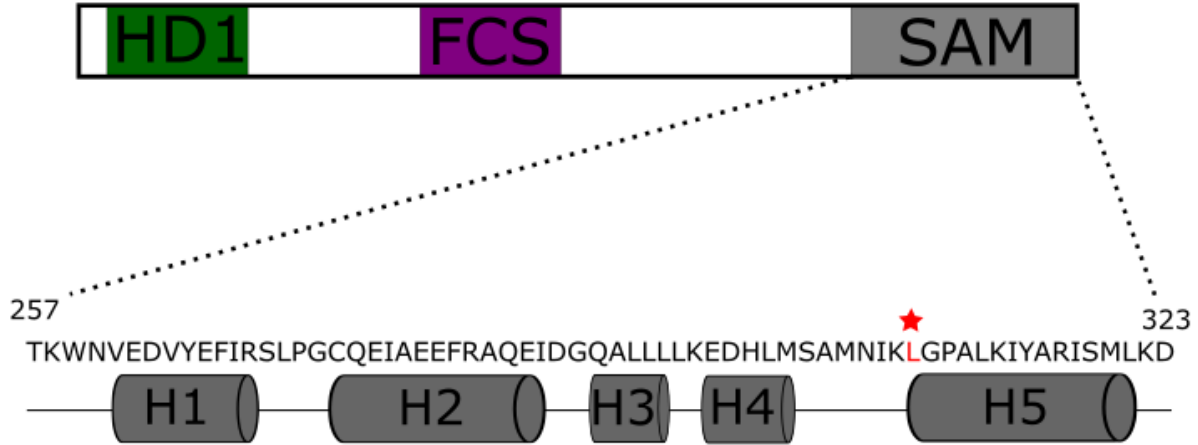


Figure 18. Schematic of PHC2-SAM domain. The PHC2-SAM domain in PHC2_b stretches from amino acids 257-323 on the C-terminus. A critical residue (indicated with a red star) is positioned at the beginning of the end-helix (H5). Hydrophobic interactions occur between the leucine of H5 and the stretch of apolar residues on the mid-loop (H3) of a separate PHC2 protein. Further disruption of the end-helix and mid-loop interaction disassociates PHC2-PHC2 interactions further inhibiting oligomerization of PRC1.

To investigate previously associated phenotypes with the PHC2-L307R mutant, we transiently transfected either PHC2 wild-type or PHC2 L307R into HeLa cells with an empty pBABE vector as a control. After transfection, we then used immunofluorescence using both an anti-FLAG and anti-BMI1 antibody. The goal was to observe whether transiently expressing the L307R mutant would eliminate polycomb body formation compared to the wild type. We observed that overexpression of the pBABE-FLAG-PHC2 wild-type vector enhanced polycomb body formation as evident by the identical visualization when stained with both the anti-FLAG and anti-BMI1 antibodies indicating that these nuclear bodies are indeed structures formed from polycomb proteins (Figure 19). Conversely, overexpression of the pBABE-FLAG-PHC2 L307R mutant eliminated polycomb body formation which was indicated by the lack of nuclear body formation in positively transfected cells (Figure 19). This result further mimicked the phenotype observed in PHC2 depleted HeLa cells when stained with anti-BMI1 (Figure 16A). Additionally, based on the

point-mutation of the pBABE-FLAG-PHC2 L307R construct, the decrease in polycomb body formation should be independent of the binding between PHC2 and BMI1.

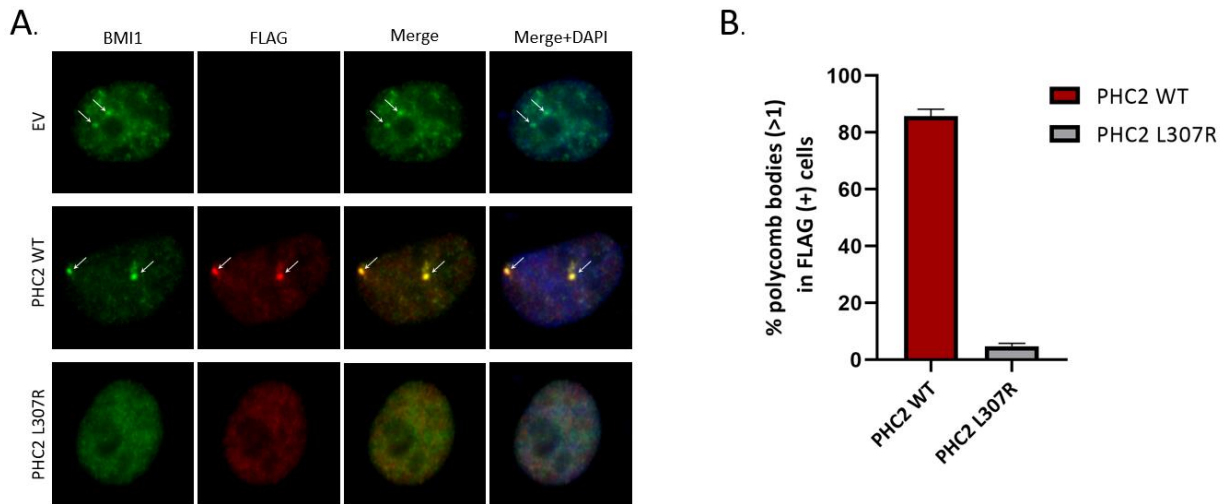


Figure 19. Overexpression of wild-type PHC2 enhances polycomb nuclear body formation while the L307R mutant diminishes formation **A.** HeLa cells were transiently transfected and overexpressed with indicated cDNA for 24 hours, fixed, and costained with anti-BMI1 and anti-FLAG antibodies. **B.** Flag positive cells were counted (n=20 each sample) and the percentage cells with polycomb bodies in the FLAG positive population were quantified. The EV (empty vector) vehicle control was used as a negative control for quantifying FLAG positive signal.

To further show that binding between PHC2 and BMI1 was not disrupted with BMI1 between the wild-type and mutant, we used an immunoprecipitation assay to confirm the binding. We first used HEK293T cells due to their high cell density and capabilities for expression of exogenously expressed proteins. We transiently transfected either the pBABE-FLAG-PHC2 wild-type or the pBABE-FLAG-PHC2 L307R constructs with a pBABE-empty vector transfection control into 293T cells. After transfection, we affinity purified the exogenously expressed constructs on FLAG-conjugated agarose beads (Thermo Scientific). As predicted, we found that expression of the pBABE-FLAG-PHC2 L307R mutant did not disrupt the binding between BMI1 when compared to the pBABE-FLAG-PHC2 wild-type (Figure 20). Thusly, this further aided in the

notion that the SAM-domain mutant decreases polycomb body formation independent of binding with BMI1 and further implicated the L307R mutation as a critical residue essential for polycomb body formation. Now that we had established that the L307R mutant construct could disrupt polycomb bodies and PRC1 polymerization while still maintaining binding with BMI1, we wanted to determine whether this mutation had implications in gene repression mechanisms at DSBs

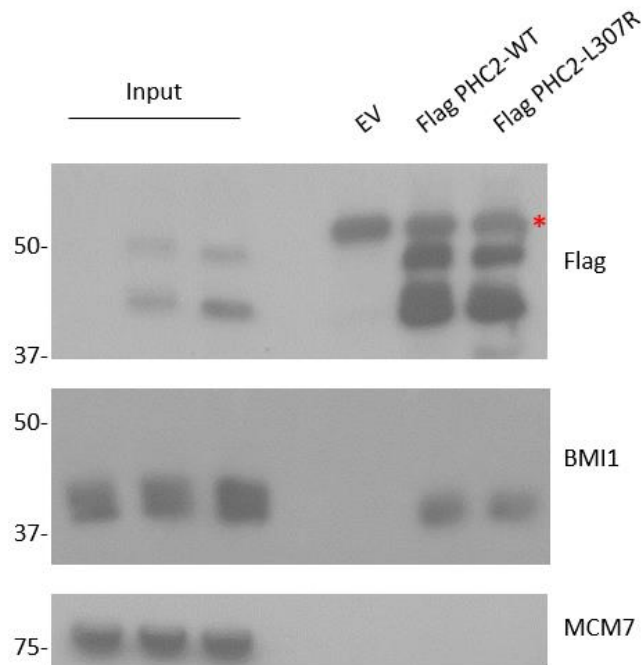


Figure 20. Overexpression of the PHC2 L307R mutant does not affect BMI1 binding. 293T cells were transiently transfected with either a pBABE-FLAG-PHC2-WT, pBABE-FLAG-PHC2-L307R, or empty pBABE vector vehicle control. 24 hours after transfection, 293T cells were harvested, lysed, and immunoprecipitated with anti-FLAG agarose beads. The beads were washed and subjected to SDS-PAGE (refer to methods) and immunoblotted with anti-FLAG, anti-BMI1 antibodies, and anti-MCM7 antibodies (washing control). Red star indicates non-specific IgG heavy chain.

Given our previous results that PHC2 depletion causes transcriptional derepression at DSBs in the Ptuner263 cell line (Figure 13B), we aimed to performed reconstitution rescue analysis with the L307R mutant. If polycomb bodies were essential for transcriptional repression

at DSBs, then reconstitution of PHC2 wild type protein would rescue the transcriptional derepression while introducing the L307R mutant would fail to do so. To test this, we used 3' untranslated region (UTR) targeting siRNA against PHC2 to selectively knockdown endogenous PHC2 protein levels. Otherwise, an siRNA targeting the coding region would also knockdown the protein expression from the exogenous plasmid. After knockdown with the 3' UTR siRNA, we transiently transfected either the pBABE-PHC2 wild type or pBABE-PHC2 L307R plasmids with an empty vector control. We observed that in Ptuner263 samples transiently transfected with wild-type PHC2, transcriptional repression was restored at the fok1 DSB marker (Figure 21). However, in the Ptuner263 cells transiently transfected with the PHC2 L307R mutant, we saw transcriptional derepression at the fok1 DSB marker indicating that the mutant was unable to restore transcriptional repression at the DSB site (Figure 21). As a result, this helped to provide a role for polycomb-mediated gene silencing at the DSB dependent upon PRC1 polycomb body formation. This suggests that PRC1 architecture dependent upon PHC2 regulates its ability to facilitate gene silencing flanking DSBs.

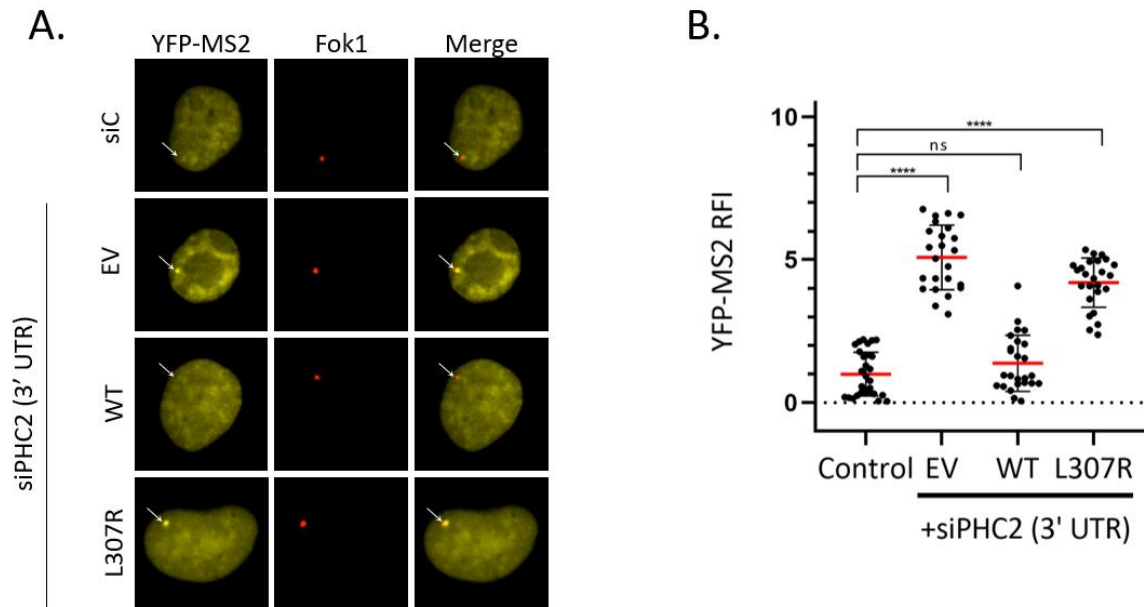


Figure 21. Reconstitution of PHC2 wild type but not PHC2 L307R mutant can rescue the transcription repressive phenotype. A. The ptuner263 cells transiently transfected with indicated PHC2 constructs (EV=empty vector) were transfected with 3' UTR targeting siRNA against PHC2 also treated with 4-OHT, shield-1, and tetracycline for 3 hours prior to fixing. B. Quantification of the YFP-MS2 RFI (refer to methods) at the fok1 spot in each condition (**** indicates P-value <0.0005). The assay was performed in triplicates (N=30).

Conclusions and Future Directions

Thus far, our work has identified a novel function for PHC2 in transcriptional repression at DSBs. We first wanted to address the extent to which PRC1, and associated polycomb proteins can repress transcription at damaged DNA. The literature has extensively implicated the BMI1-RNF2 dimer and its ubiquitin catalytic activity in mediating transcriptional repression. However, whether other PRC1 components cooperate in polycomb body formation are not addressed. As a result, we initially hypothesized that the BMI1-RNF2 dimer was specifically responsible for transcriptional repression at damage. To our surprise, we showed that PHC2 depletion contributes to transcriptional derepression at induced DSBs. Additionally, we observed that PHC2 ablation contributes to transcriptional misregulation at sites of DNA damaged induced by UV-C

radiation. These results phenocopy the transcriptional derepression phenotype previously attributed to BMI1 and RNF2. As a result, this further implicates that PHC2 can contribute to transcriptional repression at damaged DNA foci whereas previous evidence had solely focused primarily on BMI1 and RNF2. We further show that PHC2 localizes to sites of DNA damage along with BMI1 suggesting that the transcriptional repressive phenotypes are a result of a concerted effort of PRC1 proteins to promote transcriptional repression *in cis* to sites of DNA damage. Furthermore, to address whether the associated transcriptional repression phenotypes function in a linear pathway between PHC2 and BMI1, we showed that BMI1 localization to damage is ablated in PHC2 depleted cells. As a result, this work implicates that PHC2 cooperates with BMI1 in the PRC1 to suppress local transcriptional elongation in response to damage which is a novel function of PHC2.

However, it was unclear as to the precise mechanism by which PHC2 could contribute to transcriptional repression in the PRC1 at damaged chromatin. One of the most well-known phenotypes of PHC2 is its role in polycomb nuclear body formation and PRC1 architecture maintenance at developmental loci [31]. As a result, we then hypothesized that PHC2 may be essential in maintaining PRC1 architecture and promoting polycomb domains at sites of damage. However, thus far our previous phenotypes suggest that PHC2 contributes to gene silencing at damaged DNA, but it was unclear to the extent by which PRC1 architecture and polycomb body formation serves in this pathway. For example, we showed that PHC2 depletion decreases both polycomb body formation and BMI1 accumulation at damaged chromatin (Figure 17A). A possible explanation is that PHC2 depletion prevents proper PRC1 formation preventing the PRC1 oligomerization polycomb body formation. However, how might this specifically affect BMI1 foci

formation at the damaged chromatin spot? Is BMI1 still recruited but cannot form foci due to lack of PHC2? As a result, we introduced a PHC2 SAM domain mutant to address whether PRC1 oligomerization is essential in maintaining this transcriptional repressive phenotype. We found that overexpression of the PHC2 SAM domain mutant decreased polycomb body formation in positively transfected cells while not affecting binding with its partner, BMI1 (Figure 20). This suggested that the PHC2 SAM domain mutant destabilizes PRC1 polymerization rather than degrading individual PRC1 complexes. Furthermore, we found that reconstitution of a wild-type PHC2 cDNA was able to rescue the transcriptional derepression phenotype while reconstitution of PHC2 SAM domain mutant cDNA failed to rescue the phenotype (Figure 21). Overall, this suggested that PRC1 polymerization mediated by PHC2 for transcriptional repression at sites of DNA damage is essential. Our interpretation of this result is that PRC1 may still be recruited to the site of damage, but without PRC1 polymerization through PHC2's SAM domain, gene silencing is hindered. However, what is still unclear is if the BMI1-RNF2 heterodimer is first recruited to the DSB and then PHC2 binds to enhance the polymerization. Further architectural studies will be needed to identify whether PRC1 including PHC2 is recruited to the damage site or if the BMI1-RNF2 heterodimer is recruited first in a linear recruitment pathway.

A caveat to these findings, however, is that the associated phenotypes we have seen have been with an overexpression of PHC2 wild-type and the PHC2 SAM domain mutant compared to endogenous PHC2 levels. As a result, the overexpression of the constructs may contribute to these phenotypes. To address this concern, we sought to create a homozygous knock-in cell line to contain the L307R mutation with endogenous levels of protein expression. Thus, we commissioned the development of several knock-ins in the HCT116 cell line through Genomic

Engineering and iPSC Center at Washington University in St. Louis. We chose the HCT116 cell line because it is a near-diploid colon colorectal cell line useful for observing chromosomal aberrations in the presence genomic stressors Sequencing analysis confirmed the incorporation of the appropriate mutation in both PHC2 alleles in the HCT116 cell line (Figure 22). Additionally, an out-of-frame clone was generated to potentially decrease protein function (Figure 22). We then confirmed equal protein expression between each knock-in cell line compared to the wild-type and observed depletion of PHC2 in the out-of-frame clone (Figure 23A). To confirm that the L307R homozygous genotype disrupted polycomb body formation, we used immunofluorescence to detect polycomb body formation in the knock-ins. Consistently, we found that the knock-in cell lines indeed depleted polycomb body formation as well as the out-of-frame clone (Figure 23B). Next, we wanted to test whether the PHC2 L307R mutation introduced in the HCT116 cells could regulate gene silencing at DSBs. To test this, we treated cells the wild-type HCT116 cells, the L307R homozygous knock-in cells, and the PHC2-out-of-frame clones with the anticlastogenic agent bleomycin to induce DSBs. We found the introduction of the L307R mutations caused misregulation of transcription at the DSB (Supplemental Figure 1) suggesting that polycomb bodies are needed to properly silence genes at DSBs. Additionally, we wanted to test whether the introduction of the L307R mutant could possibly contribute to an increase in endogenous DSB formation or replication stress due to inhibition of gene silencing. To do so, we stained the HCT116 wild-type cells and L307R knock-ins with a γ H2AX antibody to measure an observable increase in endogenous DNA damage (Supplemental Figure 2A). We found that in the L307R knock-in cells, there was a marketable an increase in γ H2AX formation (Supplemental Figure 2B). Also, when we stained both the HCT116 wild-type cells and the L307R knock-ins, we found an

increase in p-RPA32 foci which is a marker for replication stress (Supplemental figure 3A). Taken together, these results reveal that the PHC2 L307R mutation may threaten genomic stability and cellular homeostasis. However, at this point, it is unclear to what extent PHC2 can contribute to chromosomal aberrations and repair defects contributing to genomic stability. Thus, further studies should be performed to address whether the PHC2 SAM domain mutant or PHC2 depletion can contribute to chromosomal aberrations and repair defects which have also been implicated with BMI1 depletion.

HCT116 Wild-type	Allele #1: CACCTGATGAGCGCCATGAACATCAAGCTGGGGCCCGCCCTGAAGATCTACGCCCGCATCAGCATGCTCAAGGACTCC Allele #2: CACCTGATGAGCGCCATGAACATCAAGCTGGGGCCCGCCCTGAAGATCTACGCCCGCATCAGCATGCTCAAGGACTCC	
1B8 L307R KI #1	Allele #1: CACCTGATGAGCGCCATGAACATCAAGAGAGGGGGCCCGCCCTGAAGATCTACGCCCGCATCAGCATGCTCAAGGACTCC Allele #2: CACCTGATGAGCGCCATGAACATCAAGAGAGGGGGCCCGCCCTGAAGATCTACGCCCGCATCAGCATGCTCAAGGACTCC	CTG>AGA
1E6 L307R KI #2	Allele #1: CACCTGATGAGCGCCATGAACATCAAGAGAGGGGGCCCGCCCTGAAGATCTACGCCCGCATCAGCATGCTCAAGGACTCC Allele #2: CACCTGATGAGCGCCATGAACATCAAGAGAGGGGGCCCGCCCTGAAGATCTACGCCCGCATCAGCATGCTCAAGGACTCC	CTG>AGA
1B11 Out-Of-Frame	Allele #1: CACCTGATGAGCGCCATGAACATCAAGGATGAGCGCCATGAA-TGGGGCCCGCCCTGAAGATCTACGCCCGCATCAGCATGCTCAAGGACTCC Allele #2: CACCTGATGAGCGCCATGAACATCAAGGATGAGCGCCATGAA-TGGGGCCCGCCCTGAAGATCTACGCCCGCATCAGCATGCTCAAGGACTCC	15 bp insertion and 1 bp deletion

Figure 22. Sequencing information for PHC2 knock-in cell lines. Genomic sequencing confirms the HCT116 PHC2 L307R knock-in (KI) clones (1B8 and 1E6) are homozygous for the mutation. Additionally, in the 1B11 clone, there is a 14 base pair insertion and 1 bp deletion in both alleles for a homozygous out-of-frame clone.

Additionally, the relationship between the PHC2-containing PRC1 and the DNA damage kinase ATM has yet to be fully elucidated. ATM is a key regulator in facilitating transcriptional repression *in cis* to DSBs as previously shown by Shanbhag et al. (2010). Additionally, the transcriptional elongation factor, ENL, has been implicated in an ATM-dependent pathway with BMI1 in transcriptional repression at DSBS [80]. However, this study further implicated an interaction between ENL and BMI1 in ubiquitinating H2A to repress transcription. Furthermore,

further studies would need to be performed to implicate the extent by which the PHC2-containing PRC1 may contribute to gene repression in an ATM-dependent manner.

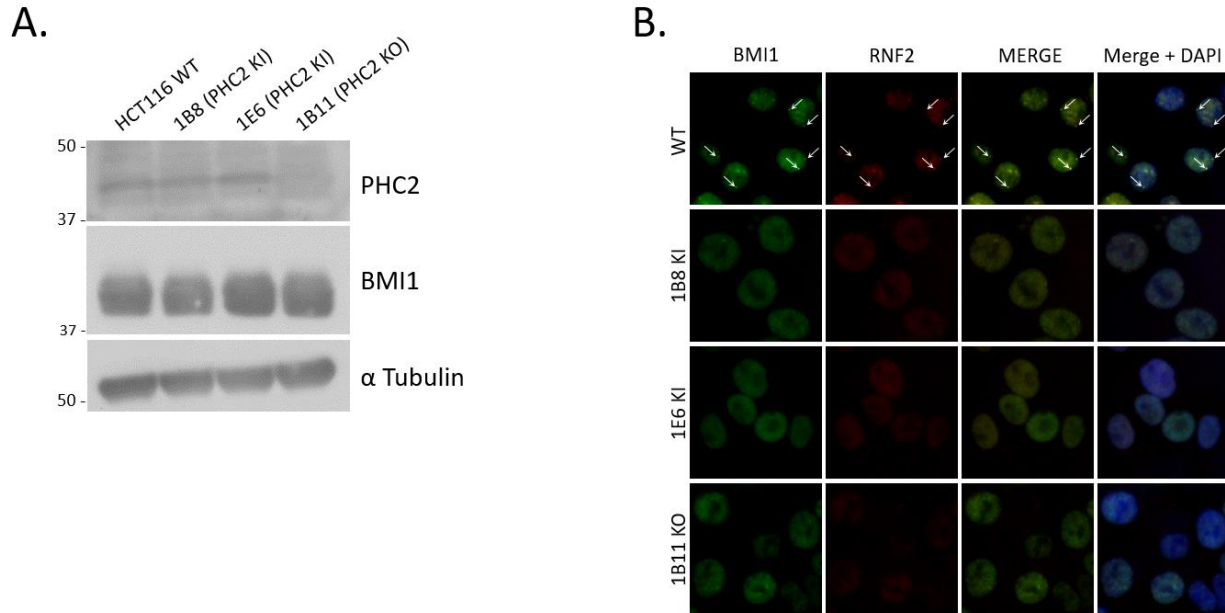


Figure 23. The L307R homozygous mutation depletes polycomb body formation in HCT116 cells. A. Western blot confirmation of equal PHC2 expression between each knock-in (KI) clones (1B8 and 1E6). The out-of-frame clone 1B11 resulted in undetectable PHC2 protein levels. B. HCT116 cells were co-stained with anti-BMI1 and anti-RNF2 antibodies for immunofluorescence. The 1B8 and 1E6 KI clones ablated polycomb body formation as well as the 1B11 out-of-frame clone.

Further evidence is needed to link a mechanism by which polycomb bodies and genomic organization may contribute to transcriptional repression at damage. For instance, it is unclear whether the polycomb proteins are actively being recruited to the damage or whether the damaged chromatin is being mobilized to a polycomb domain to facilitate repression. Given that polycomb bodies form stable contacts at defined genomic loci [31], it is plausible to suggest that the three-dimensional chromosomal organization may contribute to transcriptional repression in response to damage. It is also unclear to what extent damaged DNA, specifically DSBs, interact with specific nuclear locations to facilitate repair and promote gene silencing. Previous evidence in yeast has implicated the DSB mobilization to the nuclear periphery [97], but the notion of DSB

mobility in mammalian cells is currently under debate [100]. Furthermore, it is unclear to the extent by which contacts with the PHC2-containing PRC1 and DSB mobility at the nuclear periphery play in gene silencing at DSBs. Additional evidence regarding transcription regulated by PRC1 and nuclear periphery components will be discussed further in Chapter 5.

Chapter Five: Elucidating the Dynamics of Transcriptional Repression at DSBs Through
Interactions with Nuclear Pore Complex Proteins

Nuclear Pore Y-complex Proteins contribute to transcriptional repression at DSBs

A previous study has shown that polycomb protein homologs in *D. melanogaster* are implicated in transcription dynamics at the NPC [44]. It was suggested that interactions occur between a subset of polycomb targeted genomic locations and the NPC in regulating gene regulatory processes. Taken together, transcriptional dynamics were evaluated with two core components of the NPC, NUP107 and NUP93, where the former was suggested to regulate transcription of active genes while the latter is associated with polycomb target genes [44]. Furthermore, it is unclear why an interaction between polycomb proteins and the NPC is necessary for gene silencing. It is tempting to speculate that the 3-dimensional chromosomal organization influences an interaction in which specific polycomb-targeted genes localized in proximity to the NPC provide a scaffolding mechanism to mediate transcriptional repression. The dynamics of the interaction between the NPC and polycomb proteins has not been extensively pursued in human cells, so pursuing this concept would provide novelty in understanding PRC1-dependent gene silencing mechanisms. We then sought to address whether a polycomb-mediated transcriptional repression mechanism exists in human cells that would occur at the NPC in response to damage.

Thus far, our recent phenotypes of transcriptional repression mediated by the PHC2-containing PRC1 suggests a polycomb-body dependent mechanism. However, it is still unclear exactly how PRC1 and polycomb bodies recognize damaged chromatin for repair. We hypothesize that polycomb bodies may provide a local environment conducive to transcriptional repression, but it is unclear whether PRC1 is actively recruited to the site of damage or if the damaged chromatin is mobilized to PRC1-inclusive polycomb bodies to facilitate transcriptional repression at damage. As a result, we first sought to independently characterize any potential interaction between NPC-containing proteins and PRC1 using proteomic analysis. We pursued a mass spectrometry based proteomic analysis to observe all possible potential interactions between PHC2 and NPC proteins. We performed immunoprecipitation with samples containing a FLAG-tagged PHC2 and subjected eluates to mass spectrometry to analyze the proteomic landscape of proteins bound to PHC2. Three separate samples were submitted with two samples treated with formaldehyde to crosslink proteins to DNA. By doing so, we could also identify indirectly interacting proteins through DNA binding. After immunoprecipitation, we proceeded with western blot to confirm successful transfection and immunoprecipitation (Figure 24B). As an indicator for successful immunoprecipitation we used an anti-BMI1 antibody to identify interaction with PHC2 after pulldown (Figure 24B). After confirmation, we submitted samples to the proteomic core facility at Moffitt Cancer Research Center and found that canonical PRC1 proteins: BMI1, RNF2, and CBX4 were preferentially bound in all three immunoprecipitation samples (Figure 24C). Given these proteins are canonical binding partners with PHC2, it is useful information in evaluating the efficiency of the pulldown. Interestingly, we found several nucleoporins corresponding to specific NPC sub-complexes. For example, we found several Y-

complex nucleoporins: 43, 85, 107, 133, and 160 which makes up the nucleoplasmic and cytoplasmic ring structure [40]. Additionally, nucleoporins 37 and 93 which make up the inner ring also showed up in the mass spectrometry results (Figure 24C). Moreover, we found other factors of interest including the cohesin-SA2 complex, several DSB factors, and proteins involved in resolving replication stress. Meisenberg et al. (2019) showed that the cohesin-SA2 complex is integral for mediating transcriptional at DSBs and preventing chromosomal translocations. The implications of this will be discussed later, as we continued to focus on the potential interaction between PRC1 and the NPC.

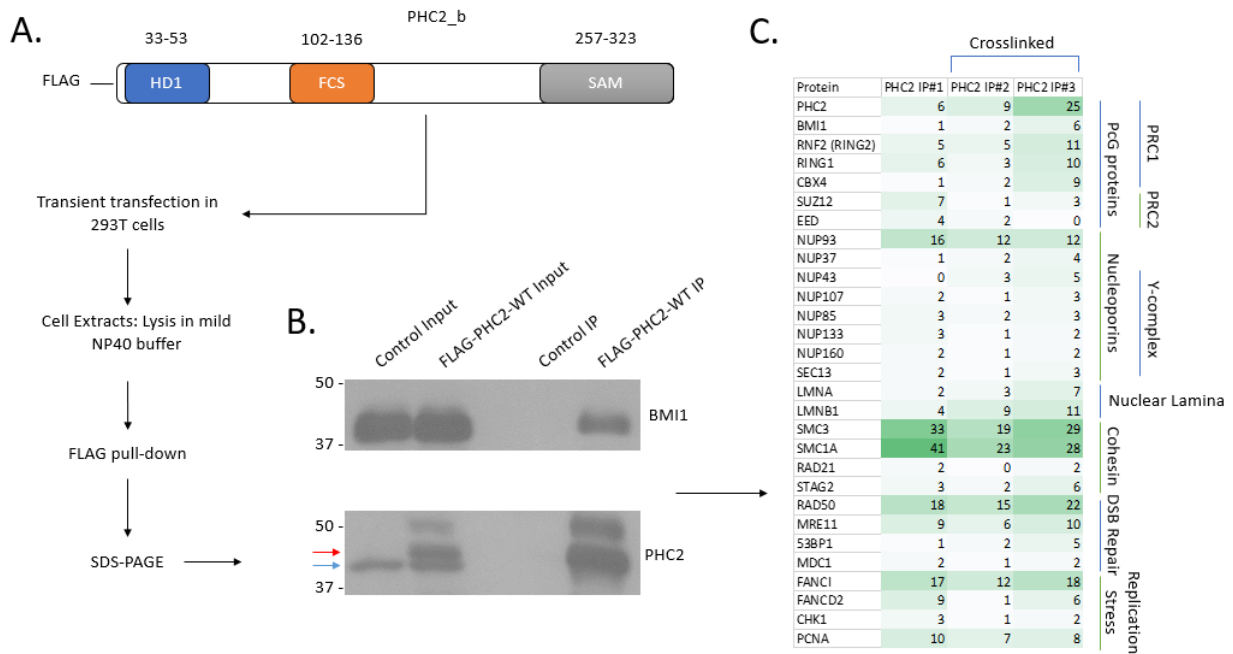


Figure 24. Workflow for immunoprecipitation mass spectrometry analysis. A. HEK293T cells were transiently transfected with a pBABE-FLAG-PHC2 plasmid harboring the isoform b cDNA. 24 hours post transfection, cells were lysed and immunoprecipitated with FLAG M2 agarose beads (refer to methods) and processed with SDS-PAGE to confirm expression and successful immunoprecipitation B. Confirmation of successful immunoprecipitation via western blot (Red arrow indicates exogenously expressed protein while blue arrow indicates endogenous protein). C. Mass spectrometry results obtained from submission of 3 samples where two indicated samples were crosslinked with formaldehyde prior to lysis. Numbers in each column represent the number of unique peptides found in each sample corresponding to the designated protein.

As a result, because we found several nucleoporins corresponding to distinct sub-complexes, we wanted to separately evaluate each of the nucleoporin's in a context of DSB-induced gene silencing. Although it had been previously suggested that NUP93 interacts with polycomb proteins to promote gene silencing while NUP107 contributes to gene activation [44], we found both proteins present in the mass spectrometry results. Therefore, it is unclear to the extent that the nucleoporins play in interacting with PRC1 to potentially lead to gene silencing. As a result, we wanted to first independently evaluate each nucleoporin's propensity to promote gene silencing in response to DNA damage. We thus pursued a screen of the NUPs using the Ptuner263 cell line to identify which NUPs function in transcriptional repression at DSBs. We treated Ptuner263 cells with siRNA targeting each NUP and evaluated whether knockdown of each nucleoporin would contribute to transcriptional derepression at the DSB further indicating an involvement in gene silencing in response to induced damage. In the screen we found that Y-complex associated NUPs (43, 85, 107, 133) contributed to transcriptional derepression at the DSB while the inner ring member NUPs (37, 93) did not show a phenotype (Figure 25). Additionally, we found that LMNA, NUP98, and NUP153 also contributed to the transcriptional derepression phenotype while other NUPs (50 and 88) did not show any significant phenotype (Figure 25). What we found to be particularly interesting is that the NUPs that displayed a phenotype were associated with Y-complex NUPs. NUPs 43, 85, 107, and 133 are core components of the scaffolding Y-complex that makes up a portion of the NPC [41]. Additionally, NUP153 had been shown to be integral for recruitment of the Y-complex to the inner nuclear membrane for NPC assembly [51]. Also, NUP98 had been shown contribute to gene regulation through a dynamic nuclear localization away from the NPC [49]. In turn, a fraction of NUP107

protein, a key Y-complex factor, associates in the nucleoplasm with NUP98 in a previously uncategorized function of NUP107 [49]. As a result, there appeared to be a clear association between Y-complex associated NUPs and transcriptional repression at DSBs. Conversely, NUPs that are not associated with the Y-complex (93, 37, 50, and 88) did not show a transcriptional repressive phenotype at DSBs (Figure 25). LMNA also showed a phenotype which was interesting, but it is unclear whether this phenotype is associated with NUPs or through a different mechanism. The potential implications of LMNA in this observed phenotype will also be addressed in a later section as we decided to pursue the potential function of NPC-associated proteins in gene silencing at DSBs. Additionally, it remains to be clear as the relative location of the gene silencing activity observed by the Y-complex nucleoporins. Because nucleoporins are canonically known to be associated with the NPC, it can be inferred that the gene silencing activity at the DSB occurs at the NPC. However, several nucleoporins have also shown to function away from the NPC [49]. This possibly suggests that the observed phenotype of transcriptional repression at the DSB could be mediated within the nucleoplasm as an “off-pore” function of the nucleoporins. Thus, we further aimed to determine if the observed phenotype of gene silencing by the Y-complex nucleoporins at the DSB could be occurring at the NPC or “off-pore.” Furthermore, we wanted to address whether the DSB showed signs of movement or relocalization within the nucleus to facilitate gene silencing at the break.

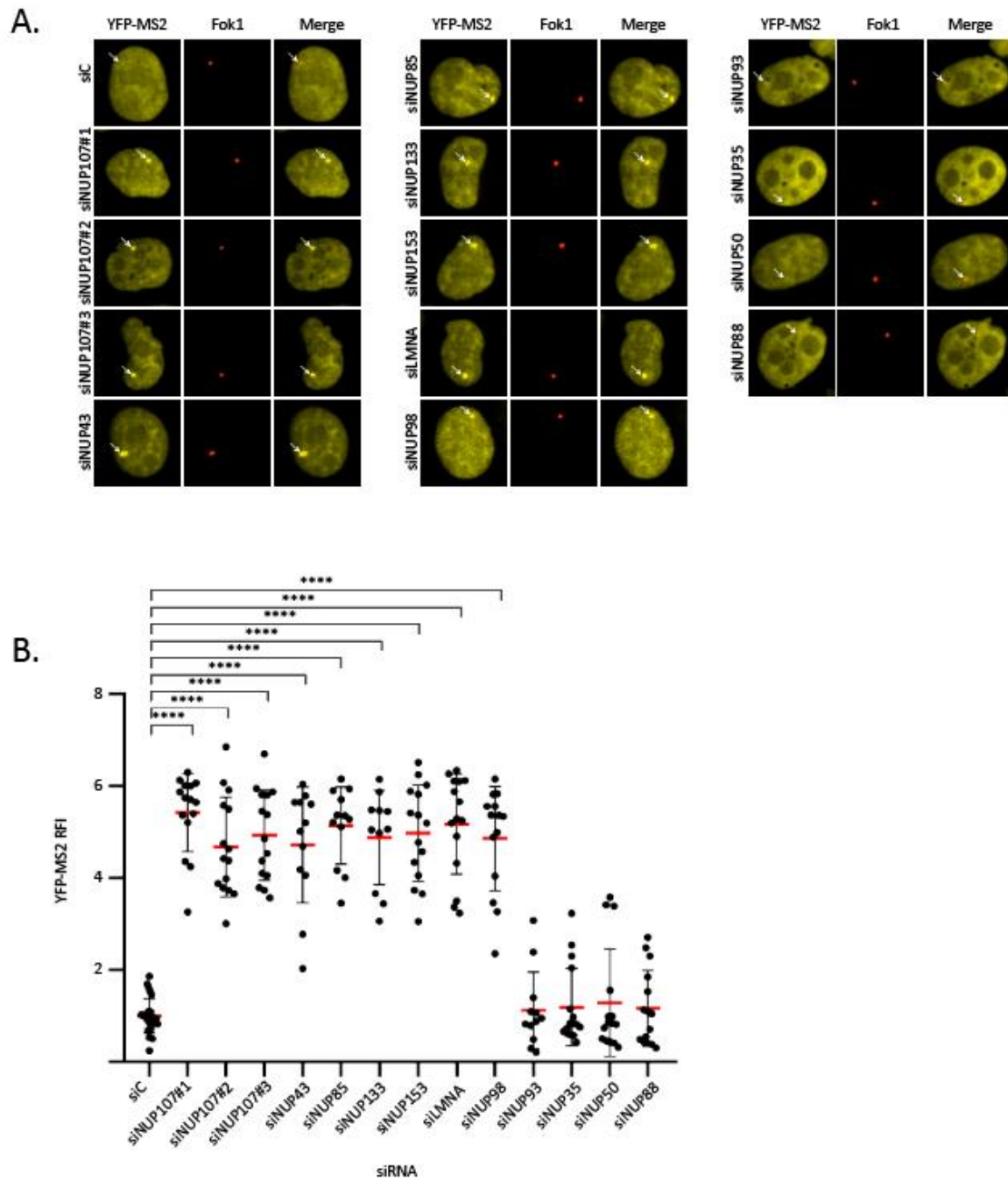


Figure 25. Screen of NUPs that contribute to transcriptional repression at DSBs. A. Ptuner263 cells were transfected with the indicated siRNAs (20 nM) for 72 hours and treated with tetracycline and 4-OHT/Shield-1 (3 hours) to induce both YFP-MS2 transcription and Fok1, respectively. C. Quantification of the YFP-MS2 RFI compared to the control condition at the Fok1 spot. The YFP-MS2 RFI (refer to methods) was quantified using ImageJ (N=15, **** indicates P-value <0.0005).

NUP107 Forms Nucleoplasmic Foci and Localizes to DSBs

We decided to focus on the nucleoporin Y-complex for several reasons. First our mass spectrometry results suggest that there is an interaction between PHC2 with Y-complex NUPs (Figure 23C). Based on our evidence, there appeared to be a connection between Y-complex associated NUPs and transcriptional repression at DSBs (Figure 24). PRC1-containing proteins also show a similar phenotype which suggests a possible interactive relationship between PRC1 and the Y-complex NUPs in repressing transcription at DSBs. Furthermore, the Y-complex factor NUP107 (Nup84 in yeast) has been previously implicated in the DDR [96-98, 104]. In yeast, persistent or “difficult to repair” DSBs relocate to the nuclear periphery through an interaction with Nup84 [96]. Through this interaction, DSBs can undergo repair at the nuclear periphery to avoid mutagenesis at these persistent DNA lesions. However, this DSB relocalization to the nuclear periphery at persistent DSBs dependent upon NUP107 has not been fully elucidated in mammalian cells. Currently, there is debate over whether DSBs remain immobilized for repair or if they display propensity for mobilization [99, 100]. In mammalian cells, several NUPs, including NUP107, are associated within the nucleoplasm in addition to the nuclear envelope further adding to the complexity in understanding how NUPs function in transcription dynamics and DSB repair in mammalian cells [49, 51]. As a result, we decided to elucidate a mechanism by which NUP107 mediates transcriptional repression at DSBs in relationship to its function as an NPC component.

Next, we wanted to determine the localization dynamics of NUP107 in mammalian cells. We previously showed that depletion of NUP107 derepresses transcription at a DSB (Figure 24), but it has yet to be determined if NUP107 specifically localizes to DSBs. As a result, we tested

whether NUP107 forms distinct foci at DSBs using the Ptuner263 cell line. In this manner, we specifically induced DSBs with 4-OHT and Shield-1 treatment. After induction of DSBs, we used immunofluorescence with an anti-NUP107 antibody to see if NUP107 foci was localized to the DSB. Surprisingly, we found that NUP107 forms distinct foci and localizes to the fok1 spot (Figure 26A). To ensure that the fok1 spot is indicative of a DSB, we also stained cells with an anti-53BP1 antibody which is a canonical DSB repair factor that rapidly localizes to DSBs (Figure 26B) [69]. As a result, this further suggests that NUP107 localizes to DSBs which is consistent with our previous finding that NUP107 depletion regulates transcription at DSBs. One thing that is intriguing is that NUP107 is an associated protein with the NPC, but the foci appear to be distinctly nucleoplasmic without clear staining of the nuclear periphery. One explanation for this phenomenon is that NUP107 has been previously shown to associate with the nucleoplasm in HeLa cells independent of the NPC [49]. The resulting visible foci could be the detectable cytoplasmic fraction of NUP107 proteins. However, given that this is a 2-dimensional view, it is still possible that the fok1 spot and the NUP107 foci could be in a different plane of the cell. For example, with this 2-dimensional approach, the visible NUP107 foci could still be associated with the NPC 3-dimensionally and not necessarily localized at the NPC. To address this, we pursued a 3-dimensional immunofluorescence approach to determine the location of the NUP107 foci. Furthermore, we wanted to confirm that the observed foci were co-localized in the same plane of the cell with this 3-dimensional approach.

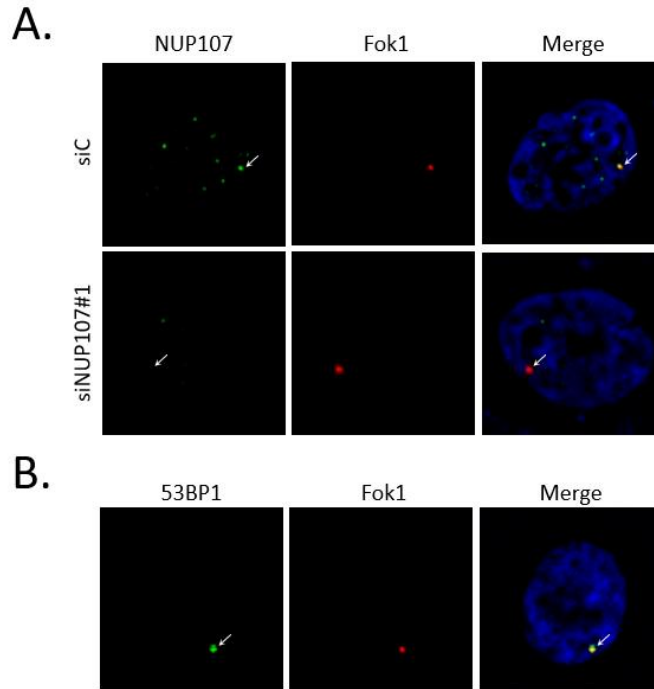


Figure 26. NUP107 forms visible foci at DSBs. A. The ptuner263 cells were treated with 4-OHT/Shield-1 for 3 hours to induce DSBs. Cells were fixed and stained with anti-NUP107 antibody and observed for foci localization at the fok1 spot. B. The ptuner263 cells were treated with 4-OHT/Shield in the same manner as in A but stained with anti-53BP1 antibody. 53BP1 localization was used as a positive control for DSB induction.

To do so, we first used an immunofluorescence approach again using the Ptuner263 cell line. Similarly, we induced DSBs by treating cells with both 4-OHT and Shield-1. We then stained the Ptuner263 cells with an anti-NUP107 antibody for immunofluorescence. However, when viewing the cells, we used a 3-dimensional deconvolution function which would take a subsequent image of the z-axis in addition to both the x-and y-axes. As a result, we were able to acquire both 2- and 3-dimensional images of NUP107 foci at the fok1 spot. Consistently, we found that NUP107 formed foci at the fok1 spot with several nucleoplasmic foci (Figure 27A). Additionally, when viewed with 3-dimensional deconvolution, the NUP107 foci inhabits the nucleoplasmic interior within the same plane of the fok1 spot (Figure 27B). This further provided evidence that NUP107 indeed localized to the DSB within the nucleoplasm. This further suggests

that at least a portion of the NUP107 population of nuclear proteins displays propensity for localization to damaged chromatin away from the NPC towards the nuclear interior. Also, this suggests that NUP107 may have serve other roles independent of its function at the NPC. On the other hand, at this point, it is still unclear to what extent NUP107 foci recruitment dynamics is stabilized at DSBs. For example, it is plausible to suggest that NUP107 may be actively recruited to DSBs to provide a tethering mechanism to the nuclear periphery given that NUP107 functions in part as a scaffold in the Y-complex at the NPC. However, further studies need to be done to elucidate a NUP107 mediated scaffolding mechanism to DSBs.

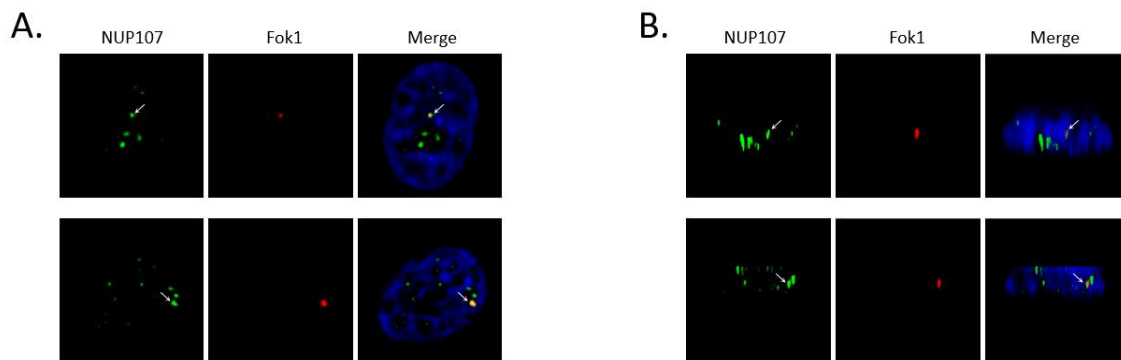


Figure 27. NUP107 localizes with DSBs in the nucleoplasm. A. The ptuner263 cells were treated with 4-OHT/Shield-1 for 3 hours to induce DSBs. Cells were fixed and stained with anti-NUP107 antibody and observed for foci localization at the fok1 spot. Images represent Fok1 localization to fok1 spots at different orientations within the nucleus. B. View of the 3-dimensional plane of the representative images in A revealing the colocalization occurs within the same plane of the nucleus.

NPC Y-Complex Proteins Regulate NUP107 Expression and Foci Formation

Next, we wanted to further understand dynamics of NUP107 localization to DSBs. Given that NUP107 binds with other NUPs in an isostoichiometric ratio to form the Y-complex [50], we wanted to test the propensity of other Y-complex member NUPs in regulating NUP107 foci at DSBs. As previously mentioned, NUPs 43, 85, and 133 are other Y-complex members in addition

to NUP107. Additionally, NUPs 98 and 153 have been implicated in interacting with NUP107 to maintain stability [49, 51]. As a result, we wanted to confirm the knockdown efficiency of the NUPs analyzed in the transcriptional repression at DSB screen. We found that depletion of NUP107's binding partner, NUP133 also reduced NUP107 expression (Figure 28). This can partially be explained by NUP107 binds with NUP133 and disruption of this stoichiometric ratio, further destabilizes the Y-complex. Additionally, we found that both NUP98 and NUP153 which are not members of the Y-complex also caused a decrease in NUP107 expression (Figure 28). A previous study by Vollmer et al. (2015), showed that NUP153 is required for proper recruitment of the Y-complex to the inner nuclear membrane. As a result, depletion of NUP153 could result in further Y-complex destabilization. However, it is unclear at this point how depletion of NUP98 might affect the expression of NUP107.

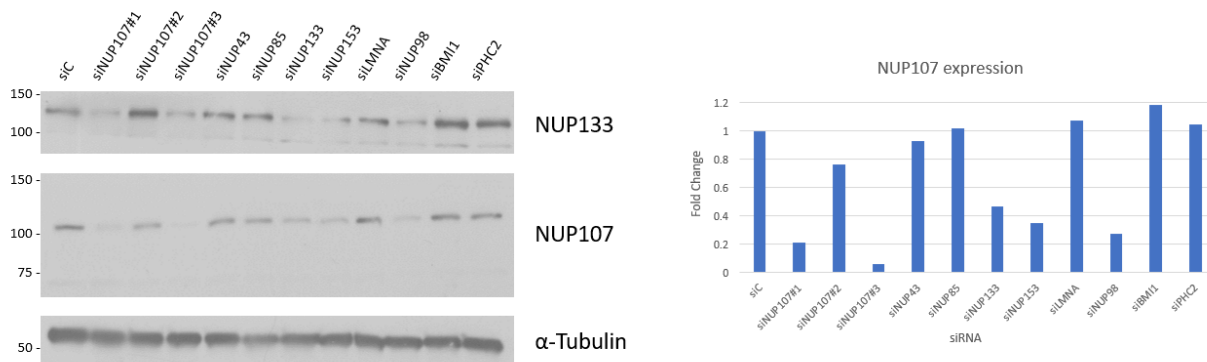


Figure 28. NUP107 expression profile after various NUPs knockdowns. A. Ptner263 cells were treated with indicated siRNA for 48-72 hours at 20 nM. Cells were lysed and subjected to SDS-PAGE and western blot analysis. Lysates were immunoblotted with anti-NUP107 antibody with α Tubulin as a control. B. Quantification of the fold change of western blot protein expression. Quantification was performed by normalizing Tubulin levels. After normalization to the loading control, the fold change in protein expression was quantified relative to the siRNA control protein expression by using ImageJ to measure the band intensity of each condition.

Additionally, we saw a slight reduction in the protein expression of NUP107 with NUP43 and NUP85 targeting siRNA (Figure 28). Conversely, we did not see a reduction in protein expression with treatment of siRNA targeting LMNA, BMI1, or PHC2 signifying that the protein expression profile of NUP107 is particularly regulating in part to NPC related proteins (Figure 28). This could also provide an explanation for the YFP-MS2 accumulation phenotype previously discovered. For instance, knockdown of NUPs that affect NUP107 expression may have caused the YFP-MS2 accumulation at the DSB by indirectly depleting NUP107 protein levels through destabilization of the Y-complex. Thus, we wanted to test if knockdown of NUP107-associated NUPs decreased NUP107 foci formation and localization to DSBs visualized through immunofluorescence. Additionally, we wanted to determine if NUP107 foci stably localizes to DSBs over a prolonged period of induced breaks.

Using the Ptuner263 cell line, we induced DSBs as two separate time points at 3 hours and 8 hours, respectively. Cells were also treated with two siRNAs targeting NUP107 and siRNAs targeting NUP133 and NUP153. We chose these siRNAs because NUP133 is the binding partner of NUP107 in the Y-complex [97] and based on our previous expression profile (Figure 28), NUP133 decreased NUP107 expression. In line with this, NUP153 had been shown to be necessary for Y-complex formation in interphase of the cell and also decreased NUP107 expression (Figure 28) [51]. We indeed found that depletion of NUP107, NUP133, and NUP153 decreased NUP107 foci formation at both 3-hour and 8-hour time points (Figure 29) which was consistent with our western blot analysis. Also, we also observed the presence of NUP107 localization to the fok1 induced DSB at both 3-hour and 8-hour time points suggesting that NUP107 may form stable foci at DSBs. Further studies need to be conducted to determine the

explicit nature of NUP107s potential function in the DDR at DSBs, but our data suggests that NUP107 may localize to aid in repressing transcription.

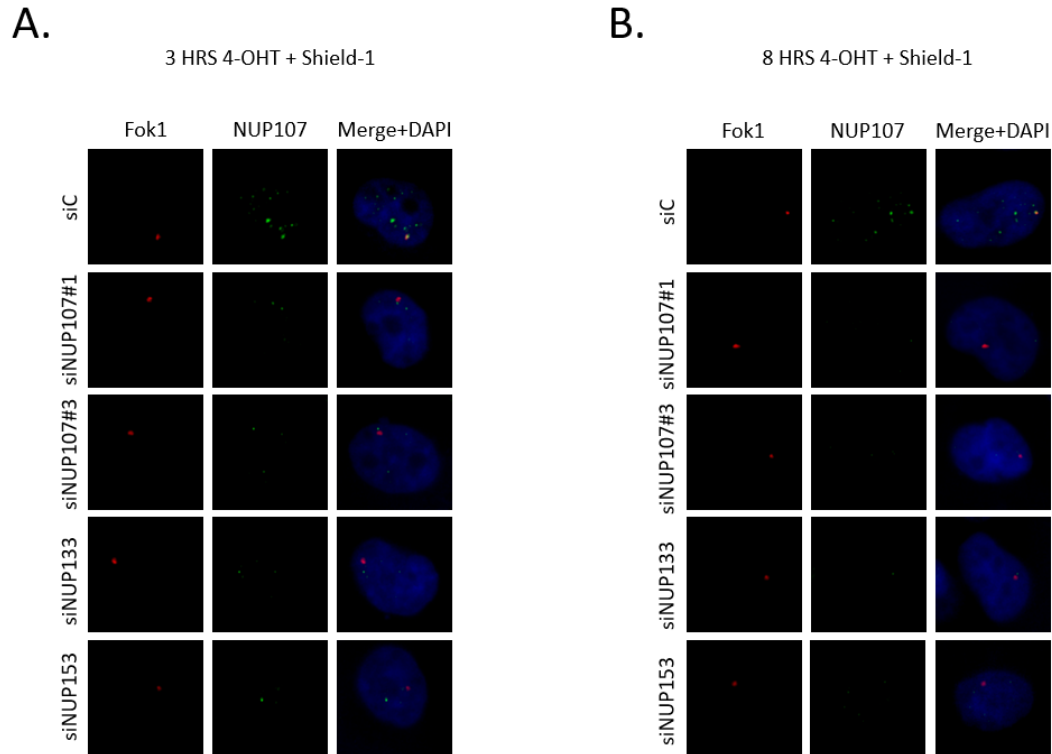


Figure 29. NUP107 is retained at DSBs over prolonged DSB induction. A. ptuner263 cells were treated with indicated siRNA for 72 hours and treated with 4-OHT/Shield-1 for 3 hours to induce the fok1 endonuclease. Cells were stained with anti-NUP107 antibody to observe colocalization at the fok1 spot. B. ptuner263 cells were treated siRNA in the same manner as in A and were treated with 4-OHT/Shield-1 for 8. Cells were also stained with the anti-NUP107 antibody as in A.

By also inducing DSBs at 3-hour and 8-hour time points, we wanted to address the concern of DSB stabilization in response to persistent DSBs. As a result, we also looked for the relative location of the fok1 spot in the nucleus between each time point. If DSBs mobilize to the nuclear periphery, we hypothesized that there would be a greater proportion of fok1 spots at the nuclear periphery at the 8-hour time point compared to the 3-hour time point. However, in either case, we did not see a clear distinction in the localization of the fok1 spot between each time

point. Several conclusions can be made from this. First, a more in-depth time course assay should be conducted to determine if the relocalization of DSBs to the nuclear periphery is a phenomena in mammalian cells. Secondly, the specific 3-dimensional organization of chromatin in the nucleus cannot be overlooked. For example, the ptuner263 cell line creates a DSB on the chromosome 1p3.6 location [76]. As a result, the chromosome may naturally occupy a location in the nucleus relatively closer to the nuclear periphery when compared to other chromosomal locations. As a result, further analysis is needed to determine the relocalization of DSBs to the nuclear periphery, specifically the NPC. Nonetheless, our data points to a mechanism where NUP107 contains distinct nucleoplasmic protein fractions can localize to DSBs away from the NPC. However, further studies should be conducted to further elucidate whether NUP107s observed transcriptional repression phenotype and localization at DSBs is dependent on a relationship with PRC1 and the Y-complex.

Chapter Six: Conclusions, Future Directions, and Clinical Significance

Polycomb Proteins in Cancer

Thus far, PcG proteins have been known to function in stem cell maintenance through transcriptional repression of developmental genes to maintain self-renewal and prevent differentiation [11, 13, 15, 17]. As a result, PcG proteins have been shown to be indispensable for self-renewal of HSCs and normal stem cells [112]. However, there is also clinical evidence to show that PcG proteins are upregulated and involved in the progression of various types of cancers [13, 14, 85, 88, 102, 113-116]. For example, BMI1 overexpression has been implicated in promoting cell growth, proliferation, and invasiveness in gastric and breast cancers [14, 113, 115]. Additionally, BMI1 overexpression has been shown to promote chemoresistance and decrease radiosensitivity in hematological malignancies and various leukemias while also demonstrating a propensity for maintaining properties of cancer stem cells (CSCs) [14, 113]. Cancer stem cells are a proportion of tumor cells that maintain “stemness” to increase proliferation and tumor growth [115]. Additionally, EZH2, a core catalytic component of PRC2, has been implicated in prostate cancer progression and cancer stem cell proliferation upon overexpression [117, 118]. Furthermore, in a study of patients with gliomas PRC2 and EZH2 have been significantly associated with gliomas and served as a prognostic biomarker [119]. Thus, PcG proteins have clinical overlapping roles in contributing to tumorigenesis and cancer stem cell maintenance. Despite there being clinical evidence in PcG proteins contributing to cancer progression, a mechanism remains to be fully elucidated.

One proposed mechanism lies in the repression of the p16^{Ink4a} and p19^{Arf} cell cycle inhibitors which regulate retinoblastoma (Rb) and p53, respectively. It was previously shown the *Ink4a/Arf* locus is important in tumorigenesis of hepatic stem cells and dependent upon BMI1 [82, 88]. For example, BMI1-null phenotypes have shown decreased repression of the *Ink4a/Arf* locus resulting in an increase in cellular senescence and decrease in proliferation, particularly in cancer stem cells [115]. On the other hand, overexpression has been implicated in an increased of repression of the *Ink4a/Arf* locus resulting in an increased in cellular proliferation lending BMI1 to have oncogenic properties [120]. However, deletion of the *Ink4a/Arf* locus fails to completely reverse the BMI1 null phenotypes suggesting there are other mechanisms contributing PcG-mediated cancer cell proliferation [113, 121]. Since, BMI1's discovery and proposed oncogenic activity, it has been heavily implicated with the progression of B-cell lymphomas [122]. As a result, small-molecule inhibitors of BMI1 have been developed, PTC596 and PTC-209, to potentially counteract BMI1 in these aggressive B-cell lymphomas [123, 124]. It was observed that BMI1 was upregulated in mantle cell lymphomas (MCL) which is a type of aggressive B-cell lymphoma. PTC596 showed promising results in phase 1 of clinical trials and showed potent anti-proliferative properties and induced apoptosis in MCL cells independent of p53 [124]. Additionally, a most recent study examined PTC596 efficacy in cells derived from glioblastoma patients and mice [123]. In this study, it was shown that PTC596 inhibited BMI1 but displayed off-target effects on PRC2 factor EZH2. While the drug showed to increase lifespan by 41 days in terminally ill mice, the expression of EZH2 was also rapidly affected. Because PRC2 also regulates developmental gene expression, there was also a reduction in H3K27me3 which could potentially

affect relapse of cancer stem pluripotency state. As a result, more studies need to be conducted to further elucidate the specificity and efficacy in clinical applications.

To date, there has been little investigation into the role of PHC2 in cancer despite its implications with BMI1 and PRC1. Looking into the cancer profile of PHC2 in the cancer genomics database, cBioportal, shows that PHC2 is frequently mutated in various cancer types suggesting that its structure is important for cellular homeostasis [125, 126]. Additionally, in an analysis of PcG expression signatures in patient-derived gliomas, PHC2 was increased in malignancies and served as a potential prognostic marker [119]. Although BMI1 has also been implicated in gliomas, there has been little investigation into the role of PHC2 in cancer. However, our work has identified a novel role for PHC2 in mediating PRC1 transcriptional silencing at damaged chromatin. Additionally, our work identified a novel role in polycomb body formation via SAM domain interactions in mediating gene silencing in response to damaged DNA. Therefore, it is plausible to suggest that the mutations acquired in PHC2's SAM domain can threaten transcriptional regulation and contribute to genomic instability and furthering the progression of tumorigenesis. However, more studies need to be conducted to make this conclusion, but our results have promising potential clinical implications in terms of maintaining cellular homeostasis in response to genotoxic stressors. Because other PcG proteins like BMI1 have been involved in various types of malignant tumors [83], specifically targeting this gene silencing pathway mechanism mediated by PHC2 may be a fruitful therapeutic target. As a result, it could be a potential therapeutic to target the PHC2-SAM domain interaction to disrupt the transcriptional landscape around DNA double-strand breaks rendering cancer cells sensitive to chemotherapeutic agents.

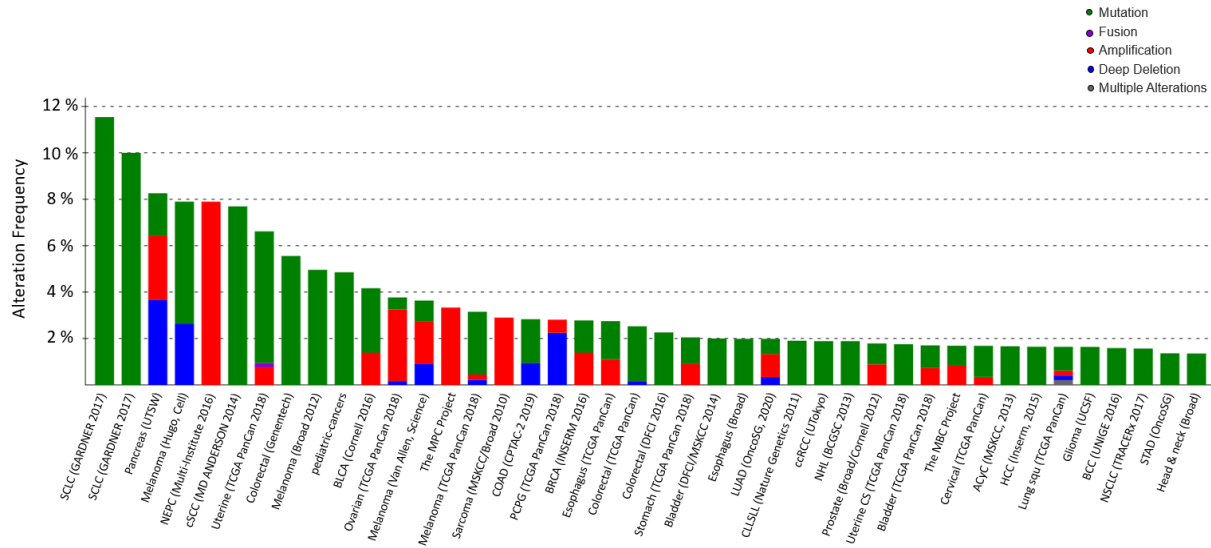


Figure 30. Cancer genomic profile of PHC2-associated cancers. Summary of alternation frequencies of PHC2 in various cancer types collected from a cancer genomic database. Adapted from Cerami et al., (2012) and Gao et al., (2013) [112,113]. Cancer types are listed in correspondence to the alteration frequency and type of alteration on y-axis (mutation, fusion, amplification, deep deletion, or multiple alterations).

Implications of Nucleoporins in Disease

In addition to our results showing PHC2's regulation of transcription at damaged chromatin, we identified an intriguing role for a nucleoporin-dependent DSB response pathway. Typically, nucleoporins have been involved in regulating transport of macromolecules through the nuclear envelope in eukaryotic cells [40]. However, additional studies are being pursued into nucleoporins regulating alternative pathways, particularly gene regulation [39, 47, 50]. In yeast, it has been observed that the NUP107-containing Y-complex provides a scaffolding for DSB repair and stressed replication fork repair [96, 98]. However, thus far, it is unclear to the extent of the role that NUP107 contributes to DSB repair in human cells. So far, our work has pointed to a role in which NUP107 can mediate transcriptional repression at DSBs. Upon DSB induction, we showed a selective transcriptional derepression of the Y-complex containing NUPs. Additionally, we observed damage foci formation of NUP107 that can extend and localize to the nucleoplasm

away from the NPC. Nonetheless, the mechanism by which NUP107 can extend into the nucleoplasm to mediate transcriptional repression at damage remains to be elucidated. In addition, it is unclear if NUP107 provides a scaffolding for repair to potentially relocate the damaged chromatin to the nuclear pore. Further studies would need to be done to confirm the notion that NUP107 mediates the relocalization of the DSBs to the nuclear pore where gene silencing can occur to maintain genomic stability. Based on our preliminary data and our mass spectrometry results, we believe there is a novel interaction between PRC1 and the nucleoporin Y-complex in preventing transcription at damaged chromatin. Given that they exhibit many of the same phenotypes and have shown propensity for binding through proteomic analysis, there is reason to suggest that damaged chromatin is being targeted to the nuclear pore where transcriptional silencing can occur. This also has clinical relevance because if PRC1 is interacting with NUP107 to silence genes *in cis* to DSBs, then disrupting this interaction could increase the radiosensitivity of cancer cells. Previous evidence has implicated that depletion of NUP107 confers decreased cell survival in response to drug treatment [96]. Thus, the increased cellular sensitivity should be pursued in the context of a NUP107-PRC1 interaction to investigate the role in cancer cell proliferation. Furthermore, there has been an association between biallelic NUP107 mutations and steroid resistant nephrotic syndrome (SRNS) through an unknown mechanism [127]. Therefore, determining a relationship between NUP107 and PRC1 may provide insight into understanding both cancer cellular sensitivity and potentially SRNS.

Potential Impact of Polycomb Proteins in Laminopathies

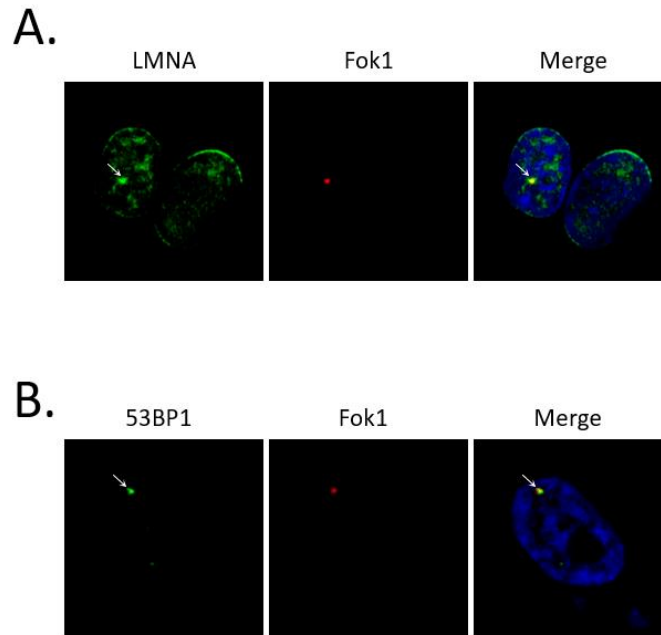


Figure 31. LMNA localizes to DSBs. A. Ptuner263 cells were seeded on coverslips and treated with 4-OHT and Shield-1 for 3 hours to induce fok1. Cells were stained with anti-LMNA antibody. B. Cells were seeded and treated in the same manner as in A. However, cells were stained with anti-53BP1 antibody to confirm the occurrence of a DSB.

In addition to cancer therapeutics, polycomb mediated gene silencing mechanism may also have implications in laminopathies such as progeria and congenital muscular dystrophy (CMD) [56, 57, 128]. Despite Lamin A having critical implications in progeria and CMD for example, a precise molecular mechanism remains to be fully understood to contributing to these laminopathies. Previous studies implicated lamin A in promoting a DSB repair response where lamin A deficiency affects 53BP1 recruitment to damage while not necessarily localizing to damage [129]. However, our preliminary data suggests that LAMIN A depletion contributes to transcriptional derepression at DSBs (Figure 26). Additionally, we identified lamin A accumulation

at DSBs induced by the fok1 endonuclease within the cellular nucleoplasm whereas lamin A had not been previously shown to localize to damage [129]. Thus, this evidence suggests that lamin A may be actively recruited to induced DSBs to function in transcriptional regulation. However, it remains to be fully elucidated how lamin A mediates the transcriptional repression at the damaged chromatin. Based on our mass spectrometry results, may interact with PHC2 so the answer may lie in an interaction between lamin A and PRC1 in the scope of the DDR. Reports have implicated PRC1 interactions with lamin A in promoting muscular stem cell renewal [57], so it is plausible that lamin A may interact with PRC1 to promote transcriptional repression in response to DNA damage. As a result, a disruption in this interaction may contribute to increased genomic instability aiding to progeria and other laminopathies, but further studies still need to be pursued.

References

1. Oudshoorn, D., G.A. Versteeg, and M. Kikkert, *Regulation of the innate immune system by ubiquitin and ubiquitin-like modifiers*. Cytokine Growth Factor Rev, 2012. **23**(6): p. 273-82.
2. Thrower, J.S., et al., *Recognition of the polyubiquitin proteolytic signal*. EMBO J, 2000. **19**(1): p. 94-102.
3. Meas, R. and P. Mao, *Histone ubiquitylation and its roles in transcription and DNA damage response*. DNA Repair (Amst), 2015. **36**: p. 36-42.
4. Pickart, C.M., *Mechanisms underlying ubiquitination*. Annu Rev Biochem, 2001. **70**: p. 503-33.
5. Nguyen, L.K., et al., *Polyubiquitin chain assembly and organization determine the dynamics of protein activation and degradation*. Front Physiol, 2014. **5**: p. 4.
6. Callis, J., *The ubiquitination machinery of the ubiquitin system*. Arabidopsis Book, 2014. **12**: p. e0174.
7. Metzger, M.B., V.A. Hristova, and A.M. Weissman, *HECT and RING finger families of E3 ubiquitin ligases at a glance*. J Cell Sci, 2012. **125**(Pt 3): p. 531-7.
8. Cao, R., Y. Tsukada, and Y. Zhang, *Role of Bmi-1 and Ring1A in H2A ubiquitylation and Hox gene silencing*. Mol Cell, 2005. **20**(6): p. 845-54.
9. Cohen, I., C. Bar, and E. Ezhkova, *Activity of PRC1 and Histone H2AK119 Monoubiquitination: Revising Popular Misconceptions*. Bioessays, 2020. **42**(5): p. e1900192.
10. Lelli, K.M., M. Slattery, and R.S. Mann, *Disentangling the many layers of eukaryotic transcriptional regulation*. Annu Rev Genet, 2012. **46**: p. 43-68.
11. Entrevan, M., B. Schuettengruber, and G. Cavalli, *Regulation of Genome Architecture and Function by Polycomb Proteins*. Trends Cell Biol, 2016. **26**(7): p. 511-525.
12. Lewis, E.B., *A gene complex controlling segmentation in Drosophila*. Nature, 1978. **276**(5688): p. 565-70.
13. Richly, H., L. Aloia, and L. Di Croce, *Roles of the Polycomb group proteins in stem cells and cancer*. Cell Death Dis, 2011. **2**: p. e204.
14. Chan, H.L. and L. Morey, *Emerging Roles for Polycomb-Group Proteins in Stem Cells and Cancer*. Trends Biochem Sci, 2019. **44**(8): p. 688-700.
15. Wang, L., et al., *Hierarchical recruitment of polycomb group silencing complexes*. Mol Cell, 2004. **14**(5): p. 637-46.
16. Gil, J. and A. O'Loughlen, *PRC1 complex diversity: where is it taking us?* Trends Cell Biol, 2014. **24**(11): p. 632-41.
17. Buchwald, G., et al., *Structure and E3-ligase activity of the Ring-Ring complex of polycomb proteins Bmi1 and Ring1b*. EMBO J, 2006. **25**(11): p. 2465-74.
18. Blackledge, N.P., et al., *Variant PRC1 complex-dependent H2A ubiquitylation drives PRC2 recruitment and polycomb domain formation*. Cell, 2014. **157**(6): p. 1445-59.
19. Taherbhoy, A.M., O.W. Huang, and A.G. Cochran, *BMI1-RING1B is an autoinhibited RING E3 ubiquitin ligase*. Nat Commun, 2015. **6**: p. 7621.
20. Colombo, M., O. Pessey, and M. Marcia, *Topology and enzymatic properties of a canonical Polycomb repressive complex 1 isoform*. FEBS Lett, 2019. **593**(14): p. 1837-1848.

21. Connelly, K.E. and E.C. Dykhuizen, *Compositional and functional diversity of canonical PRC1 complexes in mammals*. *Biochim Biophys Acta Gene Regul Mech*, 2017. **1860**(2): p. 233-245.
22. Wang, Z., et al., *A Non-canonical BCOR-PRC1.1 Complex Represses Differentiation Programs in Human ESCs*. *Cell Stem Cell*, 2018. **22**(2): p. 235-251 e9.
23. Gao, Z., et al., *PCGF homologs, CBX proteins, and RYBP define functionally distinct PRC1 family complexes*. *Mol Cell*, 2012. **45**(3): p. 344-56.
24. Gray, F., et al., *BMI1 regulates PRC1 architecture and activity through homo- and hetero-oligomerization*. *Nat Commun*, 2016. **7**: p. 13343.
25. Farcas, A.M., et al., *KDM2B links the Polycomb Repressive Complex 1 (PRC1) to recognition of CpG islands*. *Elife*, 2012. **1**.
26. Ogiyama, Y., et al., *Polycomb-Dependent Chromatin Looping Contributes to Gene Silencing during Drosophila Development*. *Mol Cell*, 2018. **71**(1): p. 73-88 e5.
27. Tsuboi, M., et al., *Ubiquitination-Independent Repression of PRC1 Targets during Neuronal Fate Restriction in the Developing Mouse Neocortex*. *Dev Cell*, 2018. **47**(6): p. 758-772 e5.
28. Fursova, N.A., et al., *Synergy between Variant PRC1 Complexes Defines Polycomb-Mediated Gene Repression*. *Mol Cell*, 2019. **74**(5): p. 1020-1036 e8.
29. Kim, C.A., et al., *Polymerization of the SAM domain of TEL in leukemogenesis and transcriptional repression*. *EMBO J*, 2001. **20**(15): p. 4173-82.
30. Kim, C.A., et al., *The SAM domain of polyhomeotic forms a helical polymer*. *Nat Struct Biol*, 2002. **9**(6): p. 453-7.
31. Isono, K., et al., *SAM domain polymerization links subnuclear clustering of PRC1 to gene silencing*. *Dev Cell*, 2013. **26**(6): p. 565-77.
32. Pirrotta, V. and H.B. Li, *A view of nuclear Polycomb bodies*. *Curr Opin Genet Dev*, 2012. **22**(2): p. 101-9.
33. Kojic, A., et al., *Distinct roles of cohesin-SA1 and cohesin-SA2 in 3D chromosome organization*. *Nat Struct Mol Biol*, 2018. **25**(6): p. 496-504.
34. Kong, X., et al., *Distinct functions of human cohesin-SA1 and cohesin-SA2 in double-strand break repair*. *Mol Cell Biol*, 2014. **34**(4): p. 685-98.
35. Cuadrado, A., et al., *Specific Contributions of Cohesin-SA1 and Cohesin-SA2 to TADs and Polycomb Domains in Embryonic Stem Cells*. *Cell Rep*, 2019. **27**(12): p. 3500-3510 e4.
36. Hill, V.K., J.S. Kim, and T. Waldman, *Cohesin mutations in human cancer*. *Biochim Biophys Acta*, 2016. **1866**(1): p. 1-11.
37. Meisenberg, C., et al., *Repression of Transcription at DNA Breaks Requires Cohesin throughout Interphase and Prevents Genome Instability*. *Mol Cell*, 2019. **73**(2): p. 212-223 e7.
38. Sanchez, A., et al., *BMI1-UBR5 axis regulates transcriptional repression at damaged chromatin*. *Proc Natl Acad Sci U S A*, 2016. **113**(40): p. 11243-11248.
39. Dicks, M.D.J., et al., *Multiple components of the nuclear pore complex interact with the amino-terminus of MX2 to facilitate HIV-1 restriction*. *PLoS Pathog*, 2018. **14**(11): p. e1007408.
40. Raices, M. and M.A. D'Angelo, *Nuclear pore complex composition: a new regulator of tissue-specific and developmental functions*. *Nat Rev Mol Cell Biol*, 2012. **13**(11): p. 687-99.
41. Weberruss, M. and W. Antonin, *Perforating the nuclear boundary - how nuclear pore complexes assemble*. *J Cell Sci*, 2016. **129**(24): p. 4439-4447.
42. Dechat, T., et al., *Nuclear lamins: major factors in the structural organization and function of the nucleus and chromatin*. *Genes & Development*, 2008. **22**(7): p. 832-853.
43. Kalousi, A. and E. Soutoglou, *Nuclear compartmentalization of DNA repair*. *Curr Opin Genet Dev*, 2016. **37**: p. 148-157.
44. Gozalo, A., et al., *Core Components of the Nuclear Pore Bind Distinct States of Chromatin and Contribute to Polycomb Repression*. *Mol Cell*, 2020. **77**(1): p. 67-81 e7.

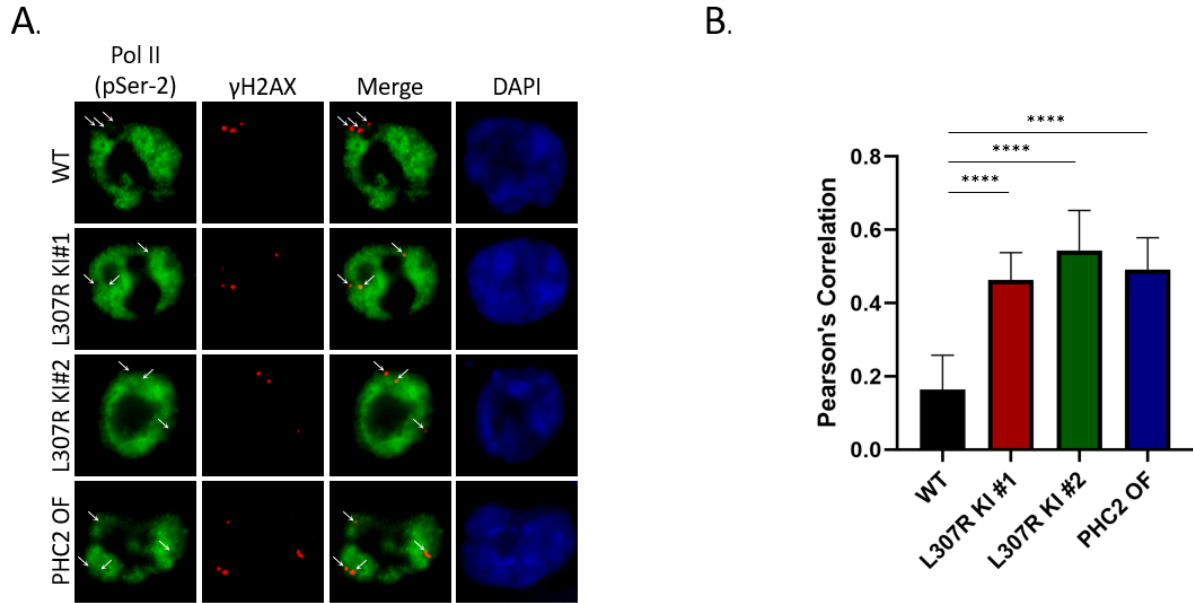
45. Fritz, A.J., et al., *Chromosomes at Work: Organization of Chromosome Territories in the Interphase Nucleus*. Journal of Cellular Biochemistry, 2016. **117**(1): p. 9-19.
46. van Steensel, B. and A.S. Belmont, *Lamina-Associated Domains: Links with Chromosome Architecture, Heterochromatin, and Gene Repression*. Cell, 2017. **169**(5): p. 780-791.
47. D'Angelo, M.A., *Nuclear pore complexes as hubs for gene regulation*. Nucleus, 2018. **9**(1): p. 142-148.
48. Jacinto, F.V., C. Benner, and M.W. Hetzer, *The nucleoporin Nup153 regulates embryonic stem cell pluripotency through gene silencing*. Genes & Development, 2015. **29**(12): p. 1224-1238.
49. Morchoisne-Bolhy, S., et al., *Intranuclear dynamics of the Nup107-160 complex*. Mol Biol Cell, 2015. **26**(12): p. 2343-56.
50. Beck, M. and E. Hurt, *The nuclear pore complex: understanding its function through structural insight*. Nature Reviews Molecular Cell Biology, 2017. **18**(2): p. 73-89.
51. Vollmer, B., et al., *Nup153 Recruits the Nup107-160 Complex to the Inner Nuclear Membrane for Interphasic Nuclear Pore Complex Assembly*. Dev Cell, 2015. **33**(6): p. 717-28.
52. Dittmer, T. and T. Misteli, *The lamin protein family*. Genome Biology, 2011. **12**(5).
53. Davies, B.S.J., et al., *The Posttranslational Processing of Prelamin A and Disease*. Annual Review of Genomics and Human Genetics, 2009. **10**: p. 153-174.
54. Worman, H.J. and S. Michaelis, *Permanently Farnesylated Prelamin A, Progeria, and Atherosclerosis*. Circulation, 2018. **138**(3): p. 283-286.
55. Eissenberg, J.C. and S. Gonzalo, *Pushing the limit on laminopathies*. Nature Materials, 2020. **19**(4): p. 378-380.
56. Marullo, F., et al., *Nucleoplasmic Lamin A/C and Polycomb group of proteins: An evolutionarily conserved interplay*. Nucleus, 2016. **7**(2): p. 103-11.
57. Bianchi, A., et al., *Dysfunctional polycomb transcriptional repression contributes to lamin A/C-dependent muscular dystrophy*. J Clin Invest, 2020. **130**(5): p. 2408-2421.
58. Friedberg, E.C., L.D. McDaniel, and R.A. Schultz, *The role of endogenous and exogenous DNA damage and mutagenesis*. Curr Opin Genet Dev, 2004. **14**(1): p. 5-10.
59. Aparicio, T., R. Baer, and J. Gautier, *DNA double-strand break repair pathway choice and cancer*. DNA Repair, 2014. **19**: p. 169-175.
60. Marechal, A. and L. Zou, *DNA Damage Sensing by the ATM and ATR Kinases*. Cold Spring Harbor Perspectives in Biology, 2013. **5**(9).
61. Berkovich, E., R.J. Monnat, Jr., and M.B. Kastan, *Roles of ATM and NBS1 in chromatin structure modulation and DNA double-strand break repair*. Nat Cell Biol, 2007. **9**(6): p. 683-90.
62. Kinner, A., et al., *Gamma-H2AX in recognition and signaling of DNA double-strand breaks in the context of chromatin*. Nucleic Acids Res, 2008. **36**(17): p. 5678-94.
63. Lukas, C., et al., *Mdc1 couples DNA double-strand break recognition by Nbs1 with its H2AX-dependent chromatin retention*. Embo Journal, 2004. **23**(13): p. 2674-2683.
64. Zannini, L., D. Delia, and G. Buscemi, *CHK2 kinase in the DNA damage response and beyond*. J Mol Cell Biol, 2014. **6**(6): p. 442-57.
65. Price, B.D. and A.D. D'Andrea, *Chromatin Remodeling at DNA Double-Strand Breaks*. Cell, 2013. **152**(6): p. 1344-1354.
66. Doil, C., et al., *RNF168 Binds and Amplifies Ubiquitin Conjugates on Damaged Chromosomes to Allow Accumulation of Repair Proteins*. Cell, 2009. **136**(3): p. 435-446.
67. Mailand, N., et al., *RNF8 ubiquitylates histones at DNA double-strand breaks and promotes assembly of repair proteins*. Cell, 2007. **131**(5): p. 887-900.
68. Kim, J.S., et al., *Independent and sequential recruitment of NHEJ and HR factors to DNA damage sites in mammalian cells*. J Cell Biol, 2005. **170**(3): p. 341-7.

69. Kakarouglas, A. and P.A. Jeggo, *DNA DSB repair pathway choice: an orchestrated handover mechanism*. Br J Radiol, 2014. **87**(1035): p. 20130685.
70. Shaltiel, I.A., et al., *The same, only different - DNA damage checkpoints and their reversal throughout the cell cycle*. J Cell Sci, 2015. **128**(4): p. 607-20.
71. D'Alessandro, G. and F. d'Adda di Fagagna, *Transcription and DNA Damage: Holding Hands or Crossing Swords?* J Mol Biol, 2017. **429**(21): p. 3215-3229.
72. Rodriguez-Gil, A., et al., *The distribution of active RNA polymerase II along the transcribed region is gene-specific and controlled by elongation factors*. Nucleic Acids Research, 2010. **38**(14): p. 4651-4664.
73. Kakarouglas, A., et al., *Requirement for PBAF in transcriptional repression and repair at DNA breaks in actively transcribed regions of chromatin*. Mol Cell, 2014. **55**(5): p. 723-32.
74. Belotserkovskaya, R., et al., *FACT facilitates transcription-dependent nucleosome alteration*. Science, 2003. **301**(5636): p. 1090-1093.
75. de Vivo, A., et al., *The OTUD5-UBR5 complex regulates FACT-mediated transcription at damaged chromatin*. Nucleic Acids Res, 2019. **47**(2): p. 729-746.
76. Shanbhag, N.M., et al., *ATM-dependent chromatin changes silence transcription in cis to DNA double-strand breaks*. Cell, 2010. **141**(6): p. 970-81.
77. Pankotai, T., et al., *DNAPKcs-dependent arrest of RNA polymerase II transcription in the presence of DNA breaks*. Nat Struct Mol Biol, 2012. **19**(3): p. 276-82.
78. Ginjala, V., et al., *BMI1 is recruited to DNA breaks and contributes to DNA damage-induced H2A ubiquitination and repair*. Mol Cell Biol, 2011. **31**(10): p. 1972-82.
79. Ismail, I.H., et al., *BMI1-mediated histone ubiquitylation promotes DNA double-strand break repair*. J Cell Biol, 2010. **191**(1): p. 45-60.
80. Ui, A., Y. Nagaura, and A. Yasui, *Transcriptional elongation factor ENL phosphorylated by ATM recruits polycomb and switches off transcription for DSB repair*. Mol Cell, 2015. **58**(3): p. 468-82.
81. Jacobs, J.J., et al., *The oncogene and Polycomb-group gene bmi-1 regulates cell proliferation and senescence through the ink4a locus*. Nature, 1999. **397**(6715): p. 164-8.
82. Bruggeman, S.W., et al., *Ink4a and Arf differentially affect cell proliferation and neural stem cell self-renewal in Bmi1-deficient mice*. Genes Dev, 2005. **19**(12): p. 1438-43.
83. Chen, H., et al., *Polycomb protein Ezh2 regulates pancreatic beta-cell Ink4a/Arf expression and regeneration in diabetes mellitus*. Genes Dev, 2009. **23**(8): p. 975-85.
84. Liu, J., et al., *Bmi1 regulates mitochondrial function and the DNA damage response pathway*. Nature, 2009. **459**(7245): p. 387-392.
85. Nacerddine, K., et al., *Akt-mediated phosphorylation of Bmi1 modulates its oncogenic potential, E3 ligase activity, and DNA damage repair activity in mouse prostate cancer*. J Clin Invest, 2012. **122**(5): p. 1920-32.
86. Chagraoui, J., et al., *An anticlastogenic function for the Polycomb Group gene Bmi1*. Proc Natl Acad Sci U S A, 2011. **108**(13): p. 5284-9.
87. Xue, L., et al., *Regulation of ATM in DNA double strand break repair accounts for the radiosensitivity in human cells exposed to high linear energy transfer ionizing radiation*. Mutat Res, 2009. **670**(1-2): p. 15-23.
88. Facchino, S., et al., *BMI1 confers radioresistance to normal and cancerous neural stem cells through recruitment of the DNA damage response machinery*. J Neurosci, 2010. **30**(30): p. 10096-111.
89. Lin, X., et al., *BMI1 reduces ATR activation and signalling caused by hydroxyurea*. Oncotarget, 2017. **8**(52): p. 89707-89721.
90. Ma, K., et al., *Common fragile sites: genomic hotspots of DNA damage and carcinogenesis*. Int J Mol Sci, 2012. **13**(9): p. 11974-99.

91. Sanchez, A., et al., *Transcription-replication conflicts as a source of common fragile site instability caused by BMI1-RNF2 deficiency*. PLoS Genet, 2020. **16**(3): p. e1008524.
92. Gomez-Gonzalez, B. and A. Aguilera, *Transcription-mediated replication hindrance: a major driver of genome instability*. Genes Dev, 2019. **33**(15-16): p. 1008-1026.
93. Hamperl, S., et al., *Transcription-Replication Conflict Orientation Modulates R-Loop Levels and Activates Distinct DNA Damage Responses*. Cell, 2017. **170**(4): p. 774-786 e19.
94. Niehrs, C. and B. Luke, *Regulatory R-loops as facilitators of gene expression and genome stability*. Nat Rev Mol Cell Biol, 2020. **21**(3): p. 167-178.
95. Klusmann, I., et al., *Chromatin modifiers Mdm2 and RNF2 prevent RNA:DNA hybrids that impair DNA replication*. Proc Natl Acad Sci U S A, 2018. **115**(48): p. E11311-E11320.
96. Nagai, S., et al., *Functional targeting of DNA damage to a nuclear pore-associated SUMO-dependent ubiquitin ligase*. Science, 2008. **322**(5901): p. 597-602.
97. Freudenreich, C.H. and X.A. Su, *Relocalization of DNA lesions to the nuclear pore complex*. FEMS Yeast Res, 2016. **16**(8).
98. Whalen, J.M., et al., *Relocation of Collapsed Forks to the Nuclear Pore Complex Depends on Sumoylation of DNA Repair Proteins and Permits Rad51 Association*. Cell Rep, 2020. **31**(6): p. 107635.
99. Lemaitre, C. and E. Soutoglou, *DSB (Im)mobility and DNA repair compartmentalization in mammalian cells*. J Mol Biol, 2015. **427**(3): p. 652-8.
100. Lottersberger, F., et al., *53BP1 and the LINC Complex Promote Microtubule-Dependent DSB Mobility and DNA Repair*. Cell, 2015. **163**(4): p. 880-93.
101. Marnef, A., et al., *A cohesin/HUSH- and LINC-dependent pathway controls ribosomal DNA double-strand break repair*. Genes & Development, 2019. **33**(17-18): p. 1175-1190.
102. Mercurio, F.A. and M. Leone, *The Sam Domain of EphA2 Receptor and its Relevance to Cancer: A Novel Challenge for Drug Discovery?* Curr Med Chem, 2016. **23**(42): p. 4718-4734.
103. Kawai, T., et al., *A heterozygous mutation in the SAM domain of p63 underlies a mild form of ectodermal dysplasia*. J Dermatol Sci, 2018. **90**(3): p. 360-363.
104. Aguilera, P., et al., *The nuclear pore complex prevents sister chromatid recombination during replicative senescence*. Nat Commun, 2020. **11**(1): p. 160.
105. Pan, M.R., et al., *Monoubiquitination of H2AX protein regulates DNA damage response signaling*. J Biol Chem, 2011. **286**(32): p. 28599-607.
106. Rastogi, R.P., et al., *Molecular mechanisms of ultraviolet radiation-induced DNA damage and repair*. J Nucleic Acids, 2010. **2010**: p. 592980.
107. Davidson, L., L. Muniz, and S. West, *3' end formation of pre-mRNA and phosphorylation of Ser2 on the RNA polymerase II CTD are reciprocally coupled in human cells*. Genes Dev, 2014. **28**(4): p. 342-56.
108. Smigova, J., et al., *Structural basis of polycomb bodies*. Folia Biol (Praha), 2014. **60 Suppl 1**: p. 13-20.
109. Tran, H.H., et al., *Native interface of the SAM domain polymer of TEL*. BMC Struct Biol, 2002. **2**: p. 5.
110. Robinson, A.K., et al., *The growth-suppressive function of the polycomb group protein polyhomeotic is mediated by polymerization of its sterile alpha motif (SAM) domain*. J Biol Chem, 2012. **287**(12): p. 8702-13.
111. Robinson, A.K., et al., *Human polyhomeotic homolog 3 (PHC3) sterile alpha motif (SAM) linker allows open-ended polymerization of PHC3 SAM*. Biochemistry, 2012. **51**(27): p. 5379-86.
112. Raaphorst, F.M., *Self-renewal of hematopoietic and leukemic stem cells: a central role for the Polycomb-group gene Bmi-1*. Trends Immunol, 2003. **24**(10): p. 522-4.

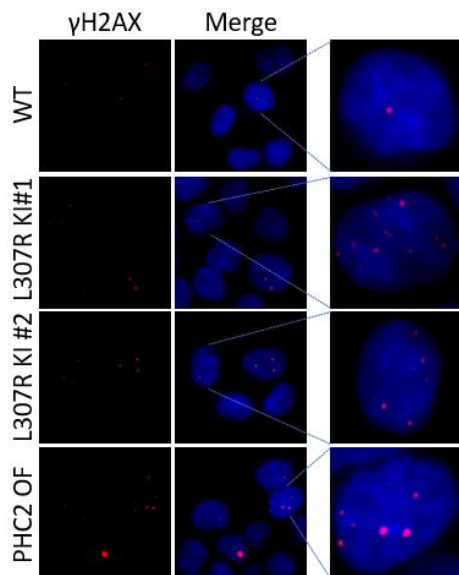
113. Wang, M.C., et al., *BMI-1, a promising therapeutic target for human cancer*. *Oncol Lett*, 2015. **10**(2): p. 583-588.
114. Yuan, B., et al., *Prognostic Value and Clinicopathological Differences of Bmi1 in Gastric Cancer: A Meta-analysis*. *Anticancer Agents Med Chem*, 2016. **16**(4): p. 407-13.
115. Srinivasan, M., et al., *Downregulation of Bmi1 in breast cancer stem cells suppresses tumor growth and proliferation*. *Oncotarget*, 2017. **8**(24): p. 38731-38742.
116. Zhu, S., et al., *BMI1 regulates androgen receptor in prostate cancer independently of the polycomb repressive complex 1*. *Nat Commun*, 2018. **9**(1): p. 500.
117. Chen, Y., et al., *RNAi targeting EZH2 inhibits tumor growth and liver metastasis of pancreatic cancer in vivo*. *Cancer Lett*, 2010. **297**(1): p. 109-16.
118. Kim, K.H. and C.W. Roberts, *Targeting EZH2 in cancer*. *Nat Med*, 2016. **22**(2): p. 128-34.
119. Hu, Q., et al., *Polycomb group expression signatures in the malignant progression of gliomas*. *Oncol Lett*, 2017. **13**(4): p. 2583-2590.
120. Chen, G., et al., *Bmi1 Overexpression in Mesenchymal Stem Cells Exerts Antiaging and Antiosteoporosis Effects by Inactivating p16/p19 Signaling and Inhibiting Oxidative Stress*. *Stem Cells*, 2019. **37**(9): p. 1200-1211.
121. Bruggeman, S.W., et al., *Bmi1 controls tumor development in an Ink4a/Arf-independent manner in a mouse model for glioma*. *Cancer Cell*, 2007. **12**(4): p. 328-41.
122. Sahasrabudhe, A.A., *BMI1: A Biomarker of Hematologic Malignancies*. *Biomark Cancer*, 2016. **8**: p. 65-75.
123. Flamier, A., et al., *Off-target effect of the BMI1 inhibitor PTC596 drives epithelial-mesenchymal transition in glioblastoma multiforme*. *NPJ Precis Oncol*, 2020. **4**: p. 1.
124. Maeda, A., et al., *Targeting of BMI-1 expression by the novel small molecule PTC596 in mantle cell lymphoma*. *Oncotarget*, 2018. **9**(47): p. 28547-28560.
125. Cerami, E., et al., *The cBio cancer genomics portal: an open platform for exploring multidimensional cancer genomics data*. *Cancer Discov*, 2012. **2**(5): p. 401-4.
126. Gao, J., et al., *Integrative analysis of complex cancer genomics and clinical profiles using the cBioPortal*. *Sci Signal*, 2013. **6**(269): p. p1.
127. Park, E., et al., *NUP107 mutations in children with steroid-resistant nephrotic syndrome*. *Nephrol Dial Transplant*, 2017. **32**(6): p. 1013-1017.
128. Chen, N.Y., et al., *Fibroblasts lacking nuclear lamins do not have nuclear blebs or protrusions but nevertheless have frequent nuclear membrane ruptures*. *Proc Natl Acad Sci U S A*, 2018. **115**(40): p. 10100-10105.
129. Gibbs-Seymour, I., et al., *Lamin A/C-dependent interaction with 53BP1 promotes cellular responses to DNA damage*. *Aging Cell*, 2015. **14**(2): p. 162-9.

Appendix I: Supplemental Information

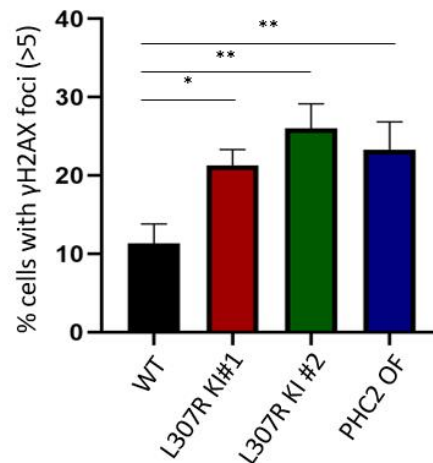


Supplemental Figure 1. PHC2 L307R mutation fails to repress transcription at DSBs. A. Indicated HCT116 cells were treated with 5 μ M bleomycin overnight to induce DSBs. Cells were fixed and co-stained with anti-pSer-2 RNA Pol II and anti- γ H2AX antibodies. B. Overlap between pSer-2 RNA Pol II signal and γ H2AX was quantified using Pearson's Correlation in ImageJ. (N=10) (**** indicates P-value <0.0005)

A.

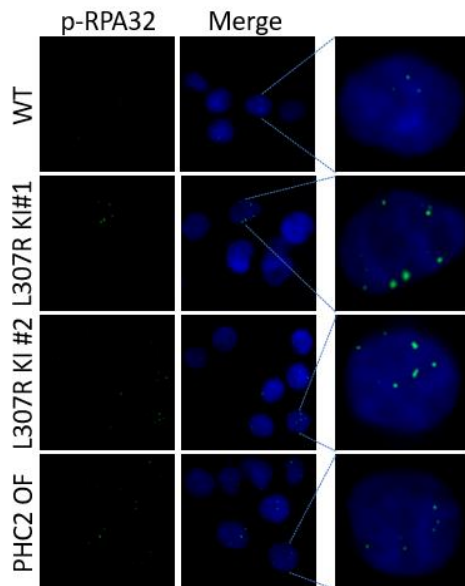


B.

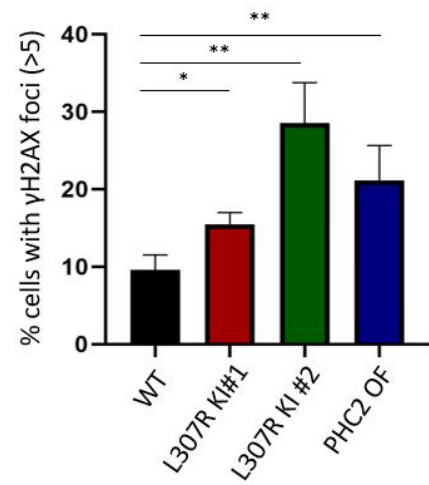


Supplemental Figure 2. PHC2 L307R mutation contributes to spontaneous DSB formation. A. Indicated HCT116 cells were seeded onto coverslips and stained with an anti- γ H2AX antibody. B. The number of nuclei were counted (N=200) in image J as well as the number of γ H2AX foci in each nuclei. The percentage of cells with greater than 5 γ H2AX foci were subsequently quantified (* indicates P-value 0.01 to 0.05, ** indicates P-value 0.001 to 0.01)

A.



B.



Supplemental Figure 3. PHC2 L307R mutation contributes replication stress. A. Indicated HCT116 cells were seeded onto coverslips and stained with an anti-p-RPA32 antibody. B. The number of nuclei were counted (N=200) in image J as well as the number of γ H2AX foci in each nuclei. The percentage of cells with greater than 5 γ H2AX foci were subsequently quantified (* indicates P-value 0.01 to 0.05, ** indicates P-value 0.001 to 0.01)